Library Declaration and Deposit Agreement

1. **STUDENT DETAILS**

   Dayal Christopher Strub

   0956563

2. **THESIS DEPOSIT**

   2.1 I understand that under my registration at the University, I am required to deposit my thesis with the University in BOTH hard copy and in digital format. The digital version should normally be saved as a single pdf file.

   2.2 The hard copy will be housed in the University Library. The digital version will be deposited in the Universitys Institutional Repository (WRAP). Unless otherwise indicated (see 2.3 below) this will be made openly accessible on the Internet and will be supplied to the British Library to be made available online via its Electronic Theses Online Service (EThOS) service. [At present, theses submitted for a Masters degree by Research (MA, MSc, LLM, MS or MMedSci) are not being deposited in WRAP and not being made available via EthOS. This may change in future.]

   2.3 In exceptional circumstances, the Chair of the Board of Graduate Studies may grant permission for an embargo to be placed on public access to the hard copy thesis for a limited period. It is also possible to apply separately for an embargo on the digital version. (Further information is available in the Guide to Examinations for Higher Degrees by Research.)

   2.4 (a) Hard Copy I hereby deposit a hard copy of my thesis in the University Library to be made publicly available to readers immediately.
   I agree that my thesis may be photocopied.

   (b) Digital Copy I hereby deposit a digital copy of my thesis to be held in WRAP and made available via EThOS.
   My thesis can be made publicly available online.

3. **GRANTING OF NON-EXCLUSIVE RIGHTS**
   Whether I deposit my Work personally or through an assistant or other agent, I agree to the following: Rights granted to the University of Warwick and the British Library and the user of the thesis through this agreement are non-exclusive. I retain all rights in the thesis in its present version or future versions. I agree that the institutional repository administrators and the British Library or their agents may, without changing content, digitise and migrate the thesis to any medium or format for the purpose of future preservation and accessibility.

4. **DECLARATIONS**

   (a) I DECLARE THAT:

   - I am the author and owner of the copyright in the thesis and/or I have the authority of the authors and owners of the copyright in the thesis to make this agreement. Reproduction of any part of this thesis for teaching or in academic or other forms of publication is subject to the normal limitations on the use of copyrighted materials and to the proper and full acknowledgement of its source.
   - The digital version of the thesis I am supplying is the same version as the final, hardbound copy submitted in completion of my degree, once any minor corrections have been completed.
   - I have exercised reasonable care to ensure that the thesis is original, and does not to the best of my knowledge break any UK law or other Intellectual Property Right, or contain any confidential material.
   - I understand that, through the medium of the Internet, files will be available to automated agents, and may be searched and copied by, for example, text mining and plagiarism detection software.

   (b) IF I HAVE AGREED (in Section 2 above) TO MAKE MY THESIS PUBLICLY AVAILABLE DIGITALLY, I ALSO DECLARE THAT:

   - I grant the University of Warwick and the British Library a licence to make available on the Internet the thesis in digitised format through the Institutional Repository and through the British Library via the EThOS service.
   - If my thesis does include any substantial subsidiary material owned by third-party copyright holders, I have sought and obtained permission to include it in any version of my thesis available in digital format and that this permission encompasses the rights that I have granted to the University of Warwick and to the British Library.

5. **LEGAL INFRINGEMENTS**

   I understand that neither the University of Warwick nor the British Library have any obligation to take legal action on behalf of myself, or other rights holders, in the event of infringement of intellectual property rights, breach of contract or of any other right, in the thesis.

Please sign this agreement and return it to the Graduate School Office when you submit your thesis.

Student's signature: ....Date: ......20th April, 2015......
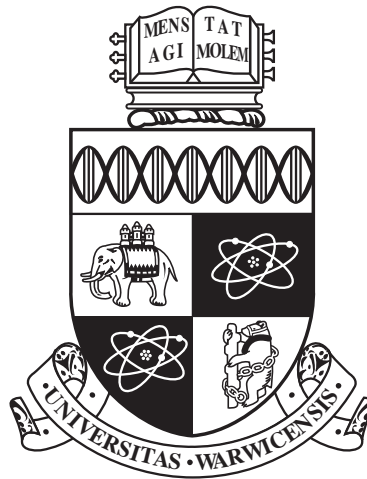
Bifurcations of transition states

by

Dayal Christopher Strub

Thesis

Submitted to the University of Warwick

for the degree of

Doctor of Philosophy

Mathematics Institute

April, 2015

THE UNIVERSITY OF
WARWICK

Contents

Acknowledgements

I would like to start by thanking my supervisor, Robert MacKay. It has been a real pleasure to work together and learn from him. Without his insight and guidance this would not have been possible.

During my undergraduate studies, I was lucky enough to be supervised, followed and guided along by Alan Champneys, Poul Hjorth and Jens Starke. They taught me a lot and prepared me for my graduate studies for which I am very grateful.

I would also like to thank a number of people that influenced the work in this thesis. Thanks to Simone Gutt, who suggested to Robert to use a symplectic connection to extend our local symplectically orthogonal foliation, Mark Roberts for pointing us to some of the literature on reduction of n-body systems and the Eckart-Sayvetz conventions [RSS06, KRT00], Robert Littlejohn and Kevin Mitchell for suggestions regarding the use of the Eckart convention and for pointing me to [LM02]. I have also discussed parts of the work presented here with a number of people, and would especially like to thank Sergios Agapiou, Gregorio Benincasa, Vassili Gelfreich, William Giles, Peter Hazard, David Kelly, Giannis Moutsinas, Georg Ostrovski, Lara Sabbagh, Arturo Vieiro, and Holger Waalkens.

The Centre Interdisciplinaire de Phénomènes Non-linéaires et de Systèmes Complexes at the Université Libre de Bruxelles hosted Robert and me from October 2010 to April 2011. This was a wonderful period, and I would like to thank in particular Pierre Gaspard and Thomas Gilbert.

Thanks also to my family and Elena Sergi, for all their love and support, and to all my WMI, Coventry, Leamington and Bear Rock friends for making these years so enjoyable.

A lot of people have helped me along the way, these are but a few.

Declarations

I declare that, to the best of my knowledge, the material contained in this thesis is original work obtained in collaboration with my Supervisor, R. S. MacKay, unless otherwise stated, cited, or commonly known.

Parts of Chapters 1 and 2 have already been published as [MS14], Chapter 3 has been re-written for publication, uploaded to the ArXiv [MS15] and submitted, whereas the questions of Section 2.3 are being considered at present and will be published once we have the answers.

Abstract

A transition state for a Hamiltonian system is a closed, invariant, oriented, codimension-2 submanifold of an energy-level that can be spanned by two compact codimension-1 surfaces of unidirectional flux whose union, called a dividing surface, locally separates the energy-level into two components and has no local recrossings. For this to happen robustly to all smooth perturbations, the transition state must be normally hyperbolic. The dividing surface then has locally minimal geometric flux through it, giving a useful upper bound on the rate of transport in either direction.

Transition states diffeomorphic to $\mathbb{S}^{2m-3}$ are known to exist for energies just above any index-1 critical point of a Hamiltonian of m degrees of freedom, with dividing surfaces $\mathbb{S}^{2m-2}$. The question addressed here is what qualitative changes in the transition state, and consequently the dividing surface, may occur as the energy or other parameters are varied? We find that there is a class of systems for which the transition state becomes singular and then regains normal hyperbolicity with a change in diffeomorphism class. These are Morse bifurcations.

Continuing the dividing surfaces and transition states through Morse bifurcations allows us to compute the flux for a larger range of energies. The effect of Morse bifurcations on the flux, as a function of energy, is considered and we find a loss of differentiability in the neighbourhood of the bifurcations.

Various examples are considered. Firstly, some simple examples in which transition states connect or disconnect, and the dividing surface may become a torus or other. Then, we show that sequences of Morse bifurcations producing various interesting transition state and dividing surface are present in reacting systems, specifically bimolecular capture processes. We consider first planar reactions, for which the reduction of symmetries is easiest, and then also spatial reactions, where we find interesting Morse bifurcations involving both the attitude degrees of freedom and the angular momentum ones.

In order to consider these examples, we present a method of constructing dividing surfaces spanning general transition states, and also a method to approximate normally hyperbolic submanifolds due to MacKay.

List of symbols

List of most used symbols in alphabetical order (Latin then Greek). Inevitably, some symbols are used for a number of objects.

a, b	(Williamson) normal form frequencies
$A(q)$	gauge potential
B^i	reactant and product regions in M
$B(q)$	Coriolis tensor
$\mathbb{B}^k$	k-ball in $\mathbb{R}^k$
$C_r(H)$	set of critical points of H
E	energy $E = H(z)$
E_k	kinetic energy
F_z	fibre at z, $F_z = \pi^{-1}(z)$
g	element of Lie group G
g_t	gradient flow, with respect to some metric
G	Lie group
h_t	Hamiltonian flow
H	Hamiltonian function
H_N	restricted Hamiltonian $H|_N = H_N$
$I(q)$	moment of inertial tensor
I_d	identity matrix
$K(q)$	reduced metric
$\tilde{K}(q)$	pseudo metric
l	body angular momentum
L	angular momentum; Lagrangian function
$\mathcal{L}_X$	Lie derivative with respect to X
m	degrees of freedom
m_i	mass of ith particle, or reduced mass
M	state space
M_E	energy level
n	number of particles
N	transition manifold
N_E	transition state
(q, p)	Darboux coordinates
Q	configuration space
$Q_{\leq E}$	Hill's region

$\mathbb{R}^k$	Euclidean k-space
S	dividing manifold
S_E	dividing surface, $S_E^{\pm}$ subsets of S_E with unidirectional flux across them
$SO(3)$	special orthogonal group (of rotations)
$SE(3)$	special Euclidean group (of rigid motions)
$\mathbb{S}^k$	k-sphere
t	time
TM	tangent bundle of manifold M
TN^ω	tangent subbundle of TM symplecitcally orthogonal to TN
T^*Q	cotangent bundle of manifold Q
$\mathbb{T}^k$	k-torus
U	potential energy function
V	effective potential energy function
$W^{\pm}$	stable and unstable manifolds of an invariant set
X_H	Hamiltonian vector field
z	point in state space M; $\bar{z}$ equilibrium or critical point
ϵ_{ijk}	Levi-Civita symbols
ε	small parameter
ϕ_E	(ergode) flux form
$\phi_E(S_E)$	flux of ergode across S_E
Φ_E	flux (of ergode) density
$\Phi_E(S_E)$	geometric flux of ergode across S_E
λ	absolute value of angular momentum, Morse index of a critical point
θ	action form
Θ	generalised action form
Θ_E	generalised action form
ρ	distribution function
ν, η, ξ	tangent vectors
ω	symplectic form; $\omega_0 = \mathrm{d}q \wedge \mathrm{d}p$ canonical symplectic form
Ω	(Liouville) phase space volume
Ω_E	energy-surface volume, or ergode

Chapter 1

Introduction

Many physical problems can be reduced to considering the rate of transport of volume between different regions of the state space[*1] of a (low-dimensional) Hamiltonian system. Such problems arise, for example, when studying chemical reaction rates [Kec67], capture and escape processes in celestial mechanics [JR+02], particle escape from charged particle storage rings [PM08], and displacement of defects in solids [TJ+85]. The state space volume of interest in these problems is that occupied by a classical ensemble derived from a "kinetic approximation", i.e. a great number of different, independent realisations of the same Hamiltonian system. The study of the evolution of ensembles, as opposed to single trajectories, involves Liouville's equation, which is reviewed Section 1.1. Since energy is conserved by the systems, it is natural to consider the rate at which energy-surface volume, or *ergode*[*2], crosses between regions as a function of the energy. The rate of transport question is stated more formally in Section 1.2, where we also recall and compare a few of the methods available to study these problems.

Both Marcelin [Mar15, Chapter 2][*3] and later Wigner [Wig37] realised that a natural way to study the rate of transport is to place a *dividing surface*[*4] between the regions of interest and consider the flux of ergode through this surface. It must divide the whole energy level into two distinct regions, such that no trajectory can pass from one region to the other without crossing it. In this case the flux of ergode through the dividing surface in one direction gives an upper bound on the rate of transport in this direction. In order to obtain a useful upper bound, Wigner [Wig37] proposed varying the dividing surface to obtain one with (locally) minimal flux. This variational definition does not determine a unique dividing surface, because one can flow any dividing

---

*1 The state space of Hamiltonian systems is often referred to as *phase space*. We prefer the dynamical systems terminology, and reserve *phases* for the "macroscopic states" of statistical mechanics, e.g. the gas phase of the reactions considered in Chapter 3.

*2 *Ergode* is Boltzmann's name for a microcanonical ensemble, see [Bru76, pages 242,367]. We shall use it interchangeably with energy-surface volume.

*3 This is a posthumous article possibly compiled by Jean Baptiste Perrin, René Marcelin's Ph.D. supervisor, seeing as he died in 1914 in WWI. The work in this article was from (one of) his 1914 theses and also from previously published articles, as explained in the brief biography by Laidler [Lai85]. This makes 2014 the centenary of the dividing surface (or *surface critique* as Marcelin called it) approach to Hamiltonian transport.

*4 Note that 'surface' (or *hypersurface*) means an (embedded) submanifold of codimension-1.

surface along the vector field and obtain another, but the minimum flux is well defined. The dividing surface approach to transport is the topic of this thesis. It is introduced in Section 1.2, and surfaces of locally minimal flux are considered in Section 1.3. This aims to be a (fairly) complete review of the fragmented literature found partly in chemistry and partly in dynamical systems.

A lot of the initial and subsequent work was done with reaction rates in mind and led to (variational) transition state theory[*5] (nicely reviewed by Keck [Kec67] and put into context by Pollak and Talkner [PT05]). In chemical reactions, one finds the basic transport scenario, which we refer to as "flux over a saddle". Here, the two regions of interest represent reactants and products and have an index-1 critical point of the Hamiltonian function between them, hence the name. For small energies above that at the critical point, the energy level is diffeomorphic to a spherical cylinder and has a bottleneck about the critical point. The dividing surface is therefore placed in the bottleneck region, thus allowing for a local analysis. It can be decomposed into two parts with oppositely directed flows, each of which spans[*6] a normally hyperbolic[*7], closed[*8], codimension-2 submanifold, the *transition state*. The basic scenario is reviewed in Section 1.4.

The general picture was given by Wigner [Wig38], though this was not the first time it appeared in print. For two degree of freedom systems, the transition states are unstable periodic orbits. This was pointed out by Pechukas [Pec76] and then used by Pollak and Pechukas [PP78], and simultaneously by Sverdlik and Koeppl [SK78][*9], to find explicit dividing surfaces spanning the family of unstable periodic orbits for systems representing collinear bimolecular reactions. These very examples had actually already been considered by De Vogelaere and Boudart [DVB55], following Wigner's suggestion to introduce a *transmission coefficient*, defined as the ratio of the number of crossings through the dividing surface leading to reaction to the total number of crossings, for systems with complex potential energies using the approach of Lemaitre and co-workers for the "allowed cone of cosmic radiation" (see references in [Wig38, DVB55]). Thus, in pioneering work that pre-dated both Pechukas et al. and the work of De Leon and co-workers on "reactive cylinders" (see e.g. [dA+90]), De Vogelaere and Boudart considered periodic orbit transition states, their bifurcations, and their stable and unstable codimension-1 manifolds that divide reactive trajectories from unreactive ones. Their use of a dividing surface spanning the unstable periodic orbit is however only implicit, which might explain why their work is relatively unknown. One can actually trace unstable periodic orbits and their invariant manifolds all the way back to the early work of Langevin on the capture, or collision, of two bodies with a

---

*5 Also often referred to as activated complex theory, or RRKM theory for unimolecular reactions.

*6 We say that a manifold S spans N if the latter is its boundary, $N = \partial S$.

*7 An invariant submanifold whose linearised normal dynamics are hyperbolic and dominate those tangent to it, see Appendix A.1.

*8 We call a manifold N closed if it has no boundary $\partial N = \emptyset$. Unfortunately, this is not the only use of "boundary" and "closed" in topology, i.e. they are also used in the sense of subsets of topological spaces.

*9 This paper has an interesting discussion on the discovery of unstable periodic orbits as solutions to the variational problem. Koeppl supposedly found this independently and at the same time as Pechukas, but only wrote up his results as a progress report for the Alfred P. Sloan Foundation.

central field [Lan05, page 279]. Here, the unstable periodic orbit of the two degree of freedom system in the invariable plane is used to find the maximum impact parameter, as the problem is considered using scattering theory. This is again an example of the basic transport scenario, and the relation to the work of Pechukas and co-workers was commented upon at the time by Chesnavich and Bowers [CB82]. The generalisation of the basic scenario to arbitrary degrees of freedom was mentioned by Pechukas [Pec76], and then considered explicitly by Toller et al. [TJ⁺85], without however restricting to energy-levels. They instead appealed to the Boltzmann distribution to restrict their attention to low energy sub-level sets of the state space. The restriction to the energy-levels was then considered by MacKay [Mac90], though for more than 2 degrees of freedom it left too much to the imagination of the reader, as the construction was then rediscovered by Wiggins et al. [WW⁺01]. In parallel, the celestial mechanics literature had also been considering the basic transport scenario about the Lagrange (index-1 critical) points in the circular restricted three-body problem. The planar case has two degrees of freedom and one finds (Lyapunov) periodic orbits, see e.g. Szebehely's note on the very long history of these orbits [Sze67, Section 5.7]. Whereas, for the spatial case it was known that these are replaced by 3-spheres since the work of Conley and his students, see [Eas67, Con68, Sac69] and references therein. These works generally focused on the stable and unstable submanifolds and their role as transport barriers, as opposed to dividing surfaces. Actually, the transition states are the energy levels of the local centre manifold about the index-1 critical point of the Hamiltonian function, as we shall recall in Section 1.4, and the fact that for general degrees of freedom these are spheres was already known since at least 1965 [Kel65].

Recently, there has been a lot of interest in the chemistry literature in understanding what happens when the energy is increased in the basic scenario and the bottleneck opens up, which may lead to more general transport problems, see e.g. [BS11, Osb08]. This leads to interesting mathematical questions and is the focus of this thesis. These scenarios will not allow for a local analysis about some critical point any more, but will instead involve global dividing surfaces and transition states that may bifurcate leading to other scenarios. Section 2.2 gives a method to construct dividing surfaces about general transition states, which uses the normal hyperbolicity of the latter. This is a necessary step in order to consider the more general transport problems.

For two degree of freedom systems, the transition states are hyperbolic periodic orbits. The bifurcations of such objects are well known and can be found in the literature, e.g. Abraham and Marsden [AM78, Section 8.6], Meyer et al. [MHO09, Chapter 11] and Hanßmann [Han07, Chapter 3]. Thus, there have been various studies of the bifurcations of periodic orbit transition states in the transition state theory literature, see e.g. [DVB55, PP78, Dav87]. Periodic orbit transition states will be briefly considered in Subsection 2.3.1 in order to set the scene for higher dimensional ones. Here we will note that even when the periodic orbits are hyperbolic, there may still be topological obstructions that stop them from being transition states. This section raises a number of questions that will not be answered in this thesis, but instead will be the subject of a future publication.

For higher degrees of freedom, the transition states are normally hyperbolic submanifolds of higher dimensions, e.g. in the basic scenario we have a $(2m-3)$-sphere. The bifurcation of such submanifolds is not much explored or understood, even though there have been a few recent studies [LTK09, TTK11, AB12]. It has been considered a hard problem because bifurcation necessitates loss of normal hyperbolicity and for submanifolds of dimension 3 or greater there are many possible consequences. However, what has been overlooked and will be considered here, is that there is a large class of systems for which normal hyperbolicity is regained immediately: the transition state develops singularities at a critical energy, i.e. points at which the manifold structure fails, but regains smoothness and normal hyperbolicity with a change in diffeomorphism type[*10]. These are *Morse bifurcations*. One could say that they occur because the energy levels undergo a Morse bifurcation themselves so the dividing surfaces, and therefore the transition states, must also undergo a change of diffeomorphism class in order to still separate these in two.

Our approach is in the spirit of Smale's "topological program" for mechanical systems[*11] with symmetries [Sma70], in which he suggested studying the diffeomorphism classes of the reduced state space, and their bifurcations, in order to understand the dynamics. We apply this to transport problems and extend it to the diffeomorphism class of the transition states and dividing surfaces. This had not been done until our recent article [MS14].

For periodic orbits, Morse bifurcations can be thought of as a number of simultaneous homoclinic bifurcations. This is mentioned in Subsection 2.3.1. However, Morse theory, which is briefly reviewed in Appendix A.3, applies to manifolds of all dimensions, so there is no limitation to the number of degrees of freedom one can consider.

Some examples of Morse bifurcations will be considered in Section 2.4. The examples will initially have 2 degrees of freedom, such that the systems are as simple as possible and the Morse bifurcations stand out. The central role played by Morse bifurcations in transport problems is then seen in the application of our results to bimolecular reactions in Chapter 3. Here, we find interesting sequences of Morse bifurcations and therefore transition states and dividing surfaces, first in planar bimolecular reactions and then spatial reactions between non-collinear molecules.

1.1 Liouvillian dynamics

We are usually interested in transport in (low dimensional) Hamiltonian systems because we want to find the rate of change of some property of a physical process that can be thought of as a macroscopic observable of a microscopic system. That is, we are interested in a physical process that can be modelled as a very high dimensional

---

[*10] This possibility was pointed out by Robert MacKay in the course of a workshop in Bristol in 2009. Some examples have also been reported in Mauguière et al. [MC+13], a paper that appeared in preprint form at about the same time as ours, [MS14].

[*11] *Simple mechanical system* are Hamiltonian system whose state space is the cotangent bundle of a Riemannian manifold (*configuration space*) with canonical symplectic form ω_0, and the Hamiltonian is the sum of the positive definite *kinetic energy*, given by the metric, and a *potential energy*.

Hamiltonian system, of the order of Avogadro's constant when dealing with molecules, which however consists a large number of weakly interacting copies of a lower dimensional systems that "represents" the change of interest. Thus, assuming that the lower dimensional systems are independent of each other, a point in the high dimensional system can be replaced by an ensemble for this low dimensional Hamiltonian system[*12]. Then the rate of change question translates to one of the rate of transport of state space volume between regions of interest, which represent the different states.

In the literature, the choice of volume or ensemble for systems representing chemical reactions generally involves a statistical assumption. The reactant molecules are assumed to be in equilibrium with a Boltzmann distribution. Establishing the equilibrium can itself be thought of as an elementary reaction. In fact, the statistical assumption is equivalent to the dynamical assumption that the distribution of vibrational energy amongst the reactants occurs on time scales that are much smaller than those for reaction. This essentially requires the whole of the region representing the reactants to be accessible and the dynamics to be chaotic in this region, see e.g. [Dav85].

The statistical assumption was put in doubt from the very beginnings of transition state theory, see e.g. Wigner's comments in [Wig38]. In fact deviations from equilibrium are not uncommon. Davis studied the transport problem associated with the distribution of vibrational energy, which he referred to as intramolecular transition state or RRKM theory, from a dynamical systems perspective [Dav85], using the results of MacKay, Meiss and Percival [MMP84] and Bensimon and Kadanoff [BK84]. These articles considered transport in two dimensional area preserving maps and were the starting point of what is now generally referred to as lobe dynamics, see e.g. [Mei92].

Let us now consider the evolution of distributions representing ensembles for Hamiltonian systems, and introduce some notation.

We are given an m degree of freedom Hamiltonian systems, which we denoted $\left(M^{2m}, \omega, H\right)$. Here M is a $2m$-dimensional differentiable manifold, ω a symplectic form[*13] on it and H a smooth function from M to $\mathbb{R}$. We shall only consider autonomous systems.

The Hamiltonian vector field X_H is defined[*14] by

$$i_{X_H}\omega = \mathrm{d}H,$$

where the interior product i contracts a vector field X and a k-form α to give a $(k-1)$-form, by

$$i_X\alpha\left(\nu_1, \cdots, \nu_{k-1}\right) = \alpha\left(X, \nu_1, \cdots, \nu_{k-1}\right),$$

for any $(k-1)$ vectors ν_i.

[*12] Some physical processes, such as chemical reactions, have to be modelled as quantum mechanical systems. Then, provided the Born-Oppenheimer approximation holds, we obtain a classical Hamiltonian systems.

[*13] A closed ($\mathrm{d}\omega = 0$), non-degenerate ($\forall z \in M$ if $\exists \nu \in T_z M$ such that $\omega(\nu, \upsilon) = 0 \ \forall \upsilon \in T_z M$, then $\nu = 0$) 2-form.

[*14] There are actually (essentially) two conventions for Hamiltonian systems, as we can choose where to put the "inescapable minus" of Hamiltonian mechanics. The convention that we use is the one found in [AM78], which is not the same as the one in [Arn89].

The vector field generates a Hamiltonian flow h_t, which is given by

$$\dot{h}_t(z) = X_H(h_t(z)), \quad h_0(z) = z_0.$$

Alternatively, using Poisson brackets, defined as $\{F, G\} = \omega(X_F, X_G)$ for two functions F, G on M, we can write the equations of motion as

$$\dot{h}_t(z) - \{h_t, H\}(z) = 0, \quad h_0(z) = z_0.$$

This equation actually holds for any smooth function on M. The flow is symplectic, i.e. it preserves the symplectic form

$$h_t^* \omega = \omega.$$

This can be seen by checking that

$$\frac{\mathrm{d}}{\mathrm{d}t} h_t^* \omega = h_t^* \mathcal{L}_{X_H} \omega = h_t^*(i_{X_H} \mathrm{d}\omega + \mathrm{d}i_{X_H}\omega) = h_t^*(0 + \mathrm{d}H) = 0,$$

where we have used Cartan's formula, $\mathcal{L}_X \alpha = i_X \mathrm{d}\alpha + \mathrm{d}i_X \alpha$, and the properties of the Hamiltonian system. Thus $h_t^* \omega$ is constant in time, and since h_0 is the identity, we obtain $h_t^* \omega = \omega$, as desired [AM78, page 188].

We can define a state-space (or Liouville) volume as

$$\Omega = \frac{1}{m!} \omega^m,$$

which is also preserved by the flow, since

$$h_t^* \Omega = \frac{1}{m!} h_t^* \omega^m = \frac{1}{m!} h_t^* \omega \wedge \cdots \wedge h_t^* \omega = \Omega.$$

This is known as Liouville's theorem. In local Darboux coordinates $z = (q, p)$, $\omega = \sum_{j=1}^m \mathrm{d}q_j \wedge \mathrm{d}p_j$ and $\Omega = \mathrm{d}q_1 \wedge \mathrm{d}p_1 \wedge \cdots \wedge \mathrm{d}q_m \wedge \mathrm{d}p_m$.

We are not interested in single trajectories, but in the evolution of ensembles, i.e. sets of initial conditions $B^1 \subset M$ with non-zero volume, $\Omega(B^1) = \int_{B^1} \Omega \neq 0$. Define $B_t^1 = h_t(B^1)$, then

$$\Omega(B_t^1) = \int_{B_t^1} \Omega = \int_{B^1} h_t^* \Omega = \int_{B^1} \Omega = \Omega(B^1),$$

so

$$\frac{\mathrm{d}}{\mathrm{d}t} \Omega(B_t^1) = 0.$$

That is, the ensemble evolves as if it were an incompressible fluid. Given this analogy, the above equation presents the Lagrangian perspective of the flow of state-space volume, which focuses on the trajectories.

we can consider the Eulerian perspective, i.e. focus on a specific location of state space, say the region $B \subset M$, and consider the flow through this region. W

Alternatively, we can introduce a distribution function representing the initial B^1-

ensemble, e.g. $\rho^1(z, 0) = \chi_{B^1}(z)$ where χ_{B^1} is the characteristic function of B^1

$$\chi_{B^1}(z) = \begin{cases} 1 \text{ if } z \in B^1, \\ 0 \text{ otherwise.} \end{cases}$$

Later, we shall normalise this to a probability distribution, for which $\int_M \rho_0^1 \Omega = 1$. Then, the distribution $\rho^1(z, t)$ at time t of a state $z \in M$ originally in B^1 at time 0 is uniquely determined by following the trajectory through z back to $z_0 \in B^1$, so

$$\rho^1(z, t) = \rho^1(z_0, 0),$$

where $z = h_t(z_0)$. Differentiating with respect to time gives

$$\frac{\mathrm{d}}{\mathrm{d}t} \rho^1(z, t) = 0,$$

and we obtain

$$(\partial_t \rho^1 + \{\rho^1, H\})(z, t) = 0.$$

This is known as *Liouville's equation*. The study of the evolution of ensembles is in fact often referred to as *Liouvillian dynamics* [Gas05, MS$^+$81] and is the starting point of statistical mechanics, cf. the equations and derivations in [Pet07, Section 2.1] or [Bal97, Section 3.2]. Most derivations make use of a Riemannian metric. Also, in the literature we often find the equation written as

$$(\partial_t \rho + \mathrm{div}(\rho X_H))(z, t) = 0,$$

since $\mathrm{d}\rho \wedge i_{X_H}\Omega = \mathcal{L}_{\rho X_H}\Omega$, and for a vector field X and a volume Ω, $\mathrm{div}(X)$ is the scalar defined by $\mathrm{div}(X)\Omega := \mathcal{L}_X\Omega$, see e.g. [Fra04, Section 4.2c]. Liouville's equation is a linear partial differential equation for the distribution function. Also, it has the opposite sign to the one appearing in the equations of motion, in the Poisson formalism.

Actually, the product assumption used to obtain the low dimensional Hamiltonian systems is only a first order kinetic approximation, since the high dimensional system will usually not be an exact product, due to interactions. When considering interacting particles in gas phase, for example, this product approximation is valid for sufficiently dilute gases, i.e. gases for which the effective range of interaction is much smaller than the inter-particle spacing, or equivalently the range of interaction is much smaller than the mean free path [Kec67]. In order to find higher order kinetic equations for the evolution of distribution functions for the low dimensional system, one usually starts with a distribution for the high dimensional system, due to the uncertainty in the microscopic initial conditions, and then uses either a BBGKY[*15] hierarchy, or some other perturbative approach to obtain a kinetic equation for the evolution of the ensembles, see e.g. [Bal97, Dor99].

Apart from Hamiltonian transport problems obtained from macroscopic rate of

---

*15 Born, Bogoliubov, Green, Kirkwood, and Yvon.

change questions, as above, others appear when we want to obtain a "statistical under-standing" of a (low) dimensional Hamiltonian system, that is chaotic say [Gas05]. For example, we may be interested in asteroids reaching Earth (or generally the planetary realm) in a reduced three-body system, see Figure 1.2, and want to study the rate of transport of some representative ensemble as opposed to single trajectories, due to uncertainties in the initial conditions.

1.2   Rates of transport

The transport question that we are interested in can be stated as follows. Given two subsets B^1, B^2 of state-space M, what is the fraction of ensemble originally in B^1 (at time 0) that is in B^2 after some time t. The ensemble is given by a probability distribution ρ^1 that is initially in B^1, i.e. $\rho^1(z, 0) = \chi_{B^1}(z)/\Omega(B^1)$, where χ_{B^1} is the characteristic function of B^1 and ρ^1 has been normalised so $\int_M \rho^1 \Omega = 1$. The ensemble evolves under the Hamiltonian flow and is represented by $\rho^1(z, t)$. We want to compute

$$\int_{B^2} \rho^1 \Omega,$$

or equivalently

$$\Omega(B_t^1 \cap B^2).$$

Actually, we want to find their rate of change.

Usually, the subsets B^i will be clear from the application. Generally, we shall assume that B^i are $2m$-dimensional, connected, disjoint subsets of M. Thus avoiding trivial transport questions, for which $\Omega(B_0^1 \cap B^2) \neq 0$. Also, we are implicitly assuming that M is connected, or if not that B^1 and B^2 are in the same component, otherwise the transport is clearly null. The compactness of the subsets depends on both M and H, for example, M might not be compact, as is often the case for simple mechanical systems, e.g. those with configuration space $\mathbb{R}^m$, and H might not be proper, or bounded from below.

Often, when the Hamiltonian system models some physical process and is therefore a simple mechanical system, the subsets of interest are naturally defined using the potential energy, or an effective potential. For example, chemical systems usually have a molecular (Born-Oppenheimer) potential U that is bounded from below, and *chemical species* (i.e. stable nuclear configuration) are associated with a given "basin" of the potential [Mez87, Section V.2]. That is, *catchment regions*[*16] C_i are defined for each critical point $\bar{z}_i$ of U. These are the basin of attraction of the critical point under the gradient flow g_t with respect to the Riemannian metric of configuration space

$$C_i = \{z \in Q | \lim_{t \to \infty} g_t(z) = \bar{z}_i\}.$$

[*16] Basins of minima, or *immits* (cf. summit) as Cayley called them, of a potential function show strong analogies with geographical catchment regions, i.e. geographical areas from where rainwater drains into a lake. The origins of the mathematical concept of a catchment region may be found in the early Morse theoretic works on topography of Cayley [Cay59] and Maxwell [Max70], who called them *dales*, or simply *basins*.
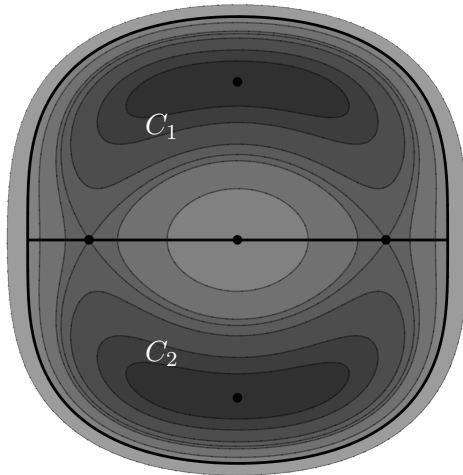
Figure 1.1: Contours over configuration space for a double-well potential energy with two index-1 critical points. Catchment regions of the two minima, restricted to energies below some given value, enclosed by thick black lines.

Catchment regions are defined for any index critical point and the dimension depends on the index, namely catchment regions of minima have dimension m, those of index-1 critical points have dimension $m-1$, etc. Catchment regions for a double well potential with two index-1 critical points, as found in narcisistic isomerisation reactions and which we shall study in Section 2.4.2, are depicted in Figure 1.1. We are only interested here in catchment regions of minima of the potential, which are then used to define the subsets in state-space for the transport problem. Thus, both configuration Q and state space M can be partitioned and B_1 and B_2 are elements of this partition. Our transport problem can then be seen as one element of a larger question, namely given such a partition what is the rate of transport of state space volume between regions. There may also be situations in which we are interested in transport from a number of regions (or one disconnected region) into another, but transport between multiple regions is probably best always divided into multiple transport problems.

Note, that the Hamiltonian or potential need not be bounded from below, as is the case for example with the effective potential of the planar circular restricted three-body problem, see e.g. [MHO09, Sections 2.3, 6.3.2]. Here, we may be interested in transport between regions in the neighbourhood of the principal masses, usually referred to as the interior realm (about the sun) and the planetary realm, or the one that is far from either, the exterior realm, see Figure 1.2. These transport problems arise when studying the capture of asteroids, or the transport of rockets for space missions [Con68, JR+02].

For general mechanical systems, the relation between the geometry of state space, the Hamiltonian function, and so the dynamics and the regions of interest can be much more complicated. Some of the literature makes simplifying assumptions such as having a compact state space that is then partitioned into compact regions of interest, which are connected subsets whose boundaries consist of parts of the boundary of M and of codimension-1 invariant manifolds, see e.g. [DJ+05].

Computing rates of transport is a non-trivial task, even numerically, which requires
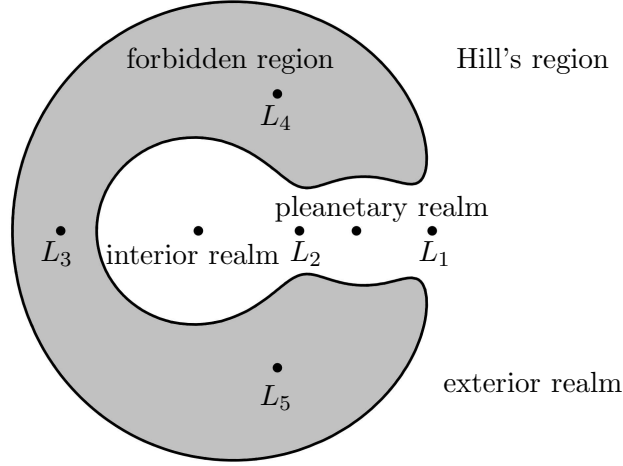
Figure 1.2: Configuration space Q for the planar restricted three-body problem with Hill's region $Q_{\leq E}$ and the forbidden region $Q_{\geq E}$ (shaded) separated by a zero-velocity curve, for some value of E above the critical energy at L_1 and below that at L_3, where L_i are the Euler-Lagrange points. The regions of interest are usually the exterior realm, the planetary realm and the interior realm, about the sun.

solving the Hamiltonian equations with the whole of B^1 as initial conditions.

Recently, Mosovksy, Speetjens and Meiss pointed out that for volume preserving, and therefore Hamiltonian, systems one only has to consider the evolution of codimension-2 subsets [MSM13]. The first dimensional reduction is obtained by noting that $\Omega = -\mathrm{d}\Theta$ where $\Theta = \frac{1}{m!}\theta \wedge \omega^{m-1}$ is a *"generalised" action form* with θ the *action form*, used to write $\omega = -\mathrm{d}\theta$, modulo global topological obstructions. In local Darboux coordinates one usually takes $\theta = \sum_{k=1}^{m} p_k \mathrm{d}q_k$. Thus, using Stoke's theorem,

$$\Omega(B_t^1 \cap B^2) = -\int_{\partial(B_t^1 \cap B^2)} \Theta = -\int_{b_t^1} \Theta - \int_{b_t^2} \Theta,$$

where we have divided $\partial(B_t^1 \cap B^2) = b_t^1 \cup b_t^2$ into components from B_t^1 and B^2, namely b_t^2 is a segment of ∂B^2 which is known, whereas b_t^1 is a segment of ∂B_t^1. Next, in order to simplify the integral over b_t^1, we write

$$\int_{b_t^1} \Theta = \int_{b_0^1} h_t^* \Theta = \int_{b_0^1} \Theta + \int_{b_0^1} (h_t^* \Theta - \Theta),$$

and

$$\int_{b_0^1} (h_t^* \Theta - \Theta) = \int_0^t \frac{\mathrm{d}}{\mathrm{d}t} \int_{b_0^1} (h_t^* \Theta - \Theta) \mathrm{d}s = \int_0^t \int_{b_t^1} \mathcal{L}_{X_H} \Theta \mathrm{d}s.$$

Then, for regular values of H,

$$\mathcal{L}_{X_H} \Theta = \mathrm{d}i_{X_H} \Theta - i_{X_H} \Omega = \mathrm{d}i_{X_H} \Theta - \mathrm{d}H \wedge i_{X_H} \Omega_E = \mathrm{d}(i_{X_H} \Theta - H \wedge \phi_E) =: \mathrm{d}\Lambda,$$

where we have used Cartan's formula and that $\phi_E := i_{X_H} \Omega_E$ (which we shall identify later as a flux form) is closed, since $\phi_E = \omega^{m-1}/(m-1)!$ [TJ$^+$85]. Mosovsky et al. call Λ the *"generalised" (state-space) Lagrangian form* because for 1 degree of freedom,
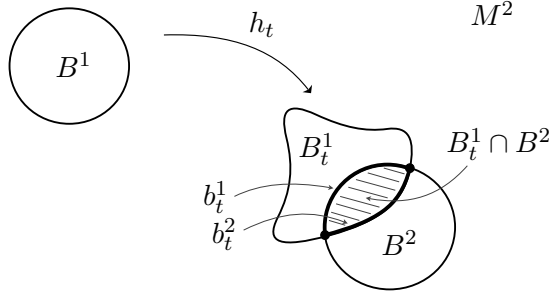
10

Figure 1.3: Depiction of an example transport scenario for a 1 degree of freedom system. We are interested in the rate of transport of state space volume from region B^1 to $B^2 \subset M$. The boundary of $B_t^1 \cap B^2$ is split into the curves b_t^1 and b_t^2, which meet at the points $\partial b_t^1 = \partial b_t^2$. Cf. [MSM13].

$\Omega = \omega$, $\omega = -\mathrm{d}\theta$ and in canonical coordinates $\mathcal{L}_{X_H}\theta = \mathrm{d}(i_{X_H}\theta - H) = \mathrm{d}(p\dot{q} - H) := \lambda$. Finally

$$\Omega(B_t^1 \cap B^2) = -\int_{b_t^2} \Theta - \int_{b_0^1} \Theta - \int_0^t \int_{\partial b_t^1} \Lambda \mathrm{d}s.$$

Thus, in order to compute the transported volume, we require the trajectories of sets that are two dimensions smaller than the whole region B^1 [MSM13]. An example of transport in a 1 degree of freedom system is depicted in Figure 1.3.

We instead return to the transport problem and notice that another simplification is available for Hamiltonian system. Since H is conserved by the flow, we can restrict our attention to the energy levels $M_E = H^{-1}(E)$ and consider the microcanonical transport problem parametrised by energy.

For regular M_E (i.e. $\mathrm{d}H$ is nowhere zero on M_E; $E \in \mathbb{R}$ is said to be a regular value of H), we can define energy-surface volume or *ergode*, Ω_E, a $(2m-1)$-form given by the relation

$$\mathrm{d}H \wedge \Omega_E = \Omega.$$

This is preserved by the Hamiltonian flow, and the transport problem becomes that of finding

$$\Omega_E(h_t(B_E^1) \cap B_E^2).$$

This will generally be simpler than the general transport problem in state space because M_E is dimension $2m-1$ and might be simpler to consider than the whole of M, e.g. when H is proper and bounded from below and M_E is closed. The regions B_E^i might also be simpler.

As the energy is varied, the diffeomorphism class of M_E may change, as we shall see in Section 2.4, leading to qualitatively different microcanonical transport problems. As for the full transport problem, the regions of interest are often defined in configuration space for mechanical systems. These are the subsets of *Hill's region* $Q_{\leq E} = U^{-1}((-\infty, E])$, where U is the potential energy function, as for the planar circular restricted three-body problem depicted in Figure 1.2.

Similarly, if the system has other symmetries and therefore conserved momenta,

these too can be reduced in order to obtain a yet lower dimensional transport problem. This shall be done for the bimolecular reactions of Chapter 3.

Actually, even when considering transport in state-space, it is generally better to restrict one's attention to sub-level sets $M_{\leq E}$. This is done by Toller et al. and justified by appealing to the properties of the Boltzmann distribution, for which higher energy-levels are less densely populated [TJ$^+$85].

Various approaches were introduced over the years to study transport problems. Classically, capture or scattering transport problems, in which two bodies approach each other and interact, were considered using scattering theory. An introduction can be found in most classical mechanics text books, e.g. [GPS02, Section 3.10]. The rate is then found by determining the reactive cross section. For two rotationally symmetric bodies, or equivalently for two distant bodies whose joint potential is very weakly dependent on the attitudes, the transport problem is simplified by considering a central field between the two bodies. This is known as the Langevin's central field capture model after Langevin very early contribution [Lan05], see e.g. review by Chesnavich and Bowers [CB82]. These examples are usually partially reduced to the invariable plane, perpendicular to the angular momentum. Here one finds an unstable periodic orbit whose codimension-1 stable and unstable manifolds act as transport barriers separating capture from non-capture trajectories. This will be clearer after Section 1.4, where we shall review the basic scenario. The codimension-1 invariant submanifolds of the unstable periodic orbits, or in higher degrees of freedom the stable and unstable submanifolds of more general codimension-2 normally hyperbolic submanifolds, act as barriers to transport. The idea of focusing on these has been proposed a number of times, see e.g. [DVB55, Dav87, dA+90, DJ$^+$05] and led to "reactive cylinder theory" in the chemistry literature and "tube dynamics" in the celestial mechanics literature.

A simpler approach, and the topic of this thesis, is the dividing surface method. Imagine a dividing surface S_E somewhere between B_E^1 and B_E^2, which is crossed by all trajectories from the former region to the latter. The positive flux of ergode through this surface gives an upper bound on the rate of transport, which can be written as the flux of B_E^1-ensemble through the boundary of B_E^2 (cf. the derivation of Liouville's equation). The flux of ergode through a codimension-1, oriented submanifold S_E of an energy level is the integral

$$\phi_E\left(S_E\right) = \int_{S_E} \phi_E,$$

where ϕ_E is the (ergode) *flux form*

$$\phi_E = i_{X_H}\Omega_E.$$

Thus, we replace integration over ∂B_E^2 of the distribution, which requires knowing its evolution, with the integral of an equilibrium distribution over an arbitrary dividing surface S_E^+. The rate may be over estimated due to the different domain, namely S_E^+ and possible recrossings of trajectories through it, as well as for systems out of equilibrium because we are replacing the integrand $\rho_E^1(z,t)\phi_E$ with ϕ_E.

Remark 1.2.1. We have chosen to use differential forms, but the equation is the same as the usual flux equation $\phi_E(S_E) = \int_{S_E} (X_H \cdot n) \operatorname{vol}_{S_E}$, where n is the unit normal to the surface (with respect to a Riemannian structure) and vol_{S_E} an infinitesimal volume element, cf. Keck [Kec67]. This is seen by rewriting the flux form as $\phi_E = i_{X_H}\Omega_E = (X_H \cdot n) \, i_n\Omega_E$ and defining $\operatorname{vol}_{S_E} := i_n\Omega_E$. See Frankel [Fra04, Section 2.9b] for more details. Use of a Riemannian structure however is an artificial crutch.

In order to obtain a useful bound on the transport, we vary the arbitrary dividing surface and replace it with a dividing surface with (close to) locally minimal flux in the chosen direction. Ideally, we would like to find a dividing surface that is crossed once and only once by each trajectory crossing from B_E^1 to B_E^2, which would have minimal flux through it and would give the actual rate of transport. Hence, we have a variational definition of the (ideal) dividing surface. However, this condition does not necessarily define a unique dividing surface because one can flow any dividing surface along the vector field and obtain another. Furthermore the minimal dividing surfaces might be hard to find in practice.

There is also a flow in the opposite direction, from B_E^2 to B_E^1, for which we could choose to consider the previous dividing surface, extended to cut all trajectories from B_E^2 to B_E^1. In order to divide the energy-level and therefore separate the two regions, we expect the surface to be closed (i.e. without boundary), otherwise trajectories could avoid it but still cross between regions. Thus, the net flux through the dividing surface will be zero, and the flux in the two separate directions equal.

Evaluating the flux integral can be simplified by noting that for regular energy levels M_E, the flux form reduces to $\phi_E = \omega^{m-1}/(m-1)!$ [TJ$^+$85], which allows us to write

$$\phi_E = -\mathrm{d}\Theta_E,$$

with the *"generalised" action form* $\Theta_E = \frac{1}{(m-1)!}\theta \wedge \omega^{m-2}$. Then, we can use Stokes' theorem to obtain

$$\phi_E(S_E) = \int_{S_E} \phi_E = -\int_{\partial S_E} \Theta_E.$$

We state this as

Theorem 1.2.2 ([Mac90])**.** *The flux of ergode through an oriented codimension-1 submanifold of an energy-level is minus the generalised action integral over its boundary.*

In general the flux form ϕ_E evaluated on the tangent space to an oriented surface is not single-signed. The flow may cross in the positive direction in some parts of S_E and the other way on other parts. Where we want to emphasise this we refer to the flux integral as "net flux".

Another theory that can be used to find bounds on the rate of transport is ergodic theory. However, it considers transport in the limit as $t \to \infty$. Smooth ergodic theory for Hamiltonian systems is briefly reviewed in [Mac94a], which focuses on its use in transport problems, and compares it with the dividing surface approach.

1.3 (Dividing) Surfaces of locally minimal flux

We will now consider which surfaces have locally minimal flux, in either direction, and the properties of such surfaces. We follow the approach of MacKay [Mac94b], which lends itself well to the general scenarios that we want to consider.

Invariant surfaces have zero flux in both directions. This is clearly a minimum value, so these surfaces are useful for transport problems because they locally separate different regions. We are interested however in surfaces that have locally minimal but not necessarily zero flux in each direction.

For a general closed, oriented surface S_E, one can decompose it into the union $S_E^+ \cup S_E^-$ of the parts of positive and negative flux[*17], with common boundary. Then we can apply the following consequence of the variational principle for odd dimensional invariant submanifolds of an energy level, in this case the boundaries of $S_E^{\pm}$.

Corollary 1.3.1 ([Mac91]). *A codimension-1 submanifold S_E^i of an energy level M_E has stationary (net) flux of ergode with respect to variations within M_E, including of its boundary ∂S_E^i, if and only if ∂S_E^i is invariant under the Hamiltonian flow.*

The proof can be found in [Mac91], which can be supplemented with the details on differentiation of integrals given e.g. in [Fra04, Section 4.3].

These stationary values of the flux are however not minima, since there exist deformations that both increase and decrease the flux. A nice way of seeing this is to consider deforming ∂S_E^i to a helix of small pitch around a part of ∂S_E^i with $X_H \neq 0$. Remembering that X_H must be tangent to ∂S_E^i for stationary values, we find that the flux increases if the pitch has one sign and decreases if it has the other [Mac94b].

We therefore consider (unsigned) *geometric flux* of ergode though S_E, denoted $\Phi_E(S_E)$. For this, we define the (ergode) *flux density* $|\phi_E|$ by

$$|\phi_E|(\nu_1, ..., \nu_{2m-2}) = |\phi_E(\nu_1, ..., \nu_{2m-2})|, \quad \forall \nu_i \in T_z M_E,$$

and integrate it over S_E. For a brief introduction to densities and density bundles see e.g. Lee [Lee03, Chapter 14].

For an arbitrary dividing surface, $\Phi_E(S_E) \geq |\phi_E(S_E)|$, with equality if and only if the flux is unidirectional through the surface. By unidirectional, we mean single-signed, as this occurs when the Hamiltonian vector field X_H is unidirectional across S_E. To see this, write $\Omega_E = dG \wedge \Omega_E^S$, where $G(z) = 0$ is the regular equation defining S_E, then

$$\phi_E = i_{X_H} \Omega_E = i_{X_H} dG \wedge \Omega_E^S + dG \wedge i_{X_H} \Omega_E^S,$$

but $dG(\nu_i) = 0$ for all ν_i tangent to S_E so $i_{X_H} dG$ gives the sign. Thus, decomposing our closed dividing surface as $S_E = S_E^+ \cup S_E^-$, where $S_E^{\pm}$ are not necessarily connected, gives

$$\Phi_E(S_E) = \phi_E(S_E^+) - \phi_E(S_E^-) = 2\phi_E(S_E^+) = -2\phi_E(S_E^-),$$

[*17] By "positive" we mean "non-negative", and by "negative" we mean "non-positive" but the terminology is too cumbersome.
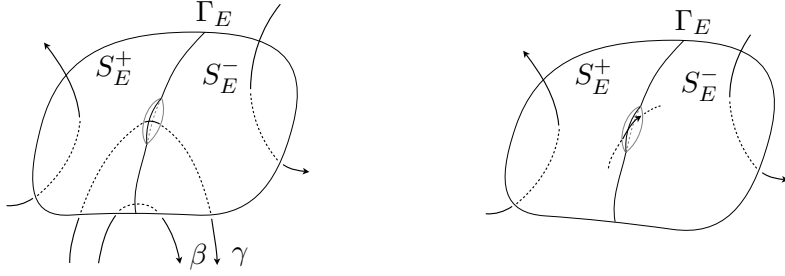
Figure 1.4: Proof of Theorem 1.3.2. Left: $\Phi\left(S_E\right)$ can be decreased if Γ_E is not invariant under X_H, shown here by trajectories β and γ touching and crossing S_E, generated by a vector field X_H not tangent to Γ_E, together with a deformation about Γ_E along γ that decreases $\Phi\left(S_E\right)$. Right: $\Phi\left(S_E\right)$ can be decreased if a nearby orbit intersects S_E twice in opposite directions.

since the flux is equal and opposite through S_E^+ and S_E^-. Asking for minimal flux in either direction is therefore the same as asking for minimal geometric flux. Furthermore, closed surfaces either have both stationary net and geometric flux or neither.

The idea is therefore to consider dividing surfaces S_E that are the union of two, not necessarily connected, surfaces $S_E^\pm$ of unidirectional flux that span a closed, invariant, codimension-2 orientable submanifold N_E in the energy level, M_E. Then $S_E^\pm$ have stationary flux, by Corollary 1.3.1, and the geometric flux is

$$\Phi_E\left(S_E\right) = -2\phi_E\left(S_E^-\right) = -2\int_{S_E^-} \phi_E = 2\int_{N_E} \Theta_E,$$

where we have chosen the orientation of N_E so that it is ∂S_E^-. To show that this situation leads to locally minimal geometric flux, we first need the following

Definition. An oriented surface S has *local recrossings* if for all $\varepsilon > 0$ there exists an orbit segment $z(t)$, $t_0 \le t \le t_1$, that intersects S in opposite directions at times t_0 and t_1, and for which

$$0 < d(z(t), S) < \varepsilon \quad \text{for all} \quad t \in (t_0, t_1),$$

where d denotes distance.

Then, we are ready for

Theorem 1.3.2 ([Mac94b]). *A codimension-1 orientable submanifold S_E of an energy-level has locally minimal geometric flux if and only if it can be decomposed into surfaces S_E^i of unidirectional stationary flux and S_E has no local recrossings.*

The proof can be found together with the theorem in [Mac94b], we re-propose it here for the Hamiltonian case.

Proof. Without loss of generality, we represent S_E as the zero-set of some smooth function $G : M_E \to \mathbb{R}$ with $dG \ne 0$ on S_E, so $S_E = \{z \in M_E | G(z) = 0\}$. To divide S_E into unidirectional parts $S_E = \cup_i S_E^i$, we consider

$$\Gamma_E = \{z \in S_E | dG(X_H) = 0\},$$

15

which gives $S_E \backslash \Gamma_E$ composed of parts $\hat{S}_E^i$. These are enlarged to S_E^i including the invariant parts such that their union is the whole of S_E.

Assume that S_E has locally minimal geometric flux. Then S_E has stationary flux, so its boundary ∂S_E is invariant under the Hamiltonian flow, by Corollary 1.3.1, i.e. X_H is tangent to ∂S_E. Now, the vector field X_H is tangent to $\partial S_E^i \backslash \partial S_E$, otherwise we could deform S_E and decrease $\Phi_E(S_E)$, as seen in Figure 1.4, contradicting our assumption that the geometric flux is minimal. Therefore X_H is everywhere tangent to ∂S_E^i, meaning that they are invariant and that S_E^i have stationary flux, again by Corollary 1.3.1. Finally, if S_E^i has local recrossings, which must be near Γ_E since the sign of the flux changes, we can decrease $\Phi_E(S_E)$ by lifting S_E locally, again contradicting the assumption, see Figure 1.4.

Conversely, assume that S_E is the union of surfaces S_E^i of unidirectional, stationary flux. Then the flux through S_E is the sum of those through S_E^i and so stationary. Thus, the geometric flux is also stationary, but we want (locally) minimal geometric flux. The only places where a small deformation would make a difference to $\Phi_E(S_E)$ are near Γ_E. However, if there are no local recrossings, lifting S_E near Γ_E cannot decrease $\Phi_E(S_E)$. This can be shown by contradiction: if $\Phi_E(S_E)$ can be decreased by a small change, then there are points on S_E whose orbit sneaks back to S_E. $\qquad\square$

1.4 Basic transport scenario: flux over a saddle

This is the case of an autonomous Hamiltonian system $\left(M^{2m}, \omega, H\right)$ with a non-degenerate index-1 critical point $\bar{z}_1$ of H. It provides an example of a closed, invariant, codimension-2 submanifold of the energy levels spanned by two codimension-1 submanifolds of unidirectional flux with no local recrossings.

About $\bar{z}_1$, we have the Williamson normal form [Wil36]

$$H(z) = E_1 + \frac{a}{2}\left(y^2 - x^2\right) + \sum_{j=1}^{m-1} \frac{b_j}{2}\left(v_j^2 + u_j^2\right) + H_n(z), \quad H_n(z) = \mathcal{O}(3),$$

where we ask that a, $b_j > 0$, and $z = (q, p) = (u, x, v, y)$ are canonical coordinates with (x, y) the hyperbolic degree of freedom and $(u, v) = (u_1, ..., u_{m-1}, v_1, ..., v_{m-1})$ the elliptic ones [Arn89, Appendix 6]. In the chemistry literature these are called the reaction and bath coordinates, respectively. Note that we do not need the higher-order normal forms found in some of the transition state theory literature, see e.g. [WW$^+$01, UJ$^+$02].

We now consider the topology of the energy levels about $\bar{z}_1$. First we consider them to second order, where they are given by

$$M_E = H_2^{-1}(E) = \left\{ z \in M \,\middle|\, \frac{a}{2}\left(y^2 - x^2\right) + \sum_{j=1}^{m-1} \frac{b_j}{2}\left(v_j^2 + u_j^2\right) = \Delta E \right\},$$

with $\Delta E = E - E_1$. Therefore, in a neighbourhood of $\bar{z}_1$, we can write the energy level

as the union of the graphs of two functions

$$x_\pm = \pm \sqrt{\frac{2}{a}\left(\frac{a}{2}y^2 + \sum_{j=1}^{m-1}\frac{b_j}{2}\left(v_j^2 + u_j^2\right) - \Delta E\right)},$$

over $\mathbb{R}^{2m-1}$. For $\Delta E < 0$, M_E is diffeomorphic to two copies of $\mathbb{R}^{2m-1}$, whereas for $\Delta E > 0$, the two disjoint regions connect and M_E is diffeomorphic to $\mathbb{S}^{2m-2} \times \mathbb{R}$. This is a standard Morse surgery, see Theorem A.3.4 in Appendix A.3. An important feature of the energy levels is the presence of a "bottleneck" about $\bar{z}_1$, which opens up as the energy is increased from $\Delta E = 0$. The two regions on either side of the critical point are the ones between which we want to study transport. For the topology of the energy-levels of the full system, we appeal to the Morse lemma, see Appendix A.3. This tells us that there are coordinates about the critical point, $\bar{z}_1$, for which the Hamiltonian function is quadratic. Thus, the previous study of the quadratic case is sufficient. However, the transformation giving the Morse lemma coordinates is not necessarily symplectic. Therefore, whilst these coordinates can be used to study the diffeomorphism class of M_E, they cannot be used to study the dynamics without losing the simple expression of the Hamiltonian nature of the system.

Remark 1.4.1. Note that considering a system with a saddle×centre×$\cdots$×centre equilibrium, as is often stated, is not actually the same as considering an index-1 critical point of the Hamiltonian function for general Hamiltonian systems. We could have for example one unstable dimension and an arbitrary odd index, e.g. three with $b_1 < 0$ in the Williamson normal form. Then M_E does not separate for $\Delta E < 0$, i.e. the topology is different. However, for simple mechanical systems with positive-definite quadratic kinetic energy, these cases cannot arise which is why the two situations are often confused.

We now find an invariant codimension-2 submanifold of the energy levels. The centre subspace $\hat{N} = \{z \in M | x = y = 0\}$ of the linearised dynamics about $\bar{z}_1$ extends to a centre manifold N, which can locally be expressed in the form

$$N = \{z \in M | x = X\left(u, v\right), y = Y\left(u, v\right)\},$$

with the 1-jets of X and Y vanishing at $\bar{z}_1$. Then $N_E = N \cap M_E$ is an invariant submanifold of the energy level. N_E is diffeomorphic to $\mathbb{S}^{2m-3}$. This is proved by using the Morse lemma as was done for the energy levels. The restriction of the Hamiltonian function to N is

$$H_N\left(u, v\right) = E_1 + \frac{a}{2}\left(Y^2 - X^2\right)\left(u, v\right) + \sum_{j=1}^{m-1}\frac{b_j}{2}\left(v_j^2 + u_j^2\right) + H_n\left(X\left(u, v\right), u, Y\left(u, v\right), v\right)$$

$$= E_1 + \sum_{j=1}^{m-1}\frac{b_j}{2}\left(v_j^2 + u_j^2\right) + \mathcal{O}\left(3\right).$$

Thus the origin, $\tilde{z}_1$, is a critical point of H_N with index-0. Then by the Morse lemma,

in a neighbourhood of $\tilde{z}_1$, we have $H_N(\tilde{z}) = E_1 + \frac{1}{2}\left(y_1^2 + \cdots + y_{2m-2}^2\right)$, so $N_E = H_N^{-1}(E) \cong \mathbb{S}^{2m-3}$. Finally, by Theorem A.3.3, the diffeomorphism type is valid until the next critical value of H_N (if one exists), and not just for small ΔE, a proof of which can be found in Sacker [Sac69], and was already known to Conley and his students, see [Eas67, Con68, Sac69] and references therein.

Thus, we have found our closed, invariant codimension-2 submanifold N_E of M_E and now want to show that it can be spanned by two surfaces $S_E^\pm$ of unidirectional flux with no local recrossings. In a neighbourhood of $\bar{z}_1$, we can simply choose

$$S = \{z \in M | G(z) = x - X(u,v) = 0\},$$

which spans N, and intersect it with M_E to obtain S_E, as done by Toller et al. [TJ$^+$85]. We can decompose it into the parts $S^\pm$ with $y > Y(u,v)$ and $y < Y(u,v)$ and show that the flux is unidirectional across $S^\pm$ by checking that $dG(X_H) \geq 0$ for $y > Y(u,v)$ and vice-versa. This will ensure that the halves of the dividing surface $S_E^\pm$ are unidirectional, since the energy levels are invariant. Firstly, we rewrite

$$dG(X_H) = \{G, H\} = \dot{G}(z),$$

then we find that

$$\begin{aligned}
\dot{G}(z) &= \dot{x} - DX(u,v) \cdot (\dot{u}, \dot{v})^\circ \\
&= ay + \partial_y H_n(X(u,v), u, y, v) - DX(u,v) \cdot (\dot{u}, \dot{v})^\circ,
\end{aligned}$$

where the $^\circ$ denotes that the term is evaluated on S. Now, the invariance of N, on which $x = X(u,v)$, $y = Y(u,v)$, gives us that

$$aY(u,v) + \partial_y H_n(X(u,v), u, Y(u,v), v) - DX(u,v) \cdot (\dot{u}, \dot{v})^* = 0,$$

where the * denotes that the term is evaluated on N. Subtracting the (first) invariance equation from the flux equation gives

$$\begin{aligned}
\dot{G}(z) &= a(y - Y) + \partial_y H_n(X, u, y, v) - \partial_y H_n(X, u, Y, v) - DX \cdot ((\dot{u}, \dot{v})^\circ - (\dot{u}, \dot{v})^*) \\
&= a(y - Y) + (\partial_y H_n(X, u, y, v) - \partial_y H_n(X, u, Y, v)) \\
&\quad - DX \cdot (\partial_v H_n(X, u, y, v) - \partial_v H_n(X, u, Y, v), -\partial_u H_n(X, u, y, v) + \partial_u H_n(X, u, Y, v)),
\end{aligned}$$

where $X = X(u,v)$, $Y = Y(u,v)$. In a small neighbourhood of the critical point $\bar{z}_1$, the first term dominates the others and gives the sign, since H_n denotes the higher order terms in the Hamiltonian function. Specifically, for the second term we find

$$\partial_y H_n(X, u, y, v) - \partial_y H_n(X, u, Y, v) = \int_Y^y \partial_{yy}^2 H_n(X, u, \tilde{y}, v)d\tilde{y} = \mathcal{O}\left((y - Y)\max(|y|, |Y|)\right),$$

as $\partial_{yy}^2 H(X, u, \tilde{y}, v) = \mathcal{O}(\tilde{y})$. Similarly for the last terms, which also include a $DX(u,v)$ factor. This construction is local about $\bar{z}_1$. A neater construction, semi-local about N,
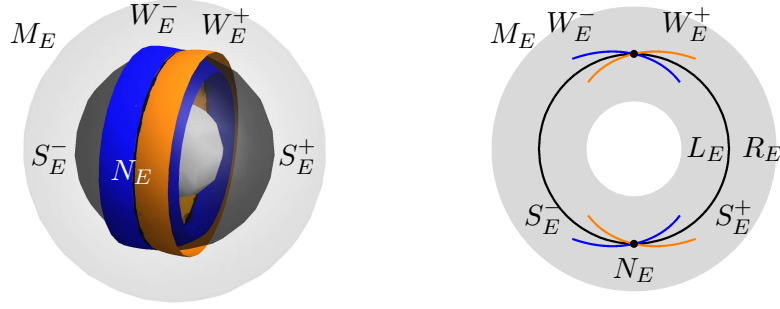
Figure 1.5: Conley representation of the quadratic approximation of the basic scenario, for some $E > E_1$, showing the energy-level M_E, the transition state N_E, its stable and unstable manifolds $W_E^\pm$ and the dividing surface $S_E = S_E^+ \cup S_E^-$. Left: full representation, right: cross-section with $z_1 = 0$.

will be presented in Section 2.2.

Remark 1.4.2. Note that the dividing surface S_E constructed above is closed, and the two halves $S_E^\pm$ are compact surfaces with boundary N_E. On the other hand, the choice $S = \{z \in M | y = Y(u, v)\}$ would not have given compact intersections with M_E.

Now, in order to apply Theorem 1.3.2 and show that our dividing surfaces have locally minimal geometric flux, we require that the dividing surfaces have no local recrossings. However, the centre manifold N is normally hyperbolic[*18] and it has stable and unstable manifolds $W^\pm$ of codimension-1 in M. Then N_E is also normally hyperbolic, as a submanifold of M_E, and $W_E^\pm$ are codimension-1 in M_E, thus dividing a neighbourhood of N_E into four sectors. Finally, since $S_E^\pm$ lie between $W_E^\pm$, unidirectionality implies that there are no local recrossings.

There is a simple asymptotic law for the flux when ΔE is small [Mac90]. In this case, N_E is given to leading order by $x = 0$, $y = 0$, and $\sum_{j=1}^{m-1} \frac{b_j}{2} \left(v_j^2 + u_j^2 \right) = \Delta E$. The generalised action is

$$
\begin{aligned}
\Theta_E &= \frac{1}{(m-1)!} \theta \wedge \omega^{m-2} \\
&= \frac{1}{(m-1)!} \left(p_1 \mathrm{d}q_1 \wedge \mathrm{d}q_2 \wedge \mathrm{d}p_2 \wedge \cdots \wedge \mathrm{d}q_{m-1} \wedge \mathrm{d}p_{m-1} + \text{ similar terms} \right),
\end{aligned}
$$

where we recall that $z = (q, p) = (u, x, v, y)$. Thus, the flux is (cf. Vineyard [Vin57])

$$
\phi_E \left(S_E^+ \right) = \frac{\Delta E^{m-1}}{(m-1)!} \prod_{j=1}^{m-1} \frac{2\pi}{b_j}.
$$

A nice way of visualising the energy level and the various submanifolds is to use the Conley representation[*19]. This method is implicit in a paper by Conley [Con68], was used by McGehee [McG69] and MacKay [Mac90], and is illustrated in [WW10]. Considering a 2 degree of freedom system and forgetting the higher order terms, the

---

[*18] Actually N is not (necessarily) compact, but the level sets N_E are invariant, so the sub-level sets $N_{\leq E}$ are compact submanifolds with (invariant) boundary N_E and normally hyperbolic.

[*19] The literature nowadays often also refers to it as the McGehee representation.

energy level M_E is given by the equation

$$\frac{a}{2}y^2 + \frac{b}{2}\left(v^2 + u^2\right) = \Delta E + \frac{a}{2}x^2, \quad \Delta E = E - E_1.$$

We have seen that for $\Delta E > 0$, M_E is diffeomorphic to $\mathbb{S}^2 \times \mathbb{R}$. The idea is therefore to represent M_E as a spherical shell in $\mathbb{R}^3$ by considering it to be a 1-parameter (x) family of 2-spheres, which we denote M_E^x. For a given x, we project the sphere M_E^x to another sphere in $\mathbb{R}^3$ by

$$\pi_x : M_E^x \to \mathbb{R}^3 : (u, v, y) \mapsto \frac{r\left(x\right)}{r_E\left(x\right)}\left(u, v, y\right) =: \left(z_1, z_2, z_3\right),$$

where $r_E\left(x\right) = \left(2\Delta E + ax^2\right)^{1/2}$ and the new radius $r\left(x\right)$ is a monotone function mapping the real line to a bounded positive interval, e.g. $r\left(x\right) = 2 + \tanh\left(x\right)$, for which $r\left(x\right) \in [1, 3]$. Under this projection, the parameterised 2-spheres M_E^x are placed concentrically in $\mathbb{R}^3$. Then we define a map taking points on M_E to $\mathbb{R}^3$ by

$$\pi : (x, u, v, y) \mapsto \pi_x\left(u, v, y\right) = \left(z_1, z_2, z_3\right),$$

which gives the desired spherical shell. The Conley representation of the quadratic approximation can be seen in Figure 1.5. This figure is only for 2 degree of freedom systems, but for m degrees of freedom, the same procedure can be applied and we can imagine projecting M_E to $\mathbb{R}^{2m-1}$.

1.5 General transport scenarios and transition states

We just saw how closed, invariant, codimension-2 submanifolds of the energy levels are the key to constructing surfaces with locally minimal geometric flux in the basic scenario. As we are interested in what happens in the basic scenario when the energy is increased further, and in other more general transport scenarios that are not governed by a local analysis, we give the following

Definition. A *transition state* for a Hamiltonian system is a closed, invariant, oriented, codimension-2 submanifold of an energy-level that can be spanned by two surfaces of unidirectional flux, whose union divides the energy-level into two components and has no local recrossings.

"Transition state"[*20] is not an ideal name because it is a set of states, not a single one. Furthermore, it is not a set of intermediate states on paths from reagents to products like the dividing surface, because it is invariant. The chemistry literature often also uses the term for dividing surfaces. This confusion might be due to the fact that in the basic scenario, the projection of both the transition state and the standard choice of dividing surface onto configuration space are the same. In fact, Pechukas

---

*20 M. King attributes the term to Johannes N. Brønsted, from circa 1922, but does not give a reference [Kin82]. Another common term in the chemistry literature is "activated" complex, state or surface, see e.g. Henriksen and Hansen [HH08, page 140].

and co-workers coined the term "periodic orbit dividing surface" (PODS), whereas the periodic orbits are transition states. For all of these reasons, MacKay [Mac90] avoided using the term. However, it is by now established terminology and we choose to stick with tradition.

In the basic scenario, the transition states are level sets of the Hamiltonian function restricted to the centre manifold. For more general transport scenarios, we expect invariant, codimension-2 submanifolds of state space, composed of the union of transition states over an interval of energy. These, and the centre manifolds of the basic scenario, we will refer to as *transition manifolds*.

We have been using *dividing surface* to refer to codimension-1 submanifolds of an energy level that divide it into two parts. The union of the dividing surfaces with different energies will be referred to as a *dividing manifold*. This is a codimension-1 submanifold, locally dividing state space.

In Section 2.1, we will comment on the properties of transition manifolds. Then, in Section 2.2 we show how to span an invariant, orientable codimension-2 submanifold of state space that is normally hyperbolic and has orientable stable and unstable manifolds by a local dividing manifold.

In the recent literature, both transition states and transition manifolds are often referred to simply as NHIMs, for normally hyperbolic invariant manifold. This terminology inevitably becomes confusing when passing to general transport scenarios that may posses multiple normally hyperbolic submanifolds, not all necessarily transition manifolds. Also, examples of transition manifolds that are not normally hyperbolic can be found, such as the symmetric disconnecting example of Subsection 2.4.2 with $a_1 \leq a_2$.

Examples of more general transport scenarios, than the basic one, will be seen in the examples of Subsections 2.4.1 and 2.4.2, and in the bimolecular reactions of Chapter 3.

Chapter 2

Transition states and dividing surfaces

Many transport scenarios, including the basic one for energies significantly above the saddle, cannot be considered locally about a critical point. The picture is therefore more complicated than the simple one for flux over a saddle.

In the easiest case, that is systems with 2 degrees of freedom, the transition states, being closed and 1-dimensional, are periodic orbits. Thus, their possible bifurcations are well known, and can be found in the literature, e.g. Abraham and Marsden [AM78, Section 8.6] and Hanßmann [Han07, Chapter 3]. A crucial feature of the transition state in the basic scenario is its normal hyperbolicity, which ensures that dividing surfaces constructed about it have locally minimal geometric flux. This may be lost at higher energies. However, for periodic orbits, we know what to expect when normal hyperbolicity is lost because normally elliptic periodic orbits also persist, see e.g. Meyer et al. [MHO09, Chapter 9] on the continuation of periodic orbits. These bifurcations however affect the underlying transport problem, see e.g. [DVB55, PP78, Dav87]. Unlike hyperbolic periodic orbits elliptic periodic orbits cannot be spanned by surfaces with no local recrossing. Other topological obstructions, such as the knot type or the twisting of the stable and unstable manifolds may also prevent hyperbolic periodic orbits from being a transition state. These may appear when the periodic orbit undergoes a bifurcation. The bifurcations of periodic orbit transition states are considered briefly in Subsection 2.3.1 in order to introduce these issues. This Subsection will raise more questions that it answers. A thorough theoretical and numerical study of periodic orbit transition states, which should answer all of these questions and more, is currently under way. This will hopefully provide some insight into higher dimensional transition states as well.

For more degrees of freedom, the transition states in the basic scenario are normally hyperbolic $(2m - 3)$-spheres. The bifurcations of higher dimensional normally hyperbolic submanifolds is not much explored. Recently, there have been studies proposing different approaches and partial normal form methods, see [LTK09, TTK11, AB12] and references therein. Nonetheless, bifurcations involving the loss of normal hyperbolicity are still not well understood.

What has been overlooked though is that there is a large class of systems for which the transition state develops singularities, i.e. points at which the manifold structure fails, at some energy E_b and then reforms as a non-diffeomorphic normally hyperbolic submanifold for energies above E_b. The dividing surfaces also undergo a similar bifurcation. In this case, we can say exactly what happens. The context for these bifurcations is that there is a normally hyperbolic submanifold in the full state space, the transition manifold, denoted N. For example, starting from the basic scenario the transition manifold is an extension of the centre manifold beyond a local neighbourhood of the index-1 critical point. The transition states are then the level-sets of the Hamiltonian function restricted to the transition manifold, $N_E = H_N^{-1}(E)$, and they undergo a Morse bifurcation. This occurs when H_N has a critical point and can be studied using Morse theory, see Appendix A.3. These bifurcations and their effect on transport problems, such as the bimolecular reactions of Chapter 3, are the main topic of this thesis.

The critical points of the restricted Hamiltonian function H_N are also critical points of the Hamiltonian function. For the Morse bifurcations, these will be of index one or higher relative to H_N, and hence of index two or higher relative to H. There have been studies regarding the role of higher index (than one) critical points in transport problems, see e.g. [EW09, CEW11, HU$^+$11]. These have however focused on the higher index critical points and a neighbourhood about these, and thus not searched for the global submanifolds beyond this neighbourhood. By considering Morse bifurcations, we therefore answer some of the questions raised in these papers.

The effect that the Morse bifurcations have on the flux of ergode through the dividing surface is considered in Section 2.5.

2.1 Properties of transition manifolds

Some properties of centre manifolds (in Hamiltonian systems) are recalled in Appendix A.2. Namely, they are normally hyperbolic and also symplectic, meaning that the restriction ω_N of the symplectic form to N is non-degenerate.

The centre manifold about an index-1 critical point is furthermore unique, by Theorem A.2.1.

Corollary 2.1.1. *For autonomous Hamiltonian systems, the centre manifold about a non-degenerate index-1 critical point of the Hamiltonian is unique.*

Proof. Consider an autonomous Hamiltonian system $\left(M^{2m}, \omega, H\right)$ with a non-degenerate index-1 critical point $\bar{z}_1$ of H, as for the basic scenario. The local centre manifold N about $\bar{z}_1$ can be written as the union of its invariant energy level sets, the transition states N_E, that are diffeomorphic to $\mathbb{S}^{2m-3}$, as we saw in Section 1.4. Thus motion in the centre manifold is bounded and by Theorem A.2.1, N is unique. $\qquad\square$

One could similarly check the centre manifolds of critical points of other index by considering their Williamson normal form [Arn89, Appendix 6].

The normal hyperbolicity of the centre manifold as a submanifold of state space ensures that of the transition states within an energy level, provided that they are

smooth manifolds. This in turn prevents local recrossings of the dividing surfaces. Thus, for the basic scenario with higher energies, we must consider normally hyperbolic extension of the centre manifold beyond a local neighbourhood of the index-1 critical point. These too will be symplectic, as seen in the examples, since symmetrically normally hyperbolic submanifolds of Hamiltonian systems that satisfy a spectral gap condition (implicit in our definition, in Appendix A.1) are symplectic, as pointed out by Marco [Mar] and Gelfreich and Turaev [GT14]. See Proposition A.1.2 and its proof for details.

Thus, when invariant submanifolds that are normally hyperbolic in some neighbourhood become degenerate, they lose normal hyperbolicity, as seen in the axi-symmetric case of the disconnecting example, Section 2.4.1. This could be used to check the stability of potential transition manifolds. The converse is not true, that is loss of normal hyperbolicity does not imply loss of symplectic nature. This can be seen in the symmetric connecting example of Subsection 2.4.2 with $a_1 \leq a_2$. This case also provides an example of a transition manifold that is not normally hyperbolic.

2.2   Constructing dividing manifolds

In the basic scenario, we have seen how to construct a local dividing manifold spanning the local codimension-2 centre manifold about the critical point $\bar{z}_1$. For more general transport scenarios, we may have an invariant, codimension-2 submanifold N of state space M on which the restriction of the Hamiltonian H_N is bounded from below and proper, such that the level sets are closed, invariant, codimension-2 submanifolds N_E of the energy levels M_E. In this section, we will show how to construct a codimension-1 submanifold S with no local recrossings, composed of two halves that span N and across which the flow is unidirectional, provided N is normally hyperbolic and its stable and unstable manifolds are orientable[*21]. Note that normally hyperbolic submanifolds that satisfy a spectral gap condition (implicit in our definition, in Appendix A.1) are symplectic (Proposition A.1.2) and that symplectic submanifolds are automatically orientable. In order for S to locally divide M, N must be embedded "nicely", as one can imagine transport scenarios with a submanifold N embedded in a non-trivial state space that is not divided by a codimension-1 spanning surface (see also discussion in Subsection 2.3.1). Provided S does locally separate M, restricting S to an energy level will give a dividing surface S_E with locally minimal geometric flux, demonstrating that S is a dividing manifold, N a transition manifold and N_E a transition state.

The construction requires a *fibration* of a neighbourhood $U \subset M$ of N. This is a manifold U (called the *total space*) together with a projection $\pi : U \to N : z \mapsto \tilde{z}$ to a manifold N (the *base space*) such that the *fibres* $F_{\tilde{z}} = \pi^{-1}(\tilde{z})$ are submanifolds, and a

---

*21 Even for orientable normally hyperbolic submanifolds, this is not necessarily the case. An example of an orientable, codimension-2 normally hyperbolic submanifold with non-orientable stable and unstable manifolds is the orbit cylinder formed by a family of inversion hyperbolic periodic orbits (with negative characteristic multipliers) parametrised by the energy in a 2 degree of freedom system. This has local stable and unstable manifolds diffeomorphic to a Möbius strip cross an interval, and emerges for example, out of a period doubling bifurcation of an elliptic periodic orbit [AM78, page 599].
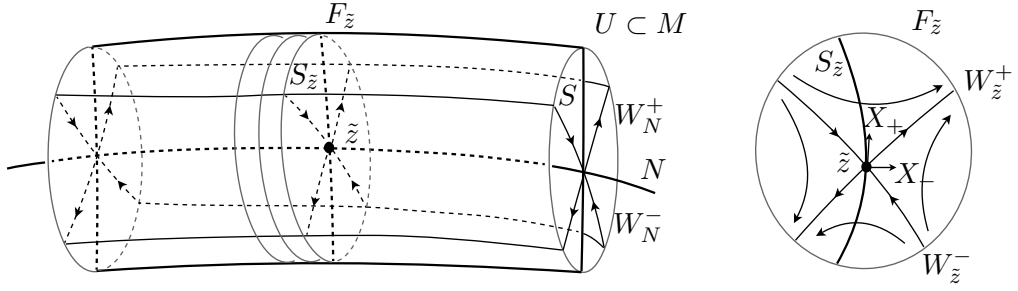
Figure 2.1: Schematic representation of a condimension-2 normally hyperbolic submanifold N and a fibration of a neighbourhood U used to find a dividing manifold S spanning N.

local trivialisation $\psi_i : \pi^{-1}(V_i) \to V_i \times F$, where V_i is a set in an open covering of N, and F is a fixed manifold (the *standard fibre*). It is usually denoted (U, N, π, F). The tangent spaces to the fibres give a *vertical subbundle*, Vert, of the tangent bundle TM

$$\mathrm{Vert}_z = \ker \mathrm{d}_z \pi = T_z F_{\tilde{z}},$$

for all points $z \in U$. Then, a choice of *horizontal subbundle*, Hor, gives a splitting[*22] of the tangent bundle

$$TM = \mathrm{Vert} \oplus \mathrm{Hor}.$$

Furthermore, we shall consider a *symplectic fibration*, for which the fibres are symplectic submanifolds of the total space, see e.g. Guillemin, Lerman and Sternberg [GLS96, Chapter 1]. With our symplectic total space, we can choose the symplectic form of the fibre $F_{\tilde{z}}$ to be $\omega_{F_{\tilde{z}}}$, the restriction of ω. We then say that ω is *fibre-compatible*. Asking that the fibration is symplectic adds a constraint, but in exchange we can associate to ω a symplectic splitting, by defining the horizontal subbundle to be symplectically orthogonal to the vertical subbundle, i.e.

$$\mathrm{Hor}_z = \mathrm{Vert}_z^{\omega} := \{\xi \in T_z M | \omega(\xi, \eta) = 0 \ \forall \eta \in \ \mathrm{Vert}_z\}.$$

We choose a specific symplectic fibration π, by introducing coordinates. The fibres are 2-dimensional (the codimension of N in M), symplectically orthogonal to the symplectic base space N and $H_{F_{\tilde{z}}}$ has only one non-degenerate, index-1 critical point $\tilde{z}$, recalling that we are considering a small neighbourhood U of N. Other choices of fibration are possible. However, these conditions alone are not sufficient to define fibrations that can be used in our construction of dividing manifolds. For any symplectic fibration for which the fibres are symplectically orthogonal to the base space N, $\tilde{z}$ is a critical point of $H_{F_{\tilde{z}}}$ since N is normally hyperbolic and we are considering a symplectic splitting $TM_N = TN \oplus^{\omega} \mathrm{Vert}_N$, so $X_H(\tilde{z}) = X_{H_N}(\tilde{z}) + X_{H_{F_{\tilde{z}}}}(\tilde{z})$, where $i_{X_{H_{F_{\tilde{z}}}}} \omega_{F_{\tilde{z}}} = \mathrm{d}H_{F_{\tilde{z}}}$, and $X_{H_{F_{\tilde{z}}}}(\tilde{z}) = 0$ by invariance. Given $\tilde{z} \in N$, the symplectic neighbourhood theorem

---

*22 This defines a *connection* on the fibration. However, to avoid confusion with the affine connection on the tangent (fibre) bundle $\tau : TM \to M$, we avoid this terminology.

[MS98, Theorem 3.30] provides Darboux coordinates $z = (u, x, v, y)$ such that

$$\omega = \mathrm{d}u \wedge \mathrm{d}v + \mathrm{d}x \wedge \mathrm{d}y,$$

and

$$N = \{x = y = 0\}.$$

We shall often write $z = (h, n)$ with $h = (u, v)$, and $n = (x, y)$. Temporarily, we choose the following fibres

$$F_{\tilde{z}} = \{h = \tilde{h}\},$$

where $\tilde{z} = (\tilde{h}, 0)$. Linearising (vertically) about N, we find

$$H(h, n) = H(h, 0) + \frac{1}{2} n^T D_{nn}^2 H(h, 0) n + \cdots,$$
$$=: H_N(h) + \frac{1}{2} n^T H_N^2(h, 0) n + \cdots,$$

using the invariance of N, so

$$\dot{h} = J_N D_h H_N(h) + \cdots,$$
$$\dot{n} = J_F D_n H_N^2(h) n + \cdots.$$

Note that the stable and unstable manifolds of $\tilde{z}$, $W^{\pm}(\tilde{z})$, are tangent to $F_{\tilde{z}}$ at $\tilde{z}$, since $T_{\tilde{z}} W^{\pm}(\tilde{z}) \perp_\omega T_{\tilde{z}} N$ (see p.82), but that they are not subsets of the fibres. We now change coordinates and choose our actual fibres. These will contain $W^{\pm}(\tilde{z})$, i.e. we shall make the strong stable and unstable manifolds $W^{\pm}(\tilde{z}) \subset W^{\pm}(N)$ vertical and use the new coordinates to choose a specific fibration. Merely asking that $W^{\pm}(\tilde{z}) \subset F_{\tilde{z}}$ does not give a fibration for which $\tilde{z}$ is a non-degenerate, index-1 critical point of $H_{F_{\tilde{z}}}$ (and might also not be necessary). We change coordinates to $z = (u_2, x, v_2, y)$ such that

$$W^{\pm}(\tilde{z}) = \{h_2 = \tilde{h}_2, g_{\tilde{z}}^{\pm}(x, y) = 0\},$$

where $\tilde{z} = (\tilde{h}_2, n)$. This change of coordinates is achieved in two steps, and is part of the transformation to Fenichel normal form coordinates, see e.g. [Jon95, Chapter 3] and [JT09, Section 2]. First, we define

$$(u_1, v_1) = \pi^-(u, x, v, y),$$

where π^- is the projection taking points in the strong stable manifolds to their base points in N, i.e. $\pi_{\tilde{z}}^-(h, n) = \tilde{h}$ for $(h, n) \in W^-(\tilde{z})$, then we define

$$(u_2, v_2) = \pi^+(u_1, x, v_1, y),$$

where π^+ is equivalent to π^- but for $W^+(\tilde{z})$. Noting that $\pi^{\pm}(h, 0) = h$, we can write $\pi^{\pm}(h, n) = h + \Pi^{\pm}(z) n$. This change of coordinates is symplectic since $W^{\pm}(\tilde{z})$ are trajectories, so $\pi_{\tilde{z}}^{\pm}$ are given by the Hamiltonian flow. Dropping the subscripts, we

choose the fibres to be

$$F_{\tilde{z}} = \{h = \tilde{h}\}.$$

A schematic representation of the fibration is given in Figure 2.1. For this choice of fibres $D_n H_N^2(h)$, or equivalently $D^2 H_{F_{\tilde{z}}}(0)$ since $X_H|_{F_{\tilde{z}}} = X_{H_{F_{\tilde{z}}}}$, is a non-degenerate matrix with one negative and one positive eigenvalue. This can be seen by completing the change of coordinates to Fenichel normal form $z = (u, q, v, p)$ in which the strong stable and unstable manifolds are straight, and by normal hyperbolicity the vertical dynamics is given by

$$\dot{q} = a^+(z)q,$$
$$\dot{p} = -a^-(z)p,$$

with $a^\pm(z) > 0$, see e.g. [Jon95, Chapter 3]. The symplectic form is canonical with $\omega_{F_{\tilde{z}}} = \mathrm{d}q \wedge \mathrm{d}p$, as can be seen by considering the straightening transformation since the strong stable and unstable manifolds are 1-dimensional, so we know the first derivative of the H_{F_z} and can differentiate it to find the second, which is non-degenerate at N since $a^\pm(z) > 0$.

Given this fibration, we can choose vector fields $X_\pm$ tangent to the fibres such that

$$\omega(X_-, X_+) > 0, \quad \mathcal{L}_{X_-}\mathcal{L}_{X_-}H < 0 \text{ and } \mathcal{L}_{X_+}\mathcal{L}_{X_+}H > 0.$$

Note that the Lie derivative $\mathcal{L}_X A$ of a 0-form (i.e. a function) A is just $\mathcal{L}_X A = X(A) = \mathrm{d}A(X)$, but this last notation does not lend itself to being applied twice. Locally, in Fenichel normal form coordinates, a possible choice of of vector fields is $X_+ = \partial_q + \partial_p$ and $X_- = \partial_q - \partial_p$, cf. Figure 2.1.

We then define

$$S_{\tilde{z}} = \{z \in F_{\tilde{z}} | \mathcal{L}_{X_-}H(z) = 0\} \text{ and } S = \cup_{\tilde{z}} S_{\tilde{z}}.$$

Again, $\mathcal{L}_{X_-}H = \mathrm{d}H(X_-)$ and we are asking that the derivative of H in the direction of X_- is zero. This dividing manifold S spans N and is an orientable, codimension-1 submanifold of M. Orientability following from that of the stable and unstable manifolds. However, we must check the flux of state space volume across S. Note that if the state space flux is unidirectional, then so is the flux of ergode, since the energy-levels are invariant. The transverse component of X_H across $S_{\tilde{z}}$ is

$$\mathrm{d}\left(\mathcal{L}_{X_-}H\right)(X_H) = \mathcal{L}_{X_H}\mathcal{L}_{X_-}H.$$

To find its sign, firstly we note that $\mathcal{L}_{[X_H, X_-]}H = \mathcal{L}_{X_H}\mathcal{L}_{X_-}H - \mathcal{L}_{X_-}\mathcal{L}_{X_H}H = \mathcal{L}_{X_H}\mathcal{L}_{X_-}H$, since $\mathcal{L}_{X_H}H = \mathrm{d}H(X_H) = 0$. Here $[X, Y] = XY - YX$ is the Lie bracket of vector fields (thought of as differential operators, as in $X(A) = \mathrm{d}A(X)$). Next, $\mathcal{L}_{X_+}H$ is single signed across each half of $S_{\tilde{z}}$ because $\tilde{z} \in N$ is a critical point of $\mathcal{L}_{X_+}H$, but

27

$\mathcal{L}_{X_+} \mathcal{L}_{X_+} H < 0$ on the whole of $F_{\tilde{z}}$, thus $\tilde{z}$ is a minimum. Therefore, we ask that

$$\mathcal{L}_{[X_H, X_-]} H = -c_{\tilde{z}} \, \mathcal{L}_{X_+} H, \quad c_{\tilde{z}} \in \mathbb{R}_+,$$

which is compatible with the initial assumptions.

In practice, it is easier to check the conditions if the vector fields $X_\pm$ are Hamiltonian, so we choose functions $A_{\tilde{z}}^\pm : F_{\tilde{z}} \to \mathbb{R}$ and define $X_\pm = X_{A_{\tilde{z}}^\pm}$, where $i_{X_{A_{\tilde{z}}^\pm}} \omega = \mathrm{d} A_{\tilde{z}}^\pm$. Then using Poisson brackets, defined as $\{A, B\} = \omega(X_A, X_B)$ for two functions on M, and considering $A_{\tilde{z}}^\pm$ as functions on the whole of M, we can rewrite the conditions satisfied by the vector fields as

$$\{A_{\tilde{z}}^-, A_{\tilde{z}}^+\} > 0, \quad \{\{H, A_{\tilde{z}}^-\}, A_{\tilde{z}}^-\} < 0 \text{ and } \{\{H, A_{\tilde{z}}^+\}, A_{\tilde{z}}^+\} > 0,$$

and the new conditions, ensuring that the flux is unidirectional, as

$$\{A_{\tilde{z}}^-, A_{\tilde{z}}^+\} > 0, \quad \{H, A_{\tilde{z}}^-\} = c_{\tilde{z}} \, A_{\tilde{z}}^+ \text{ and } \{\{H, A_{\tilde{z}}^+\}, A_{\tilde{z}}^+\} > 0,$$

where we have used the two relations $\mathcal{L}_{X_A} B = \{B, A\}$ and $[X_A, X_B] = X_{\{B,A\}}$, see e.g. [AM78, Section 3.3]. Thus, we have actually found that

$$S_{\tilde{z}} = \{z \in M | A_{\tilde{z}}^+(z) = 0\}.$$

Now, seeing as $\tilde{z} \in N$ is an index-1 critical point of the Hamiltonian function restricted to $F_{\tilde{z}}$, it has Williamson normal form

$$H_{F_{\tilde{z}}}(x, y) = \frac{a_{\tilde{z}}}{2} \left(y^2 - x^2 \right) + \mathcal{O}(3), \quad a_{\tilde{z}} \in \mathbb{R}_+,$$

about $\tilde{z}$. We can then choose $A_{\tilde{z}}^-(z) = y$, $A_{\tilde{z}}^+(z) = -x$, for example.

The dividing surfaces S_E are then simply given by intersecting the dividing manifold with the energy levels. We must check that these are closed and have no local recrossings. In order to check that S_E is closed, we show that the sub-level set $S_{\leq E} = \{z \in S | H_S(z) \leq E\}$ is compact. To check that $S_{\leq E}$ is compact, we restrict the fibration to $\pi|_{S_{\leq E}} : S_{\leq E} \to N_{\leq E}$, which has a compact base space $N_{\leq E}$ by choice, and compact fibres $S_{\leq E, \tilde{z}}$ as we can see from $H_{F_{\tilde{z}}}$ in normal form, and thus a compact total space $S_{\leq E}$, as desired. The dividing surface S_E does not have local recrossings by the same argument as for the local dividing surfaces in the basic scenario. N_E is a normally hyperbolic submanifold of M_E, and $W_E^\pm$ are codimension-1. Then for each $\tilde{z} \in N$, $W_E^\pm(\tilde{z}) = \{z \in M | y \mp x = 0, \ H(z) = E\}$, so $S_E^\pm$ lie in-between $W_E^\pm$ and unidirectionality implies no local recrossings.

This construction generalises, and reduces to, Toller et al.'s local construction [TJ$^+$85] for the basic scenario

$$S = \{z \in M | G(z) = x - X(u, v) = 0\},$$

see Section 1.4. In this case, the fibres symplectically orthogonal to N are given by

$$F_{\tilde{z}} = \left\{ u - \tilde{u} = \tilde{X}_v \left[y - \tilde{Y} \right] - \tilde{Y}_v \left[x - \tilde{X} \right], \ v - \tilde{v} = \tilde{X}_u \left[y - \tilde{Y} \right] - \tilde{Y}_u \left[x - \tilde{X} \right] \right\},$$

where $\tilde{z} = \left(\tilde{X}, \tilde{u}, \tilde{Y}, \tilde{v} \right)$ is a point in N, $\tilde{X} = X\left(\tilde{u}, \tilde{v} \right)$, $\tilde{X}_i = \partial_i X\left(\tilde{u}, \tilde{v} \right)$ and similarly for Y. The rest follows.

2.3 Bifurcations and obstructions for transition states

Periodic orbit transition states for two degree of freedom Hamiltonian systems are the simplest example of transition states. Their bifurcations and breakdown are therefore archetypes of those for general transition states. The properties and bifurcations of periodic orbits of Hamiltonian systems are briefly reviewed paying particular attention to (changes in) the topology of the periodic orbits (cf. Ghrist et al. [GHS97, Chapter 4]), and the geometry of the global *orbit manifold*, i.e. the global two-dimensional (possibly branched and disjoint) submanifold N of state space containing all the periodic orbits of the system and obtained by continuing the individual orbit cylinders through bifurcations. This will raise a number of questions regarding the role of periodic orbits in transport problems, most of which will not be answered here.

The same questions are then asked for higher dimensional transition states in subsection 2.3.2.

2.3.1 Periodic orbit transition states

Parametrised families of periodic orbits are generic for Hamiltonian systems. This is the contents of the regular orbit cylinder theorem.

Theorem 2.3.1 (Regular orbit cylinder theorem). *If N_E is a closed orbit of (M^4, ω, H), and one is not a characteristic multiplier, then it is contained in a regular orbit cylinder N, i.e. a submanifold diffeomorphic to $\mathbb{S}^1 \times \mathbb{B}^1$ that is transversal[*23] to every energy-level and has $N_E = N \cap M_E$. Furthermore, the orbit cylinder N is symplectic (with ω_N non-degenerate).*

Remark 2.3.2. The proof of Theorem 2.3.1 can be found in any textbook on Hamiltonian systems, e.g. [AM78, Section 8.2]. Most of the literature however does not mention the symplectic nature of N. This follows from the Hamiltonian flow box, or rectification, theorem which states that given a regular point $z \in M$, i.e. one for which $\mathrm{d}H(z) \neq 0$, there exist Darboux coordinates (q, p) in a neighbourhood of z such that $q_1 = t$, $p_1 = H$, $\dot{q}_1 = 1$, $\dot{p}_1 = 0$, $\dot{q}_2 = 0$, $\dot{p}_2 = 0$ [MHO09, Section 8.3]. Thus $N = \{z \in M | q_2 = Q_2(p_1), \ p_2 = P_2(p_1)\}$ and $\omega_N = \mathrm{d}q_1 \wedge \mathrm{d}p_1$.

In general, the regular orbit cylinder cannot be extended for all energies without encountering either a critical point of H or a closed orbit for which the hypothesis of Theorem 2.3.1 fails. These lead to bifurcations.

[*23] Recall, we say that two submanifolds $X, Y \subset M$ are *transversal*, and write $X \pitchfork Y$, if $T_z X + T_z Y = T_z M$ for all $z \in X \cap Y$.

Before considering bifurcations, we shall ask whether there are topological obstructions that can prevent a hyperbolic periodic orbit from being a transition state for a two degree of freedom system. There are two different points to consider, the first is the topology of the energy levels M_E and the embedding of the periodic orbits N_E in these. That is, the topology of M_E can obstruct the existence of dividing surfaces. Similar obstructions are found when trying to construct transverse and complete Poincaré surfaces of section. Their existence for two degree of freedom systems is a very studied topic, starting with the works of Poincaré and Birkhoff, see [BDW96] and references therein. Other topological obstructions may come from the topology of the periodic orbit itself. One generally keeps track of these properties, which may change when periodic orbits bifurcate, by considering (numerical) invariants. Two (topological) properties of periodic orbits are encoded in the *Maslov index*, which counts the number of times the stable and unstable manifolds wind around the orbit in one period[*24] [Rob92], and the *link* or *knot type*.

We shall first consider the Maslov index. The local stable and unstable manifolds $W^\pm(N_E)$ of a hyperbolic periodic orbit N_E are two dimensional ribbons. These may wind around the periodic orbit, as they do for *inversion hyperbolic*[*25] periodic orbits, with negative real characteristic multipliers, that emerge from a period doubling bifurcation. In this case, the local invariant manifolds form Möbius bands. An inversion-hyperbolic periodic orbit has Maslov index-1. In general, a periodic orbit with Maslov index-$2k$ has stable and unstable manifolds with k twists.

Clearly, an inversion hyperbolic periodic orbit N_E with Maslov index-1 cannot act as a transition state because we cannot place an orientable dividing surface S_E spanning N_E between the non-orientable invariant manifolds. Locally S_E would have to be a Möbius strip, which if closed by gluing a disk $\mathbb{B}^2$ would be diffeomorphic to a Klein bottle. The same is true for all periodic orbits with odd Maslov index, whereas for periodic orbits with even index and therefore orientable but twisted local invariant manifolds it might still be possible to form orientable spanning surfaces by gluing two non-trivial surfaces with boundary the circle.

The Maslov index is usually defined for closed curves in Lagrangian submanifolds [MS98, Section 2.3]. Recall that a submanifold W of a symplectic manifold (M, ω) is said to be *Lagrangian* if for all $z \in W$ the tangent space $T_z W$ is Lagrangian, i.e. the symplectic complement to the tangent space

$$T_z W^\omega = \{\nu \in T_z M | \omega(\nu, \xi) = 0 \ \ \forall \xi \in T_z W\}$$

satisfies $T_z W^\omega = T_z W$. This implies that W has half the dimension of M and that ω vanishes on W. The definitions of the Maslov index coincide because the invariant manifolds of hyperbolic periodic orbits are Lagrangian, as we shall now recall.

[*24] Ghrist et al. [GHS97] instead refer to the *self-linking number* of the periodic orbit, that is the linking number of the link composed of the periodic orbit and a boundary of one of the local invariant manifold ribbons.

[*25] These are also referred to as *flip* (hyperbolic), or *Möbius* periodic orbits.

Proposition 2.3.3. *For a 2 degree of freedom Hamiltonian system, the stable and unstable manifolds $W^{\pm}(N_E)$ of an (inversion) hyperbolic periodic orbit N_E are submanifolds of the energy level M_E containing N_E, and both have dimension 2. Furthermore, they are Lagrangian submanifolds of state space (M^4, ω).*

Proof. The stable and unstable manifolds are submanifolds of the energy level M_E by definition, seeing as they consist of trajectories asymptotic to N_E and energy is conserved. Their dimension can be deduced from the constraints on the characteristic multipliers of Hamiltonian periodic orbits. To see why $W^{\pm}(N_E)$ are Lagrangian, we first note that for points $z \in N_E$, the tangent manifolds $T_z W^{\pm}$ are Lagrangian by considering the splitting of $T_z M$ as by the Williamson theorem. Thus $\omega(\eta_1, \eta_2) = 0$ for $\eta_i \in T_z W^{\pm}$, and the symplectic form must vanish throughout $W^{\pm}$ because the Hamiltonian flow preserves ω. Finally, since $\dim(W^{\pm}) = 2$ and ω vanishes, $W^{\pm}$ are Lagrangian. $\square$

Actually, we can also define a Maslov index for elliptic periodic orbits [Sug00]. This allows us to follow the index through bifurcations in which the stability of the periodic orbit changes.

Another topological property of periodic orbits is their *knot* or *link type*. Periodic orbits are diffeomorphic to $\mathbb{S}^1$, but for 2 degree of freedom systems they can be embedded in their energy level in non-trivial ways, i.e. they may be knotted or linked[*26]. Two good references are the classic book of Roflsen [Rol03], and Ghrist et al. [GHS97], which considers knots arising in dynamical systems.

Periodic orbits that are local, i.e. contained in a subset of M_E diffeomorphic to $\mathbb{R}^3$, avoid the global topological obstructions mentioned previously. In the literature, links are usually embedded in $\mathbb{S}^3$, which can be thought of as $\mathbb{R}^3$ plus a point at infinity (by considering the stereographic projection). This is boundaryless and easier to work with than $\mathbb{R}^3$, e.g. when dealing with link-complements.

Given some collection of periodic orbits forming a link N_E, we ask whether this can be spanned by orientable surfaces of unidirectional flux. We recall that all links have a *Seifert surface*.

Proposition 2.3.4. *Any link N_E in $\mathbb{S}^3$ has at least one Seifert surface, that is a connected, oriented surface spanning[*27] N_E.*

The proof is constructive and known as *Seifert's algorithm* [Rol03, Section 5.4]. However, the Seifert surface it produces depends on the chosen *link-diagram* (or presentation), i.e. the projection of the link N_E onto the plane with a convention for the crossings.

We can thus span any link with an orientable (Seifert) surface. Spanning a given link on either side with one (or two) of its Seifert surfaces and then taking the union of these will thus give a closed oriented surface, which separates the ambient energy-level.

[*26] Note that all knots "untangle", i.e. are equivalent to the *unknot* (a closed curve whose embedding in $\mathbb{S}^3$ is the boundary of an embedded disk) in dimensions 4 or higher.

[*27] In the literature, the terminology often inverts the roles, saying that N_E *bounds* the surface S_E.

However, we want Seifert surfaces that admit flows that are unidirectional across them. We recall that a knot or link N_E in $\mathbb{S}^3$ is said to be *fibred* if there is a family of Seifert surfaces S_t parametrised by points t in the circle $\mathbb{S}^1$, such that for two distinct points t and τ the intersection of S_t and S_τ is exactly N_E. That is, the *link complement* of fibred knots, $N_E^c = \mathbb{S}^3 \setminus N_E$, can be written as a (surface) fibre bundle over the circle [Rol03, Section 10.H]. In $\mathbb{S}^3$, these knots are the ones for which we can find a spanning (Seifert) surfaces through which the flux of ergode is unidirectional. They are in fact used to construct global Poincaré surfaces of section, see e.g. [BDW96].

Fibred links are a subset of all links, which satisfy certain conditions, see e.g. [Rol03, Section 10.H]. One of these is that the Alexander polynomial $A(t)$ of fibred links N_E in $\mathbb{S}^3$ is monic, i.e. its first and last non-zero coefficients are ± 1. Thus the only twisted knots that can be fibred are the trefoil, the figure of eight, and the unknot. Also, all torus knots and links are fibred, and all closed positive braids are fibred links [BW83]. However, in general M_E is not diffeomorphic to $\mathbb{S}^3$, so this does not provide a complete answer regarding which hyperbolic periodic orbits may be transition states.

We now turn to bifurcations, at which periodic orbits may change stability or topological properties. We shall only consider the energy, which parametrises the orbit cylinders, as a bifurcation parameter. This is a natural parameter for Hamiltonian systems.

The bifurcations of periodic orbits can be divided into those that produce a branching (or termination) of the orbit manifold, such as (Lyapunov) creations and homoclinic bifurcations[*28], those that result in a change of stability of the periodic orbits, such as centre-saddle bifurcations, and those that combine both cases above, such as period doubling bifurcations.

We would like to classify the different transport scenarios for 2 degree of freedom systems, and understand which periodic orbits can act as transition states. Seeing as the orbit manifold, or parts of it, will act as a transition manifold, we are also interested in their geometry, especially their smoothness, branching and symplectic nature, which was answered with Theorem 2.3.1. These are not generally the focus of the bifurcation theory literature.

Clearly, bifurcations that result in the loss of normal hyperbolicity of the periodic orbit break the transition state condition, as elliptic periodic orbits cannot be spanned by dividing surfaces with no local recrossings.

On the other hand, bifurcations that lead to branchings of the orbit cylinder without a change of stability can lead to a change in diffeomorphism class of the transition state, leading to a union, or link, of periodic orbits. The simplest branching bifurcation is the (Lyapunov) creation at an index-1 critical point of the Hamiltonian in the basic scenario, at which a periodic orbit transition state is born [AM78, Section 8.6]. Another class of bifurcations that involve the branching of the orbit manifold are homoclinic bifurcations. In the simplest case, a regular orbit cylinder terminates at a critical energy E_c with a homoclinic orbit asymptotic to a hyperbolic equilibrium point, or index-2 critical point of the Hamiltonian function. The period of the orbits in the cylinder tends

---

*28 Homoclinic bifurcations are also known as *homoclinic*, or *infinite period, blow-up*.

to infinity and the orbits tend to the homoclinic orbit as E tends to E_c [VF92]. Recall that the stable and unstable manifolds of an equilibrium point lie in the energy level containing the equilibrium. This follows from their definition and the conservation of energy. Thus W^+ and W^- may intersect transversely along homoclinic orbits, which are then said to be *non-degenerate*. More generally, Hamiltonian systems often have a number of homoclinic orbits asymptotic to the same hyperbolic equilibrium, or multiple hyperbolic equilibria at a given E_c and heteroclinic orbits. This leads to multiple homoclinic bifurcations, involving multiple periodic orbits, which may also tend to a number of heteroclinic orbits. There are essentially two possible bifurcations for the orbit manifold. In the first, the manifold consists of orbit cylinders for E both above and below E_c, all terminating at the homoclinic orbits and joining smoothly to form a global, symplectic orbit manifold. These are *Morse bifurcations*[*29]. The simplest example is that of two homoclinics to a single index-2 critical point of H and an orbit manifold that is locally a "pair of pants", as seen in the connecting example in Section 2.4.2. The other class of bifurcations occurs when the orbit cylinders are only present for E either above or below E_c and the global, possibly branched, orbit manifold disappears as E passes through E_c. In this situation, the orbit manifold terminates. These bifurcations are found in chaotic scattering and known as *"abrupt bifurcations"* [BGO90].

For simple mechanical two degree of freedom systems, one can tell which homoclinic bifurcation occurs at a critical energy E_c by using the heteroclinic shadowing theorem of Turaev and Shilnikov [TS89] and Baesens et al. [BCM13]. This gives the existence of periodic orbits shadowing sequences of *admissible* non-degenerate heteroclinic orbits. For general Hamiltonian systems, those with more degrees of freedom than two, and for higher index critical points there is no theorem that can be used to decide which bifurcation occurs at a given critical value of the energy. One must therefore try to construct a smooth normally hyperbolic codimension-2 submanifold through E_c and then consider its level sets.

2.3.2 Higher dimensional transition states

Similarly, we are interested in higher dimensional transition states and their bifurcations and obstructions. However, it is not straight forward to study the bifurcations of these high dimensional submanifolds, let alone define and enumerate all their possible topological properties. In two degrees of freedom, links cover all periodic orbit transition states, whereas in general degrees of freedom, transition states can undergo Morse bifurcations and change diffeomorphism class altogether.

Knot theory does generalise to spheres, and possibly other high dimensional submanifolds, namely a knot is an embedding of a submanifold N^n in M^m, and if non-trivial (that is not isotopic to the trivial embedding) it is said to be knotted, see e.g. [Rol03, Chapter 11]. Transition states will always be codimension-2 in their energy-level, and so maybe be knotted. If N is disconnected then it may be called a link.

[*29] Morse bifurcations of periodic orbits are also called *gluing bifurcations* [GHS97, Section 4.4], *connections* [GH90], and also play a role in *"massive bifurcations"* to chaotic scattering [DG⁺90].

One would then like to ask which of the previous obstructions for periodic orbit transition states carry over to higher dimensions. This would also require understanding how to generalise the Maslov index to higher dimensional submanifolds. For general degrees of freedom, we must also check for other topological invariants that are not present for periodic orbits.

Bifurcations of high dimensional transition states that lead to a loss of normal hyperbolicity have not been explored much. It has been considered a hard problem because there are many possible consequences. Recently, there have been a few studies, e.g. in the context of transport problems see [LTK09, TTK11, AB12], but these bifurcations are still poorly understood.

What had been overlooked until now are the Morse bifurcations in which the transition manifold branches, just as for the homoclinic Morse bifurcations of periodic orbits. These shall be considered in the next Section and then again in Chapter 3.

2.4 Morse bifurcations of transition states

In a Morse bifurcation, the transition state develops singularities at a critical energy E_b, i.e. the manifold structure fails, but then regains smoothness and normal hyperbolicity with a change in diffeomorphism type. These bifurcations occur when there is a transition manifold N for some range of energies, and the Hamiltonian function restricted to the transition manifold H_N has a critical energy value E_b in this range. As the energy is varied through the critical value, the transition states, which are the energy levels of the transition manifold $N_E = H_N^{-1}(E)$, undergo a Morse bifurcation. Morse theory, which is briefly reviewed in Appendix A.3, gives the transition state after the bifurcation as a handlebody (Theorem A.3.4) from which we can tell its diffeomorphism class.

The Morse bifurcations of the transition states come with associated bifurcations of the dividing surfaces S_E, and of the energy-levels M_E. That is, the critical points of the restricted Hamiltonian H_N are also critical point, with an index that is greater by 1, of the Hamiltonian function H itself. One could say that the bifurcations of the energy levels are the reason for the bifurcations of the dividing surfaces and the transition states, in the sense that given a bifurcation of the energy levels the dividing surfaces must also bifurcate in order to still separate the two regions of interest.

Of course, knowledge of the diffeomorphism class of the transition states does not help us to compute the desired flux of ergode through the dividing surface, which requires an explicit formula for the transition state in order to perform the integration. However, it is crucial in order to understand the qualitative nature of the transport problem in question. The changes in flux as a function of energy, when the transition states undergo Morse bifurcations is considered in Section 2.5.

Degenerate critical points can also be considered, however if we are only interested in the diffeomorphism class of the transition states we may find this by perturbing the function slightly in order to obtain a Morse function with only non-degenerate critical point. Morse theory also provides bounds on the number of critical points given the

Figure 2.2: Graph of volcano potential with contour lines for the disconnecting transition states example.

topology of the transition manifold, via the Morse inequalities.

Morse bifurcations of the energy-levels were one of the key points of Smale's "topological program" for mechanical systems [Sma70], however those of transition states and dividing surfaces had been overlooked until now. For 2 degree of freedom systems, another way of looking at these bifurcations is as a combination of homoclinic bifurcations, as reviewed in Subsection 2.3.1. In the literature, these bifurcations have been found in a number of scenarios, the closest to our transport problems being the "massive bifurcations" to chaotic scattering considered by Ding et al. [DG$^+$90]. Recently, some examples of homoclinic bifurcations of periodic orbit transition states were reported by Mauguière et al. [MC$^+$13], in a paper that appeared in preprint form at about the same time as ours [MS14]. Unlike two degree of freedom systems, for which the transition states are always periodic orbits and the Morse bifurcations can only lead to connections and disconnections, for higher dimensional transition states, these can lead to a qualitatively different transition states and dividing surfaces.

We shall now consider two examples of Morse bifurcations of transition states. These are originally two degree of freedom systems, which are easier to present, but then more degrees of freedom are added to point out that Morse bifurcations are not restricted to any dimension. Further examples of Morse bifurcations will be seen in the bimolecular reactions of Chapter 3.

2.4.1 Example. Disconnecting transition states

We now turn to our first example of a Morse bifurcation. This shows one way in which the basic scenario transition state can change topology as the energy increases.

Consider a "volcano potential" given in polar coordinates as

$$U\left(x, \beta\right) = \frac{1}{2}x^2\left(2 - x^2\right)\left(1 - \varepsilon x \cos \beta\right),$$

where ε is a small positive parameter, see Figure 2.2.

The mechanical Hamiltonian function with this potential energy is then

$$H\left(x, \beta, p_x, p_\beta\right) = \frac{1}{2}\left(p_x^2 + \frac{1}{x^2}p_\beta^2\right) + \frac{1}{2}x^2\left(2 - x^2\right)\left(1 - \varepsilon x \cos \beta\right),$$

35

and we consider the Hamiltonian system with the canonical symplectic form. The Hamiltonian function has three critical points, one of which $\bar{z}_1 = (\bar{x}_c, 0, 0, 0)$ with index-1, and another $\bar{z}_2 = (\bar{x}_c, \pi, 0, 0)$ with index-2. We are interested in transport in and out of the crater and have an index-1 critical point in between, as expected for the basic scenario. Choosing x as the coordinate joining the two regions, we want to construct a transition and dividing manifold about the index-1 critical point and study the transition states and dividing surfaces over a range of energies.

In Subsection 3.2.1, we shall consider the transport problem associated with capture of a diatom by an atom restricted to the plane. We shall then note that the present disconnecting example can be viewed as the planar capture transport problem between a frozen diatom and an atom with zero total angular momentum. A similar volcano potential is seen in the ionization of hydrogen in a circularly polarized microwave field [FU95, BUF97]. The transport problem in this example is however different, as escaping from the volcano's crater does not necessarily imply ionization.

Considering the axi-symmetric case, $\varepsilon = 0$, for which a transition manifold can be found explicitly, allows us to find an approximate transition manifold for the full system and due to its normal hyperbolicity deduce that there is a true transition manifold nearby. The set of critical points of the Hamiltonian function restricted to the fibres, symplectically orthogonal to the axi-symmetric transition manifold, gives an approximate transition manifold as explained in Appendix A.1. Then the Morse bifurcations of the approximate transition states will be qualitatively the same as those of the actual transition states.

In the axi-symmetric case, the Hamiltonian function becomes

$$H_0 (z) = \frac{1}{2} \left(p_x^2 + \frac{1}{x^2} p_\beta^2 \right) + \frac{1}{2} x^2 \left(2 - x^2 \right),$$

where β is a cyclic coordinate, so the angular momentum is conserved, $p_\beta = \lambda_\beta$. The critical points are $\bar{z}_0 = (0, \beta, 0, 0)$ and $\bar{z}_1 = (1, \beta, 0, 0)$, which are now both degenerate. Linearising about $\bar{z}_1$, we find that (x, p_x) are the hyperbolic directions, and (β, p_β) the elliptic ones. Thus, the centre subspace about $\bar{z}_1$ is $\hat{N} = \{z \in M | x = 1, \ p_x = 0\}$, and we find the centre manifold, $N_0 = \{z \in M | x = X_0 (\beta, p_\beta), \ p_x = P_0 (\beta, p_\beta)\}$ by satisfying the invariance equations

$$P_0 - \frac{p_\beta}{X_0^2} \frac{\partial X_0}{\partial \beta} = 0,$$

$$\frac{p_\beta^2}{X_0^3} - 2X_0 \left(1 - X_0^2 \right) - \frac{p_\beta}{X_0^2} \frac{\partial P_0}{\partial \beta} = 0.$$

This is done by choosing $P_0 = 0$ and X_0 satisfying $p_\beta^2 - 2X_0^4 \left(1 - X_0^2 \right) = 0$.

We have actually found a generalised centre manifold that extends beyond a small neighbourhood of $\bar{z}_1$. To check the stability of N_0, i.e. that it remains normally hyperbolic, we need to find appropriate tangent and normal coordinates and consider the linearised equations about N_0. At a point $\tilde{z} = (\tilde{X}_0, \tilde{\beta}, 0, \tilde{p}_\beta)$ on the transition manifold, the tangent vectors are taken to be $\xi_1 = \partial_\beta, \xi_2 = \tilde{p}_\beta \partial_x + 2\tilde{X}_0^3 \left(2 - 3\tilde{X}_0^2 \right) \partial_{p_\beta}$. We then
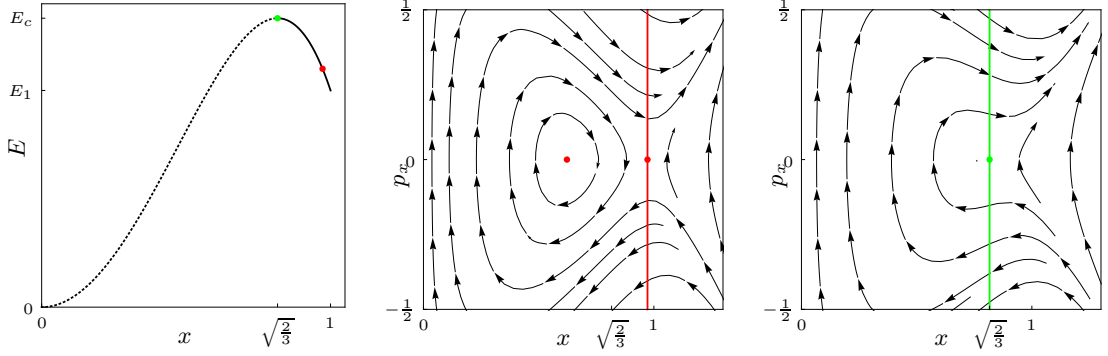
Figure 2.3: Axi-symmetric case: energy of the transition states as a function of r continued (dashed) to the elliptic periodic orbit, and flow in the (x, p_x) plane for an energy in (E_1, E_c) showing the transition state, the dividing surface and the flux through it, and for the bifurcational energy E_c.

choose a Riemannian structure, for which the length is given by

$$\mathrm{d}s^2 = \frac{c^2}{x^2}\left(\mathrm{d}x^2 + x^2\mathrm{d}\beta^2\right) + \mathrm{d}p_x^2 + \frac{1}{x^2}\mathrm{d}p_\beta^2,$$

i.e. proportional to the length in configuration space plus the kinetic energy, where the constant c balances the dimensions by having those of velocity, and is set to 1. This allows us to define vectors orthogonal to the transition manifold as $\eta_1 = 2\tilde{X}_0^3\left(3\tilde{X}_0^2 - 2\right)\partial_r + \tilde{p}_\beta\partial_{p_\beta}$ and $\eta_2 = \partial_{p_x}$. Finally, the first variation equations for $\nu = v_1\xi_1 + v_2\xi_2 + v_3\eta_1 + v_4\eta_2$ are

$$\dot{v} = \begin{pmatrix} 0 & \frac{1}{\tilde{X}_0 f(\tilde{X}_0)} & 0 & \frac{1 + 8\tilde{X}_0^2 - 12\tilde{X}_0^4}{2\tilde{X}_0^6 f(\tilde{X}_0)} \\ 0 & 0 & \tilde{p}_\beta & 0 \\ 0 & 0 & 0 & \frac{2}{\tilde{X}_0^3} \\ 0 & 0 & 2\tilde{X}_0^3(3\tilde{X}_0^2 - 2) & 0 \end{pmatrix} v,$$

where $f(\tilde{X}_0) = 1 + 7\tilde{X}_0^2 - 24\tilde{X}_0^4 + 18\tilde{X}_0^6$ and is negative in the region of interest. This choice of splitting is not invariant, but we can see that N_0 is normally hyperbolic for $X_0 \in (\sqrt{2/3}, 1]$. The point $X_0 = \sqrt{2/3}$ is the steepest point of the potential, at which the normally hyperbolic periodic orbit emanating from the critical point $\bar{z}_1$, that is the transition state, collides with the elliptic periodic orbit from the crater of the volcano in a centre-saddle bifurcation [Han07, Section 3.1]. Interestingly, at $X_0 = \sqrt{2/3}$ when normal hyperbolicity is lost, the symplectic form restricted to the transition manifold ω_N also becomes degenerate.

In the axi-symmetric case, we can use the dividing manifold construction method of Section 2.2. The fibres, symplectically orthogonal to N_0 are

$$F_{\bar{z}}^0 = \{z \in U | \beta = \tilde{\beta} + \frac{2\tilde{X}_0^3\left(2 - 3\tilde{X}_0^2\right)}{\tilde{p}_\beta}p_x, \ p_\beta = \tilde{p}_\beta\}.$$

37

Thus the restricted Hamiltonian function, linearised about $\tilde{z} \in N_0$ is

$$H_0|_{F_{\tilde{z}}^0}(z) = E_0 + \frac{1}{2}p^2 - 2\left(3\tilde{X}_0^2 - 2\right)q^2 + \mathcal{O}\left(q^3\right).$$

The functions $A_{\tilde{z}}^-(z) = p$, $A_{\tilde{z}}^+(z) = -q$ satisfy the necessary conditions of Section 2.2, and

$$S_{\tilde{z}} = \{z \in U|A_{\tilde{z}}^+(z) = \tilde{X}_0 - x = 0\}.$$

Flow in the (x, p_x) plane showing the dividing surfaces and the flux through them, for an energy in (E_1, E_c) and for the bifurcational energy E_c, are shown in Figure 2.3. There are clearly recrossings even for small energies above $\bar{z}_1$ due to the geometry of the system, but these are not local (see definition in Section 1.3). The local recrossings only appear when the transition state loses normal hyperbolicity at $X_0 = \sqrt{2/3}$.

Returning to the full system, we can now find an approximate transition manifold, N_1, by constructing a fibration of a local neighbourhood of N_0, with symplectically orthogonal fibres $F_{\tilde{z}}^0$, for $\tilde{z} = (\tilde{\beta}, \tilde{p}_\beta) \in N_0$, and then defining $N_1 = \{z \in M|d_z H_{F_{\tilde{z}}^0} = 0\}$. The symplectically orthogonal fibres are the ones used previously to find a dividing manifold for the axi-symmetric case. The Hamiltonian function restricted to the fibre $F_{\tilde{z}}^0$ is

$$H_{F_{\tilde{z}}^0}(x, p_x) = \frac{1}{2}\left(p_x^2 + \frac{1}{x^2}\tilde{p}_\beta^2\right) + \frac{1}{2}x^2\left(2 - x^2\right)\left(1 - \varepsilon x \cos\left(\tilde{\beta} + \frac{2\tilde{X}_0^3\left(2 - 3\tilde{X}_0^2\right)}{\tilde{p}_\beta}p_x\right)\right),$$

so linearising about N_0 (by letting $x = \tilde{X}_0 + \varepsilon X_1$, $p_x = \varepsilon P_1$) and taking the exterior derivative gives

$$d_z H_{F_{\tilde{z}}^0} = \frac{\varepsilon^2}{2}\left[8\left(2 - 3\tilde{X}_0^2\right)X_1 - \tilde{X}_0^2\left(6 - 5\tilde{X}_0^2\right)\cos\tilde{\beta}\right]dX_1$$
$$+ \varepsilon^2\left[P_1 - \frac{\tilde{X}_0^6\left(4 - 8\tilde{X}_0^2 + 3\tilde{X}_0^4\right)}{\tilde{p}_\beta}\sin\tilde{\beta}\right]dP_1 + \mathcal{O}\left(\varepsilon^3\right).$$

Asking that $d_z H_{F_{\tilde{z}}^0} = 0$, we obtain

$$X_1 = \frac{\tilde{X}_0^2\left(6 - 5\tilde{X}_0^2\right)}{8\left(2 - 3\tilde{X}_0^2\right)}\cos\tilde{\beta} + \mathcal{O}\left(\varepsilon\right)$$

$$P_1 = \frac{\tilde{X}_0^6\left(4 - 8\tilde{X}_0^2 + 3\tilde{X}_0^4\right)}{\tilde{p}_\beta}\sin\tilde{\beta} + \mathcal{O}\left(\varepsilon\right).$$

and so

$$N_1 = \{z \in M|x = X_0(p_\beta) + \varepsilon X_1(\beta, p_\beta) + \mathcal{O}\left(\varepsilon^2\right), \, p_x = 0 + \varepsilon P_1(\beta, p_\beta) + \mathcal{O}\left(\varepsilon^2\right)\}.$$
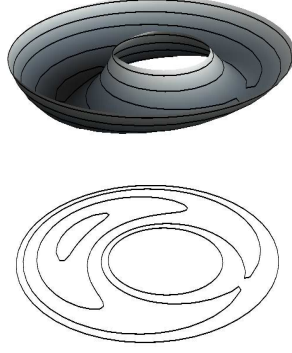
Figure 2.4: Graph of the Hamiltonian function restricted to the transition manifold H_N, over an annulus in (β, p_β), for the disconnecting example and its projections showing the transition states.

Then the restricted Hamiltonian is

$$
\begin{aligned}
H_N\left(\beta, p_\beta\right) &= \frac{1}{2}\left(\varepsilon^2 P_1^2 + \frac{1}{X^2} p_\beta^2\right) + \frac{1}{2} X^2\left(2 - X^2\right)\left(1 - \varepsilon X \cos \beta\right) \\
&= \frac{1}{2}\left(\frac{p_\beta^2}{X_0^2} + X_0^2\left(2 - X_0^2\right)\left(1 - \varepsilon X_0 \cos \beta\right)\right) - \varepsilon X_1\left(\frac{p_\beta^2}{X_0^3} - 2 X_0\left(1 - X_0^2\right)\right) + \mathcal{O}\left(\varepsilon^2\right) \\
&= \frac{1}{2} \frac{1}{X_0^2} p_\beta^2 + \frac{1}{2} X_0^2\left(2 - X_0^2\right)\left(1 - \varepsilon X_0 \cos \beta\right) + \mathcal{O}\left(\varepsilon^2\right),
\end{aligned}
$$

and is actually independent of X_1 and P_1 to first order in ε. Note that we have dropped the subscript 1. Finally, the transition states are given to order ε as the level sets of the restricted Hamiltonian function, $N_E = H_N^{-1}(E)$.

The approximate dividing surfaces are then the level sets of an approximate dividing manifold chosen to be

$$
S = \left\{z \in M \mid x = X_0\left(p_\beta\right) + \varepsilon X_1\left(\beta, p_\beta\right) + \mathcal{O}\left(\varepsilon^2\right)\right\}.
$$

This spans the approximate transition manifold, which is not invariant, so it does not have minimal geometric flux and the two halves will not be unidirectional, in general. However, there are true transition manifold and dividing manifold nearby. The true transition manifold due to normal hyperbolicity and the true dividing manifold by our construction of Section 2.2.

We now consider the topology of the transition states and the dividing surfaces. Starting with the transition state, we find that within the normally hyperbolic region, the restricted Hamiltonian function H_N has critical points $\tilde{z}_1 = (0, 0)$ and $\tilde{z}_2 = (\pi, 0)$ with $X_0 = 1$. These have index $\tilde{\lambda}_1 = 0$ and $\tilde{\lambda}_2 = 1$, and energies $\frac{1}{2}(1 - \varepsilon)$ and $\frac{1}{2}(1 + \varepsilon)$, respectively. Starting from the critical point with least energy, $\tilde{z}_1$, by the Morse lemma and Theorem A.3.3, for energies below that at $\tilde{z}_2$ the transition state is diffeomorphic to a circle, $\mathbb{S}^1$. Increasing the energy and passing the critical point $\tilde{z}_2$ results in a bifurcation and the topology of N_E changes, according to Theorem A.3.4, to $2\mathbb{S}^1$, see Figure 2.4. Thus, we have found our first example of a transition
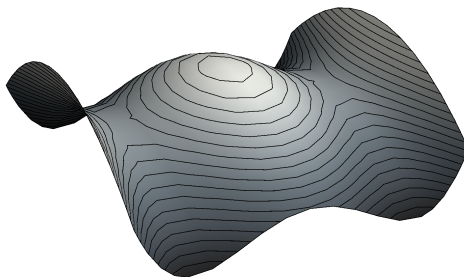
Figure 2.5: Graph of the potential energy in the connecting transition states example.

state Morse bifurcation, and therefore of a transition state not diffeomorphic to $\mathbb{S}^{2m-3}$, namely $2\mathbb{S}^1 \ncong \mathbb{S}^1$. Similarly, we see that the dividing surface bifurcates and changes from a sphere $\mathbb{S}^2$ to a torus $\mathbb{T}^2$. It can be useful for extrapolation to higher degrees of freedom to write the transition state as $\mathbb{S}^0 \times \mathbb{S}^1$ ($\mathbb{S}^0$ being the two-point set $\{\pm 1\}$) and the dividing surface as $\mathbb{S}^1 \times \mathbb{S}^1$.

Care must be taken in studying the Morse bifurcations, as the critical points of the restricted Hamiltonian functions are also critical points of the original Hamiltonian and therefore cause a change in the topology of the energy levels. In this example, the bottleneck opens up and the energy levels change topology, but we can still distinguish two regions and consider transport between them.

Morse theory applies to manifolds of all dimensions. This example can therefore be coupled to another (or more) oscillating degree of freedom to give a 3 degree of freedom system with Hamiltonian function

$$H\left(z\right) = \frac{1}{2}\left(p_x^2 + \frac{p_\beta^2}{x^2}\right) + \frac{x^2}{2}\left(2 - x^2\right)\left(1 - \varepsilon x \cos \beta\right) + \frac{b}{2}\left(v^2 + u^2\right) + \delta V\left(x, \beta, u\right).$$

In the uncoupled case, with $\delta = 0$, there is no energy transfer with the new degree of freedom, so we can effectively consider the original volcano system and the oscillator separately. For energy above the maximum on the volcano rim in the volcano degree of freedom, the transition state bifurcates from $\mathbb{S}^3$ to $\mathbb{S}^2 \times \mathbb{S}^1$ and the dividing surface from $\mathbb{S}^4$ to $\mathbb{S}^3 \times \mathbb{S}^1$. A small perturbation, $\delta \neq 0$, couples the degrees of freedom, but the normally hyperbolic transition manifold persists, along with the Morse bifurcation, so the same scenario occurs. Specific examples of higher degree of freedom systems exhibiting this Morse bifurcation will be seen in Section 3, where we consider bimolecular reactions.

2.4.2 Example. Connecting transition states

This example is found in applications such as narcissistic isomerisation reactions, that is chemical reactions in which a given molecule changes from one of its stereoisomers to the mirror image. References to this and other chemical reactions in which this bifurcation appears can be found in Ezra and Wiggins [EW09], where this example is also considered. They however focus on a neighbourhood of the index-2 critical point

40

of the Hamiltonian function and the influence of this critical point on the transport, whereas we consider the complete picture.

The Hamiltonian system in question has $T^*\mathbb{R}^2$ as its state space, with its canonical symplectic form and the Hamiltonian function

$$H(z) = \frac{a_2}{4} + \frac{a_1}{2}\left(y^2 - x^2\right) + \frac{a_2}{2}\left(v^2 - u^2\right) + \frac{a_2}{4}u^4,$$

where $z = (x, u, y, v)$ and $a_1, a_2 \in \mathbb{R}^+$. The critical points of the Hamiltonian function are the origin, $\bar{z}_0$, and $\bar{z}_\pm = (0, \pm 1, 0, 0)$, with index 2 and 1, respectively.

We are interested in transport between the two regions on either side of the two index-1 critical points and therefore the x-axis, see Figure 2.5. We therefore expand the Hamiltonian function about these critical points by shifting the u-axis, namely $u = \pm 1 + \tilde{u}$ to get

$$H(z) = \frac{a_1}{2}\left(y^2 - x^2\right) + \frac{a_2}{2}\left(v^2 + 2u^2\right) + H_n(z),$$

with the higher order terms $H_n(z) = \pm a_2 u^3 + a_2 u^4/4$, where the tildes have been dropped. Thus the centre subspaces of the critical points are seen to be $\hat{N}(\bar{z}_\pm) = \{z \in M | x = y = 0\}$. Seeing as the system is uncoupled, the (local) centre manifolds can be chosen to be equal to the centre subspaces.

The two centre manifolds form part of a larger codimension-2 invariant submanifold, given by

$$N = \{z \in M | x = y = 0\},$$

for which we must check the stability, ensuring that we have normal hyperbolicity and so a transition manifold. This is done by linearising the vector field about N and comparing the linear flows in the the normal, with $\eta_1 = 2^{-1/2}\left(\partial_x - \partial_y\right)$ and $\eta_2 = 2^{-1/2}\left(\partial_x + \partial_y\right)$, and the tangent, with $\xi_1 = \partial_u$ and $\xi_2 = \partial_v$, directions. The linearised equations of motion, about a point $\tilde{z} = (\tilde{u}, \tilde{v})$ in N, are

$$\dot{v} = \begin{pmatrix} 0 & a_2 & 0 & 0 \\ a_2 - 3\tilde{u}^2 & 0 & 0 & 0 \\ 0 & 0 & a_1 & 0 \\ 0 & 0 & 0 & -a_1 \end{pmatrix} v,$$

where $\nu = v_1\xi_1 + v_2\xi_2 + v_3\eta_1 + v_4\eta_2$. The normal dynamics are clearly hyperbolic. Instead, the dynamics tangent to N depend on the point $\tilde{z}$ on the manifold. For $\left(a_2 - 3\tilde{u}^2\right) < 0$ the motion is elliptic, whereas for $\left(a_2 - 3\tilde{u}^2\right) > 0$ it is hyperbolic. Although in this uncoupled system we do not need N to be normally hyperbolic, we do to continue the conclusions to cases with small coupling. We therefore compute a condition ensuring that the normal dynamics still dominates the tangent one. The coefficient $\left(a_2 - 3\tilde{u}^2\right)$ is greatest when $\tilde{u} = 0$, thus with $a_1 > a_2$ the transition manifold is normally hyperbolic. In the basic scenario, (half of) the normally hyperbolic degree of freedom gives the transport direction. At the critical point $\bar{z}_0$ however, the two directions "compete" because the tangent dynamics becomes hyperbolic. If the transition
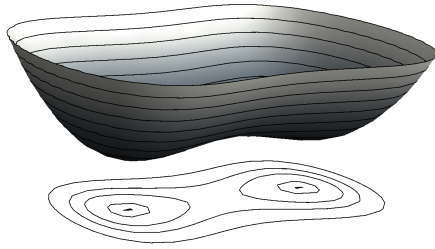
Figure 2.6: Graph of the Hamiltonian function restricted to the transition manifold for the connecting example and its projections, the transition states.

manifold stays normally hyperbolic, i.e. the potential energy (surface) is steepest in the x direction, then the transport coordinate is preserved.

Finding a dividing manifold for this example is easy due to the lack of coupling. A simple fibration of a neighbourhood of N has fibres given by $F_{\tilde{z}} = \{u = v = 0\}$. Restricting the Hamiltonian function to such fibres gives the necessary normal form Hamiltonian. The functions $A_{\tilde{z}}^-(z) = y$, $A_{\tilde{z}}^+(z) = \{H, A_{\tilde{z}}^-\} = -a_1 x$ then satisfy the necessary conditions of Section 2.2. Therefore, a dividing manifold is given by

$$S = \{z \in M | x = 0\}.$$

As usual, we can write the transition states as level sets of the Hamiltonian function restricted to N,

$$H_N(u, v) = \frac{a_2}{4} + \frac{a_2}{2}(v^2 - u^2) + \frac{a_2}{4}u^4.$$

This has the origin, $\tilde{z}_0$, and $\tilde{z}_\pm = (\pm 1, 0)$ as its critical points, with indices $\tilde{\lambda}_0 = 1$, $\tilde{\lambda}_\pm = 0$. Thus the transition states bifurcate and change from $2\mathbb{S}^1$ to $1\mathbb{S}^1$. That is, as the energy is increased, the periodic orbits emanating from $\tilde{z}_\pm$ meet in homoclinic bifurcations at $\tilde{z}_0$ and connect to become one. For energies below that at $\bar{z}_0$, this example therefore exhibits a transition state different from the usual basic scenario periodic orbit. This transition state is however the disjoint union of two periodic orbits, so if we had restricted our attention to a single index-1 critical point, we could have easily missed this more global picture.

Similarly, by considering H_S, we find that two dividing surfaces diffeomorphic to $\mathbb{S}^2$ about the index-1 critical points of H connect to form a single sphere, $\mathbb{S}^2$, as the energy is increased. The energy levels also bifurcate as we pass the critical point $\bar{z}_0$. Starting with an energy just above that at $\bar{z}_\pm$ and increasing it, we see that the two bottlenecks open up until they meet and become one, with the two regions of interest remaining the same.

We have considered here the uncoupled, symmetric case in which the three critical points are aligned on $x = 0$ with $u \to -u$ symmetry. However, due to the persistence of normally hyperbolic submanifolds, adding coupling between the (x, y) and (u, v) degrees of freedom will not alter the conclusions about the bifurcation. For this, the normal hyperbolicity condition $a_1 > a_2$ is essential. We could also break the $u \to -u$

symmetry, in which case the saddles have different energy, so as the energy increases we first obtain one $\mathbb{S}^1$ then $2\mathbb{S}^1$, followed at the index-2 energy by qualitatively the same transition to $1\mathbb{S}^1$.

Now consider coupling our example to another oscillating degree of freedom. The Hamiltonian function for this could be

$$H\left(z\right) = \frac{a_2}{4} + \frac{a_1}{2}\left(y^2 - x^2\right) + \frac{a_2}{2}\left(v^2 - u^2\right) + \frac{a_2}{4}u^4 + b\left(p^2 + q^2\right) + \delta V\left(x, u, q\right).$$

In the uncoupled case with $\delta = 0$, the transition state bifurcates from $2\mathbb{S}^3$ to $1\mathbb{S}^3$ and the dividing surface from $2\mathbb{S}^4$ to $1\mathbb{S}^4$. In the coupled case, provided the coupling is sufficiently small, we can treat it as a perturbation of the uncoupled case and invoke the persistence of normally hyperbolic submanifolds to obtain topologically the same picture.

2.4.3 Other Morse bifurcations

If we restrict our attention to 2 degrees of freedom simple mechanical Hamiltonian systems, the critical points of the restricted Hamiltonian H_N can only have index 0 or 1. At index-0 critical points a transition state is "created", whereas at critical energies corresponding to index-1 critical points, seeing as the transition state is closed, the transition state is generically a *figure eight* (more complicated cases can occur if there are several critical points with the same energy). Thus, the only generic bifurcations scenarios are the connection and disconnection ones found in Subsections 2.4.1 and 2.4.2.

It should be noted however, that this limitation on the types of Morse bifurcations of the transition states does not place significant restrictions on the bifurcations of the dividing surfaces. Just as we have found genus-1 dividing surfaces (as well as genus-0), we expect any genus surface should be possible. We expect that limitations will instead come from the transport problems and that these dividing surfaces will only appear in Hamiltonian systems for which the transport problem is not well defined.

For natural systems with 3 degrees of freedom or higher, we have seen how the connecting and disconnecting scenarios with index-1 critical points of the restricted Hamiltonian function can be coupled to other degrees of freedom. Such systems may also have higher index critical points, which will give rise to other Morse bifurcations. Explicit examples of connecting, disconnecting and also higher index Morse bifurcations will be seen in the next section in which a hypothetical class of planar bimolecular reactions is considered as an application of the previous sections. Here we find various sequences of Morse bifurcations.

2.5 Flux of ergode as a function of energy

Once we have chosen a dividing surface S_E, the rate of transport is found by computing the flux of ergode through it in a given direction. In this Section, we address the differentiability of the flux as a function of energy, which determines the shape of the

graph. This is necessary in order to connect to experiments such as in [MX⁺91] (a different RS MacKay, we hasten to add!). Our approach is similar to that of Van Hove in his study of the singularities in the elastic frequency distribution of crystals [Van53], which is related to the singularities of density of states, now known as Van Hove singularities. Also, Hoveijn has considered the differentiability of the volume of level sets of submanifolds of $\mathbb{R}^n$ [Hov08].

Recall from Section 1.2, Theorem 1.2.2, that for regular energy levels M_E, the flux through a surface S_E^+ with boundary N_E is

$$\phi_E\left(S_E^+\right) = -\int_{N_E} \Theta_E,$$

where $\Theta_E = \frac{1}{(m-1)!}\theta \wedge \omega^{m-2}$ is a "generalised" action form. In order to compute the flux, we may therefore focus on the transition states, as opposed to the dividing surfaces, provided the latter do not break down. We shall assume this to be the case.

As a function of energy, the flux through local dividing surfaces in the basic transport scenario was already considered in Section 1.4, and is given by

Proposition 2.5.1. *The flux $\phi_E\left(S_E^+\right)$ through a dividing surface S_E^+ in the neighbourhood of an index-1 critical point of the Hamiltonian H, with energy E just above the critical value E_1, is given to leading order by*

$$\phi_E\left(S_E^+\right) = \frac{\Delta E^{m-1}}{(m-1)!}\prod_{i=1}^{m-1}\frac{2\pi}{b_i},$$

where $\Delta E = E - E_1 > 0$ and b_j are the normal form frequencies.

Proof. In the basic transport scenario, for small $\Delta E = E - E_1 > 0$, the transition state $N_E = H_N^{-1}(E)$ is a small $(2m-3)$-sphere, so it is sufficient to consider the leading orders of the restricted Hamiltonian H_N in Williamson normal form. The integral can then be computed, for example, by passing to canonical action-angle variables, $J_i = (v_i^2 + u_i^2)/2$ and $\theta_i = \arctan(v_i/u_i)$, and using Stokes theorem to integrate the volume of the ball $N_{\leq E}$ instead of the generalised action over N_E. □

Increasing the energy E further above that of the index-1 critical point E_1, we find that $N_E \cong \mathbb{S}^{2m-3}$ until the next critical value of H_N, by Theorem A.3.3. Assuming that the dividing surface doesn't break down as the energy is increased, the (set of) critical points of H_S, $C_r(H_S)$ is equal to that of H_N, $C_r(H_S) = C_r(H_N)$. Furthermore, N is invariant, so $C_r(H_N) \subset C_r(H)$. The next step is therefore to consider the flux as a function of energy away from critical values.

Proposition 2.5.2. *For regular values E of the restricted Hamiltonian H_N, the flux $\phi_E(S_E^+)$ through the dividing surface S_E^+ with $\partial S_E^+ = N_E$ is C^r as a function of the energy E if H_N is itself C^r.*

Proof. In order to check that the flux is C^r, we consider an $e < E$ for which there are no critical values of H_N in $[e, E]$ and write $N_E = g_{E-e}(N_e)$, where g_t is the unit-speed

gradient flow (with respect to some metric) satisfying

$$\dot{g}_t(z) = -\frac{\text{grad}H_N}{|\text{grad}H_N|^2}(g_t(z)),$$

which carries N_e into N_E, see e.g. [Mil63, Section I.3]. Then the flux can be written as

$$\phi_E(S_E^+) = \int_{N_e} g_{E-e}^* \Theta_E.$$

Now, since N_e is a regular level set it contains only regular points and we can choose coordinates $z = (u, v) = (u_1, \cdots, u_{2m-3}, v) \in N$ so that $N_e = \{z \in N | v = 0\}$. N_E can be written as a graph over N_e, namely

$$N_E = \{z \in N | H_N(z) = E\} = \{z \in N | v = \bar{v}_E(u)\},$$

by the implicit function theorem, as $dH \neq 0$. The function $\bar{v}_E$ is C^r if H_N is C^r. The gradient flow of points in N_e gives $g_{E-e}(u, 0) = (u, \bar{v}_E(u))$. Finally, the pull-back $g_{E-e}^* \Theta_E$ contains first order derivatives of $\bar{v}$ with respect to u, but these will not affect the smoothness of the flux as a function of E, which is therefore C^r (in E). We are implicitly using a chart for the whole of N, which might not be possible. If not, we would have to find a finite number of simplices to triangulate N_e (which is compact) and then consider the flow of simplices individually, as explained in detail in [Hov08]. $\square$

Note 2.5.3. Even if H is C^∞, H_N need not be very smooth, the most derivatives we can typically assume being given by the ratio of normal to tangential expansion at N. This is usually referred to as the spectral gap condition, see e.g. [Fen71, HPS77].

We shall therefore focus on the differentiability of the flux for E near critical values E_i. Global transition states cannot generally be defined in terms of local coordinates. However, by Theorem A.3.4 the sub-level sets just above a Morse bifurcation of index-λ can be written as a handlebody, composed of a lower sub-level set that contributes a C^r term to the flux, by Proposition 2.5.2, and a handle diffeomorphic to $\mathbb{B}^\lambda \times \mathbb{B}^{2(m-1)-\lambda}$. Thus, we deduce that possible changes in the differentiability of the flux occur in a neighbourhood of the critical point, the contribution from the rest being C^r and we will assume that r is sufficiently large. For more details see [Hov08]. Hence, in order to find the smoothness of the flux as a function of the energy, we shall evaluate the integrals only over the handle region, see Figure A.3.

Proposition 2.5.4. *The flux through a dividing surface S_E^+ with small $\Delta E = E - E_2$ where E_2 is a critical value with a single index-2 critical point of H is a C^{m-2} function of the energy E, provided H_N is C^r and r is larger than $m - 2$, where $\partial S_E^+ = N_E$.*

Proof. We want the contribution to the flux from a neighbourhood U of an index-2 critical point of H, so we must integrate the generalised action Θ_E over N_E restricted to U or equivalently, by Stokes' theorem, the volume ϕ_E over $N_{\leq E}|_U$

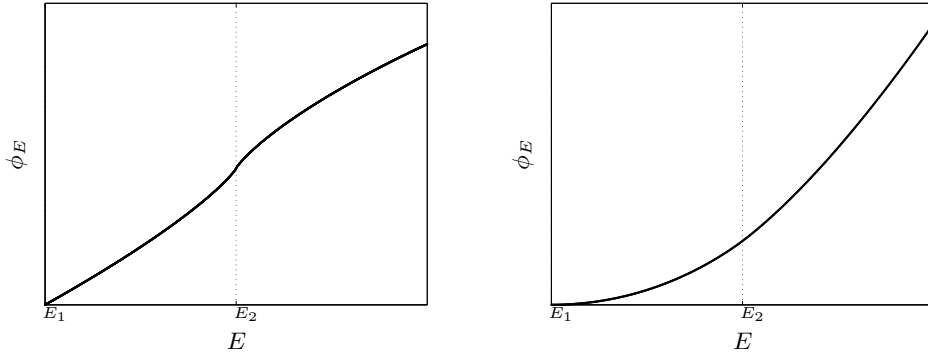$$\int_{N_{\leq E}} \phi_E = \frac{1}{(m-1)!} \int_{N_{\leq E}} \Omega_N,$$

45

Figure 2.7: Graphs of ϕ_E as a function of energy E for a transition state undergoing a disconnecting Morse bifurcation at E_2, cf. Subsection 2.4.1. Left: two degree of freedom system. Right: three degree of freedom system.

where $\Omega_N = \omega^{m-1}$, as $\phi_E = \omega^{m-1}/(m-1)!$. Since N is normally hyperbolic, it is symplectic by Proposition A.1.2, and there is a canonical linear transformation to Williamson normal form coordinates in which

$$H_N(z) = H_2(z) + H_n(z) = \frac{a_1}{2}\left(v_1^2 - u_1^2\right) + \sum_{j=2}^{m-1} \frac{b_j}{2}\left(v_j^2 + u_j^2\right) + H_n(z),$$

assuming that $H_N(\bar{z}_2) = E_2 = 0$. Then $\Omega_N = \Omega_N^0 = dz_1 \wedge \cdots \wedge dz_{2m-2}$.

Alternatively, the isochoric Morse lemma (see Remark A.3.2) gives H_N as a polynomial in H_2, $\Psi(H_2)$ and the standard volume form Ω_N^0.

By the Morse lemma (see Remark A.3.2), we can find a smooth near-identity transformation F such that

$$F^* H_N = H_2,$$
$$F^* \Omega_N^0 = \psi(H_2)\Omega_N^0 = (1 + \tilde{\psi}(H_2))\Omega_N^0.$$

If we write $N^2_{\leq E} = H_2^{-1}((-\infty, E])$, then

$$\int_{N_{\leq E}} \Omega_N = \int_{N^2_{\leq E}} \Omega_N^0 + \int_{N^2_{\leq E}} \tilde{\psi}(H_2(z))\Omega_N^0.$$

In order to find the differentiability of $\phi_E(S_E)$ with respect to E, it is sufficient to consider the first integral, as it contains the lowest order terms in ΔE and we are interested in $\Delta E \to 0$. Computing this integral, restricted to a neighbourhood of $\bar{z}_2$, we find a term of the form

$$|\Delta E|^{m-1} \ln|\Delta E| \text{ for } \Delta E < 0,$$
$$-\Delta E^{m-1} \ln|\Delta E| \text{ for } \Delta E > 0,$$

which limits the smoothness of the flux as a function of the energy to C^{m-2}, as well as polynomial terms in ΔE, cf. [Hov08]. $\qquad\square$

Graphs of ϕ_E as a function of E for a transition state undergoing a disconnecting

46

Morse bifurcation, as in Subsection 2.4.1, can be seen in Figure 2.7. One is a graph for flux through a dividing surface spanning a periodic orbit transition state of a two degree of freedom system, for which we see the log-like infinite slope singularity at the index-1 Morse bifurcation, whereas the other is a graph of the flux for a three dimensional transition state of a three degree of freedom system. For systems with more degrees of freedom than two, the Morse bifurcations do not have a significant effect on the flux, which varies C^{m-2} smoothly through these.

Similarly, we can consider how the flux changes at Morse bifurcations involving a critical point of any index. Ultimately, we are studying the differentiability of the volume of level sets about critical values. This has been studied by Hoveijn [Hov08], who tells us that the smoothness will always be limited to C^{m-2}, irrespective of the index λ for $\lambda \geq 1$. However, the nature of the discontinuity does depend on the index [Hov08, Proposition 9].

In conclusion, except when the number m of degrees of freedom is small, Morse bifurcations do not have a significant effect on the flux of ergode, which varies C^{m-2} smoothly through these. Provided $m - 2 < r$, the Morse bifurcation will cause a small kink in the graph of $\phi_E(S_E^+)$ over E. We do not however expect that these will be visible from experimentally obtained reaction rates, in which other physical considerations probably have a larger impact on the shape of the graph.

Chapter 3

Application. Morse bifurcations in bimolecular reactions

3.1 Introduction. Reaction, capture and rates of transport

One way of finding rates of reaction is to consider rates of transport in a low dimensional Hamiltonian system representing the specific reaction. Some of the first examples studied using transition state theory consisted of bimolecular reaction in gaseous phase,

$$A + B \to \text{products},$$
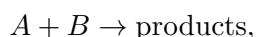
where the two (polyatomic) molecules are denoted A and B. Provided the Born-Oppenheimer approximation holds, we can pass from the quantum mechanical system to a classical one, namely the Hamiltonian system for the motion of the nuclei interacting via a potential given by the (ground state) energy of the electrons[*30] as a function of the internuclear coordinates. Then, as outlined in Chapter 1, by assuming that this extremely high dimensional (of the order of Avogadro's constant) Hamiltonian system is, at any instant, the product of "reacting" two molecule sub-systems that are independent of each other, we may consider consider the evolution of an ensemble of individual reactions in this low dimensional Hamiltonian sub-system. For this assumption to hold, we require the gas to be sufficiently dilute. Finally, we can restrict our attention to the energy levels, and consider the flow of ergode, as a function of the energy. Thus, finding (microcanonical) reaction rates translates to finding the rate of transport of ergode between regions representing reactants and products.

We shall consider transport between the region representing two distant molecules (reactants) and the region in which the molecules are close. The latter region does not however generally constitute the products[*31]. This is the *capture* transport problem associated with the necessary first step of the molecules getting close enough to react.

[*30] Assumed non-degenerate and hence a smooth energy function, else it can have conical singularities, see e.g. [DYK04].

[*31] Association and recombination reactions are largely limited to reactions in condensed phase or solvent, see e.g. [HH08, Chapter 1]

The *capture rate* (sometimes also called *collision rate*) provides an upper bound on the reaction rate, as we do not expect all captured trajectories to proceed to the products region [CSB80]. Note that, there might actually be multiple product regions, however for the capture process between two molecules there is only one final region of interest.

Capture rates are crucial for many physical processes, and have a long history dating back at least to 1905 with Langevin's early contribution [Lan05]. See e.g. review by Chesnavich and Bowers [CB82]. Two common assumptions are usually found in the literature. Firstly, the reacting Hamiltonian systems are assumed to have Euclidean symmetry, that is to be invariant under translations and rotations. This is the case for gas phase reactions with no background (electro-magnetic) field. The Hamiltonian system can then be reduced to a family of systems, in centre of mass frame, parametrised by the angular momentum. Secondly, the energy is taken to be below those at which the two molecules dissociate and centrifugal and Coriolis forces to be sufficiently weak such that the molecules are well defined and in the small vibrations regime[*32]. These assumptions allow us to distinguish between intermolecular degrees of freedom (distance and relative attitudes of the molecules) and intramolecular ones. We too shall consider systems that satisfy these assumptions.

We want to find the rate of capture, which we shall assume can be thought of as transport between regions on either side of a non-degenerate maximum $\bar{x}_c$ of the effective potential with respect to the intermolecular distance x. In the literature, this maximum is generally assumed to be a centrifugal maximum obtained by balancing the repulsive centrifugal terms with the attractive long distance potential energy. Alternatively, $\bar{x}_c$ could be a non-degenerate chemical maximum of the bimolecular potential and therefore of the effective potential for small angular momentum.

Provided $\bar{x}_c$ is sufficiently large, such that capture occurs in a region where the potential is only weakly dependent upon the attitudes of the molecules, and sufficiently non-degenerate, we shall see that fixing the intermolecular distance degree of freedom to the maximum value gives a normally hyperbolic transition manifold, which can be spanned by a dividing manifold satisfying $x \approx \bar{x}_c$. The restriction of these manifolds to the energy levels gives dividing surfaces and transition states, which we shall refer to as *capture* transition states. The literature often refers to them as *orbiting* or *loose* transition states [CB82, Pec76].

Some analysis of the structures in reaction dynamics in rotating molecules has been done recently in [CW12, KK11a], but we are interested in the interaction of two rotating molecules.

The central field model, in which the attitudes of the colliding pair are ignored, is attributed to Langevin [Lan05]. In this very early work, one already finds capture periodic orbit transition states. However Langevin, like many after him, considers the capture process using scattering theory. Introductions to scattering theory can be found in most books on classical mechanics, e.g. [GPS02, Section 3.10]. For a comparison

---

[*32] We are implicitly assuming that the molecules are *normal*, i.e. that they have a rigid equilibrium configuration. Molecules that are not normal are referred to as *anomalous*. We avoid the term *rigid*, as it might lead to confusion with the rigid body limit, in which the vibrations have been suppressed.

of the scattering theory and the dividing surface approaches to capture problems see [CB82].

Non-central fields were considered later, starting with the works of Pechukas [Pec80] and Chesnavich, Su and Bowers [CSB80]. The intramolecular degrees of freedom consist of small vibrations, by assumption. Instead, as the energy is varied, the intermolecular attitude degrees of freedom, as well as the angular momentum one, will generally be involved in interesting sequences of Morse bifurcations of the capture transition states and dividing surfaces. Physically, the Morse bifurcations involving the attitude degrees of freedom reflect the fact that as the energy is increased the molecules can capture each other for a greater range of relative attitudes, i.e. the "cone of acceptance" for capture, as it is called in the chemistry literature, opens up. That is the energy-levels change diffeomorphism class, thus causing changes in the dividing surfaces and transition states also. The simplest examples consist of planar reactions. Therefore in Section 3.2, we consider planar capture between an atom and a diatom in detail, and then also present the Morse bifurcations for diatom-diatom reactions without repeating the details. The spatial case is considered in Section 3.4, after we have reviewed symplectic reduction of n-body systems in Section 3.3. We choose to use the coordinates that one obtains via the gauge theoretic approach to cotangent bundle reduction as outlined by Littlejohn and Reinsch [LR97], and reviewed in Appendix A.4.

Following the transition states through the Morse bifurcations allows us to compute the flux through the dividing surfaces for energies above the critical values, and thus find the reaction rates for a larger range of energies.

Whether captured pairs then go on to react can be thought of as a further transport problem and will generally involve other transition states and dividing surfaces, possibly associated to other maxima $\bar{x}_i$ of the effective potential. We shall refer to these as *reaction* transition states, though they are often also called *tight* transition states. The capture and reaction transition states are therefore in series. The simplest case will be when these are distant and the level sets of separate transition manifolds. However, even when "separate" their stable and unstable manifolds, which act as transport barriers, will intersect, possibly in non-trivial ways, determining the reaction "channels". Some trajectories joining reactants and products might roam in the region between the two (capture and reaction) dividing surfaces, that is follow trajectories with a non-monotonic intermolecular distance in time, before finally crossing the reaction dividing surface. This is to be expected because of coupling between degrees of freedom, and was recently given as an explanation of what chemists have been calling *roaming reactions* [MC+14, BS11].

Reaction rates have an equally long history as capture rates, and bimolecular reactions have played the role of test problems since the early days of transition state theory (as noted in [Wig38]). The transport problems associated with reaction tend to be harder, both because there is usually no separation of scales that one can use to simplify the system and because the chemical potentials are at best not simple and often degenerate. Similarly to how the first capture models were simplified by making the fields central, reaction rates were first, and largely still, considered for collinear and
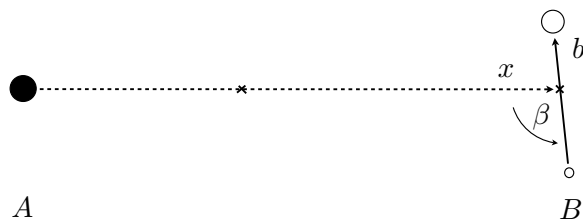
Figure 3.1: Choice of Jacobi vectors and reduced coordinates for planar atom-diatom reactions.

planar systems with zero angular momentum. The simplest bimolecular reactions, after those between atoms, are the ones between an atom and a diatom, such as the transfer reaction between H and H_2, in which a H atom swaps partner. In the collinear regime, these have two degrees of freedom, so possible transition states are periodic orbits. These have been found to bifurcate and loose normal hyperbolicity, see e.g. [DVB55, PP78, Dav87], according to the well known bifurcations of periodic orbits, see e.g. [AM78, Chapter 8]. These examples lack the attitude degrees of freedom which we shall see are involved in the Morse bifurcations for the capture transition states.

3.2   Planar reactions

Reactions with planar initial conditions, that is initial positions and momenta confined to a plane, remain in this plane for all successive times. Such systems constitute an invariant subset of all n-body systems that is a particularly simple and easy to reduce, via changes of coordinates involving the symmetries and momenta, assuming the angular momentum is non-zero. Reduced planar systems have no angular momentum degree of freedom and no coordinate singularities at collinear configurations. Planar reactions are therefore ideal as first examples of Morse bifurcations of the capture transition states, and associated dividing surfaces. We now present two examples, namely planar atom-diatom and diatom-diatom reactions. Symmetries and reduction of n-body systems are discussed in Section 3.3.

3.2.1   Example. Planar atom-diatom reactions

The simplest non-trivial example is planar reactions between an atom and a diatom. We shall consider reactions with no background (electro-magnetic) field. In this case, the molecular potential is a translationally and rotationally invariant function, and the Hamiltonian system possesses Euclidean symmetry. Furthermore, by Noether's theorem, the linear and angular momenta are conserved. Therefore, the system can be reduced, as explained in Section 3.3.

   The planar reduced three-body Hamiltonian system, parametrised by the angular

51

momentum λ, is the mechanical system $(T^*\mathbb{R}^3_+, \omega, H)$, with

$$H(z; \lambda) = \frac{1}{2}\left(\frac{1}{m}p_x^2 + \frac{1}{m_b}p_b^2 + \left(\frac{1}{m_b b^2} + \frac{1}{mx^2}\right)\left(p_\beta - \frac{m_b b^2}{mx^2 + m_b b^2}\lambda\right)^2\right) + V(q; \lambda),$$

$$V(q; \lambda) = \frac{1}{2}\frac{\lambda^2}{mx^2 + m_b b^2} + U(q)$$

and

$$\omega = \mathrm{d}x \wedge \mathrm{d}p_x + \mathrm{d}b \wedge \mathrm{d}p_b + \mathrm{d}\beta \wedge \mathrm{d}p_\beta,$$

where the coordinates are the intermolecular distance x, the attitude β and length b of the diatom, and their canonical momenta, depicted in Figure 3.1. V is the effective potential of the reduced system with the centrifugal term. The parameters are the reduced masses m and m_b, and the magnitude of the angular momentum λ. The notation is the same as the one we will use for spatial reactions between non-collinear molecules in Section 3.4.

We have chosen canonical coordinates, in which the Coriolis term is in the Hamiltonian function, as opposed to the more appropriate non-canonical coordinates that move this term to the symplectic form and simplify the Hamiltonian function, see discussion in Appendix A.4. This choice is motivated by our need to scale the system and desire to have all scale effects restricted to the Hamiltonian function for easy comparison.

For energies below that at which the diatom dissociates, we have a two-body capture problem. We shall restrict our attention to this scenario. The reduced coordinates and their momenta then split into intermolecular (x, β) and intramolecular b degrees of freedom.

The diatom will have an equilibrium configuration in the joint atom-diatom potential. This corresponds to a non-degenerate minimum $\bar{b}(x, \beta)$ of the potential with respect to the intramolecular distance b. We shall assume that this minimum is highly non-degenerate, i.e. that the diatom is strongly bonded. Then, provided the centrifugal and Coriolis forces on the diatom are not too strong, the diatom will vibrate about its equilibrium without significant distortion, so the size of the diatom $\bar{b}(x, \beta)$ is essentially constant.

The intermolecular terms of the potential will be repulsive at short ranges, possibly have a number of chemical maxima with respect to the intermolecular distance x (and therefore minima) in the mid ranges, and be attractive at long ranges, see Figure 3.2. The attractive long range (van der Waal) terms can be found qualitatively by considering the interactions between the charges of the atom and the diatom. As a function of the intermolecular distance, these are inverse k-power terms with $k \geq 4$ [Sto13]. The molecular potential is then summed to the repulsive centrifugal term to give the effective potential. In the long (physical) range, provided the attractive potential falls off faster than the centrifugal potential as $x \to \infty$, i.e. $k > 2$, the effective potential has a centrifugal maximum $\bar{x}_\lambda(b, \beta; \lambda)$. In the short (chemical) range of the potential, the chemical maxima of U with respect to x imply chemical maxima of V for λ small with respect to the slope of U at the maxima. In either case, as λ
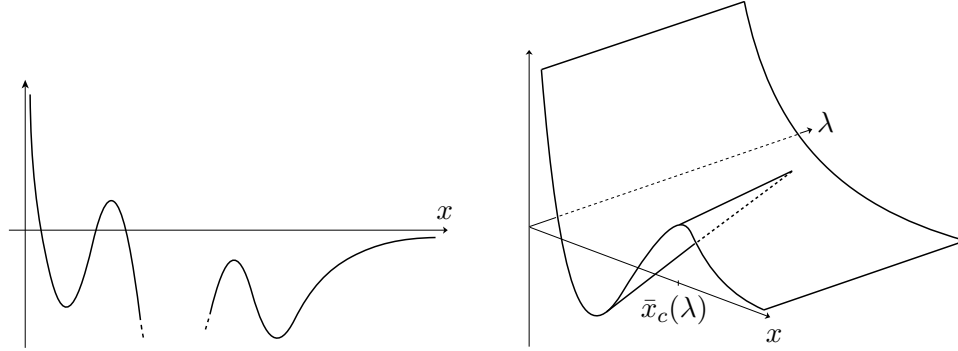
Figure 3.2: Left: Typical graph of molecular potential restricted to the intermolecular distance, with repulsive short range, attractive long range and extrema in between. Right: Example graph of the effective potential over the intermolecular distance and angular momentum (x, λ) showing the disappearance of the intermolecular maximum $\bar{x}_c$, via centre-saddle bifurcations.

increases the maxima will "collide" with the minima and disappear, see Figure 3.2.

We want to find the rate of capture of the atom and the diatom, which we shall think of as transport between the regions on either side of the largest maximum, $\bar{x}_c(b, \beta; \lambda)$. If $\bar{x}_c$ is large with respect to the length of the diatom, the capture and reaction transport problems are separate, provided of course that reactions occurs at small intermolecular distances. This separation of scales will allow us to simplify the Hamiltonian.

To introduce our assumptions into the Hamiltonian, we must scale the variables. For simplicity, we shall ignore any scaling effects due to mass differences by assuming that the masses of the atom and the diatom are similar, so set $m = m_b = 1$. Ideally, this would be taken care of when constructing the Hamiltonian system by non-dimentionalising the variables. Note that normalised or mass-weighted Jacobi coordinates do not remove the mass dependence, but instead just move it to the coordinates. The molecular scale $|x|$, $|b|$ is small with respect to $\beta \sim 1$, however by scaling the time, we can ignore this relative scale.

We start by introducing the capture scale, i.e. setting $b = \varepsilon_c \tilde{b}$ and $p_b = \varepsilon_c^{-1} \tilde{p}_b$ with $0 < \varepsilon_c \ll 1$, since we are interested in a neighbourhood of the capture maximum $\bar{x}_c$, which we take to be of order 1. Essentially, ε_c is the difference between the size of the diatom and it's distance to the atom, however in practice it is chosen such that

$$U(q; \varepsilon_c) = \varepsilon_c^{-2} U_b(\tilde{b}) + U_c^0(x) + \varepsilon_c^2 U_c^2(q; \varepsilon_c).$$

We are assuming that for distant atom-diatom systems, the potential energy is of this form, with very weak dependence on the attitude of the diatom since the pair are distant. This is the case for potential energies that are inverse power functions of the intermolecular distance, which can be expanded using Legendre polynomials.

Dropping the tildes, the Hamiltonian function expands into

$$H(z; \lambda, \varepsilon_c) = \varepsilon_c^{-2} \left(\frac{1}{2} p_b^2 + \frac{1}{2} \frac{p_\beta^2}{b^2} + U_b(b) \right) + \frac{1}{2} p_x^2 + \frac{1}{2} \frac{(p_\beta - \lambda)^2}{x^2} + U_c^0(x)$$
$$+ \varepsilon_c^2 U_c^2(q; 0) + \mathcal{O}\left(\varepsilon_c^4 \right).$$

We note that β first appears in H at order ε_c^2, so $p_\beta = \lambda_\beta + \mathcal{O}\left(\varepsilon_c^2 \right)$ with constant λ_β. Furthermore, the system separates into slow and fast degrees of freedom, i.e. at order ε_c^{-2} we find the fast oscillations of the diatom plus a "centrifugal" term for the diatom, at order ε_c^0 there is the intermolecular (capture) dynamics, and then there are the higher order terms. Up to order ε_c^0, the x and b degrees of freedom are uncoupled, and $p_\beta = \lambda_\beta$. Comparison with the disconnecting example of Section 2.4.1, shows that it could be interpreted as being the Hamiltonian representing capture between an atom and a frozen diatom, with zero angular momentum $\lambda = 0$ and a maximum in the molecular potential U with respect to the distance x.

Next, we linearise the diatom's length about the equilibrium configuration $\bar{b}_0$ of the diatom by setting $b = \bar{b}_0 + \varepsilon_b \tilde{b}$ and $p_b = \varepsilon_b^{-1} \tilde{p}_b$ with $0 < \varepsilon_b \ll 1$. The constant ε_b is chosen such that

$$U(q; \varepsilon) = \varepsilon_c^{-2} \left(U_b(\bar{b}_0) + \frac{1}{2} \varepsilon_b^2 \partial_{bb}^2 U_b(\bar{b}_0) \tilde{b}^2 + \cdots \right) + U_c^0(x) + \varepsilon_c^2 U_c^2(q; \varepsilon_c)$$
$$= \varepsilon_c^{-2} \left(\bar{U}_b^0 + \frac{1}{2} \varepsilon_b^{-2} \bar{U}_b^2 \tilde{b}^2 \right) + U_c^0(x) + \varepsilon_c^2 U_c^2(q; \varepsilon_c) + \mathcal{O}\left(\varepsilon_b^3 \right),$$

where $\bar{U}_b^2$ is order one, and $\varepsilon = (\varepsilon_c, \varepsilon_b)$. Recall that we are assuming $\partial_{bb}^2 U_b(\bar{b}_0)$ to be large. This scaling ensures that the leading order terms of the potential with respect to the coordinates are of the same order as their conjugate momenta in the kinetic energy. Thus, the Hamiltonian function becomes

$$H(z; \lambda, \varepsilon) = \varepsilon_c^{-2} \varepsilon_b^{-2} \frac{1}{2} \left(p_b^2 + \bar{U}_b^2 b^2 \right) + \varepsilon_c^{-2} \frac{1}{2\bar{b}_0^2} p_\beta^2 + \left(\frac{1}{2} p_x^2 + \frac{1}{2x^2} (p_\beta - \lambda)^2 + U_c^0(x) \right)$$
$$+ \varepsilon_c^2 U_c^2(\bar{b}_0, x, \beta; 0) + \mathcal{O}\left(\varepsilon_c^4, \varepsilon_b^1 \right),$$

where again we have dropped the tildes.

We shall further simplify our Hamiltonian by setting $p_\beta = \varepsilon_c^2 \tilde{p}_\beta$, i.e. considering $\lambda_\beta = 0$. This is a non-canonical scaling, since $\beta \sim 1$. General p_β is considered in the disconnecting example of Section 2.4.1. The scaled system consists of

$$H(z; \lambda, \varepsilon) = \varepsilon_c^{-2} \varepsilon_b^{-2} \frac{1}{2} \left(p_b^2 + \bar{U}_b^2 b^2 \right) + \frac{1}{2} p_x^2 + \frac{1}{2x^2} \lambda^2 + U_c^0(x)$$
$$+ \varepsilon_c^2 \left(\frac{1}{2\bar{b}_0^2} p_\beta^2 + \frac{1}{x^2} p_\beta \lambda + U_c^2(\bar{b}_0, x, \beta; 0) \right) + \mathcal{O}\left(\varepsilon_c^4, \varepsilon_b^1 \right)$$

and

$$\omega = \mathrm{d}b \wedge \mathrm{d}p_b + \varepsilon_c^2 \mathrm{d}\beta \wedge \mathrm{d}p_\beta + \mathrm{d}x \wedge \mathrm{d}p_x,$$

which gives the following equations of motion

$$\dot{b} = \varepsilon_c^{-2}\varepsilon_b^{-2}p_b, \qquad \dot{\beta} = \frac{1}{\bar{b}_0^2}p_\beta - \frac{1}{x^2}\lambda, \qquad \dot{x} = p_x,$$

$$\dot{p}_b = -\varepsilon_c^{-2}\varepsilon_b^{-2}b, \qquad \dot{p}_\beta = -\partial_\beta U_c^2(\bar{b}_0, \beta, x; 0), \qquad \dot{p}_x = \frac{1}{x^3}\lambda^2 - \partial_x U_c^0(x),$$

up to order ε^0.

By assumption, the intermolecular distance degree of freedom is hyperbolic, and the intramolecular distance is in the small vibrations regime, i.e. elliptic. These dynamics are uncoupled. As the diatom rotates, the attitude degree of freedom will display both kinds of motion.

Provided the (x, p_x) degree of freedom is more strongly hyperbolic that the (β, p_β) one, that is the maximum $\bar{x}_c$ is sufficiently non-degenerate, the submanifold

$$N_0 = \{z \in M_\lambda | x = \bar{x}_c^0(\lambda), \ p_x = 0\}$$

is almost invariant and normally hyperbolic. For a centrifugal maximum, this requires that the attraction between the atom and the diatom is strong and that the angular momentum is large. Given the simplicity of the equations of motion, checking the invariance equations and the variational equations about N_0 is straightforward, once we have chosen a metric with which to define the normal directions. By normal hyperbolicity theory, there is a true normally hyperbolic submanifold N nearby.

Given N_0, we could find a better approximation as explained in Appendix A.1 and done in Subsection 2.4.1. However, for the purpose of finding the Morse bifurcations and the diffeomorphism class of the transition states, N_0 is a sufficiently good approximation.

The normally hyperbolic submanifold N is a transition manifold, as it can be spanned by a dividing manifold, as outlined in Section 2.2. The approximate transition manifold N_0 is spanned by

$$S_0 = \{z \in M_\lambda | x = \bar{x}_c(b, \beta; \lambda)\}.$$

The transition states and dividing surfaces are then approximately the level sets of the Hamiltonian restricted to the approximate transition and dividing manifolds. As the energy varies, we expect these to bifurcate. The transition states may lose normal hyperbolicity. For atom-diatom reactions, N_E are 3-dimensional manifolds, so it is not well understood how they lose normal hyperbolicity. Though, for the case of a frozen diatom, the system only has two degrees of freedom and N_E is a periodic orbit. In Section 2.4.1, we saw that these disappear in a centre saddle bifurcation. However, before the loss of normal hyperbolicity, the capture transition states will undergo changes of diffeomorphism class via Morse bifurcations.

As for the disconnecting example, if we write

$$N = \{z \in M_\lambda | x = \bar{x}_c^0(\lambda) + \varepsilon_c^2 \bar{x}_c^2(z) + \mathcal{O}\left(\varepsilon_c^4\right), \ p_x = 0 + \varepsilon_c^2 P_2(z) + \mathcal{O}\left(\varepsilon_c^4\right)\},$$
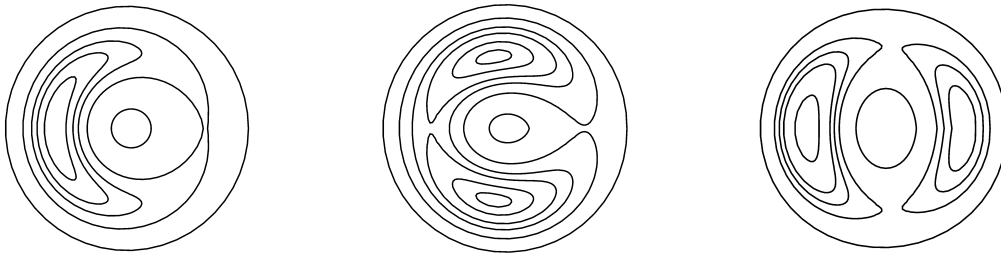
Figure 3.3: Contour plots of the frozen Hamiltonian restricted to the transition manifold H_N^β for example atom-diatom reactions. Left: case 1. Atom attracted to one of the sides of the diatom (e.g. ion plus dipole). Centre: case 2. Reaction prefers orthogonal configuration (e.g. atom plus non-symmetric non-polar diatom). Right: case 3. Reaction prefers aligned configuration (e.g. atom plus non-symmetric dipole).

we find that the Hamiltonian function restricted to the transition manifold N is independent of $\bar{x}_c^2$ and P_2 up to order ε_c^2, namely

$$H_N(z; \lambda, \varepsilon) = \varepsilon_c^{-2} \varepsilon_b^{-2} \frac{1}{2} \left(p_b^2 + \bar{U}_b^2 b^2 \right) + \varepsilon_c^2 \left(\frac{1}{2\bar{b}_0^2} v_\beta^2 + U_c^2(\bar{b}_0, \bar{x}_0^c, \beta; 0) \right) + \mathcal{O}\left(\varepsilon_c^4, \varepsilon_b^1 \right),$$

where we have used the non-canonical momentum $v_\beta = p_\beta - \frac{\bar{b}_0^2}{\bar{x}_0^2}\lambda + \cdots$, and dropped constant terms.

For E below that at which the diatom dissociates, the intramolecular degree of freedom contributes only positive definite terms to the restricted Hamiltonian function and is not involved in any Morse bifurcations. These can therefore be studied by considering the simpler (frozen) Hamiltonian function obtained by freezing the diatom, i.e. minimising H_N over (b, p_b) by setting $b = \bar{b}_0 + \text{h.o.t.}$ and $p_b = 0$ giving

$$H_N^\beta(\beta, p_\beta; \lambda, \varepsilon) = \varepsilon_c^2 \left(\frac{1}{2\bar{b}_0^2} v_\beta^2 + U_c^2(\bar{b}_0, \beta, \bar{x}_0; 0) \right) + \mathcal{O}\left(\varepsilon_c^4, \varepsilon_b^1 \right).$$

Different reactions, i.e. choices of atom and diatom, will have different potentials and different sequences of Morse bifurcations. Three example frozen restricted Hamiltonians H_N^β are depicted in Figure 3.3. The Morse bifurcations of the transition states and dividing surfaces for these examples are the following:

Case 1. Considering H_N^β, we find that $N_{\leq E}^\beta$ bifurcates from $\mathbb{B}^2$ to $\mathbb{S}^1 \times \mathbb{B}^1$. Passing to the full system, we find that the transition manifold $N_{\leq E}$ bifurcates from $\mathbb{B}^4$ to $\mathbb{S}^1 \times \mathbb{B}^3$, the transition state N_E from $\mathbb{S}^3$ to $\mathbb{S}^1 \times \mathbb{S}^2$, and the dividing surface S_E from $\mathbb{S}^4$ to $\mathbb{S}^1 \times \mathbb{S}^3$.

Case 2. Here, the two minima of U_N^β are at the same height, whereas the saddles are at different heights; the transition state goes from $\mathbb{S}^0 \times \mathbb{S}^3$ to $\mathbb{S}^3$ to $\mathbb{S}^1 \times \mathbb{S}^2$, and the dividing surface from $\mathbb{S}^0 \times \mathbb{S}^4$ to $\mathbb{S}^4$ to $\mathbb{S}^1 \times \mathbb{S}^3$.

Case 3. Here the two minima of U_N^β are at different heights, whereas the saddles are

at the same height; the transition state goes from $\mathbb{S}^3$ to $\mathbb{S}^0 \times \mathbb{S}^3$ to $\mathbb{S}^1 \times \mathbb{S}^2$, and the dividing surface from $\mathbb{S}^4$ to $\mathbb{S}^0 \times \mathbb{S}^4$ to $\mathbb{S}^1 \times \mathbb{S}^3$.

The energy-levels M_E also bifurcate along with the transition states and the dividing surfaces. That is, the critical points of the restricted Hamiltonian are also critical point, with an index that is greater by 1, of the Hamiltonian function itself. For example, in Case 1 where the atom is attracted to one of the sides of the diatom, the Hamiltonian function has an index-1 and an index-2 critical point associated with the capture maximum $\bar{x}_c$. When restricted to the transition manifold N, these are the index-0 and 1 critical points of H_N^β seen in Figure 3.3. The energy level restricted a neighbourhood of the capture maximum bifurcates from $\mathbb{B}^1 \times \mathbb{S}^3$, as is well known for the basic flux over a saddle scenario, to $\mathbb{B}^1 \times \mathbb{S}^1 \times \mathbb{S}^2$. In terms of reaction, this means that for small energies the pair can only capture if properly aligned, with the atom closest to the side of the diatom to which it is attracted, whereas for large enough energies the pair can capture for any relative attitude. The bifurcations of the energy levels are the reason for the bifurcations of the dividing surfaces and the transition states, in the sense that given the bifurcations of the energy levels the dividing surfaces must also bifurcate in order to still separate the two regions of interest.

3.2.2 Example. Planar diatom-diatom reactions

The next simplest example is that of planar diatom-diatom reactions. These examples are interesting because they have another intermolecular angle involved in the Morse bifurcations, with respect to the atom-diatom reactions.

The reduced reacting system is $\left(T^*\mathbb{R}_+^5, \omega, H\right)$ with

$$H\left(z; \lambda\right) = \frac{1}{2}\left(\frac{v_x^2}{m} + \frac{v_a^2}{m_a} + \frac{v_b^2}{m_b} + \frac{v_\alpha^2}{m_a a^2} + \frac{(v_\alpha + v_\beta)^2}{mx^2} + \frac{v_\beta^2}{m_b b^2}\right) + V\left(q; \lambda\right),$$

$$V\left(q; \lambda\right) = \frac{1}{2}\frac{\lambda^2}{mx^2 + m_a a^2 + m_b b^2} + U\left(q\right),$$

$$\omega = \sum_{i=1}^{5} \mathrm{d}q_i \wedge \mathrm{d}v_i + \lambda\left(\sum_{j=1}^{5} \partial_{q_j} A_{23}(q)\, \mathrm{d}\alpha \wedge \mathrm{d}q_j + \sum_{k=1}^{5} \partial_{q_k} A_{33}(q)\, \mathrm{d}\beta \wedge \mathrm{d}q_k\right),$$

where

$$A_{23}(q) = \frac{m_a a^2}{mx^2 + m_a a^2 + m_b b^2}, \quad A_{33}(q) = \frac{m_b b^2}{mx^2 + m_a a^2 + m_b b^2},$$

and $z = (x, \alpha, \beta, a, b, v_x, v_\alpha, v_\beta, v_a, v_b)$ are non-canonical coordinates.

We consider exactly the same scenario as for the atom-diatom reactions, namely that E is below the dissociation energy of either diatom, which are in the small vibrations regime (about their equilibrium configurations $\bar{a}, \bar{b}$), and the effective potential V has a large non-degenerate maximum $\bar{x}_c$ with respect to the distance between the diatoms. Then, for slowly rotating diatoms, $v_\alpha, v_\beta \sim \varepsilon_c^2$, there is a transition manifold in the neighbourhood of $\bar{x}_c$ approximated by

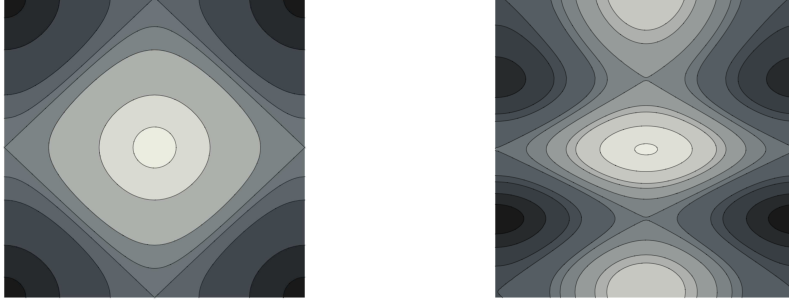$$N_0 = \{z \in M_\lambda | x = \bar{x}_c(\lambda),\ p_x = 0\},$$

Figure 3.4: Example contour plots of the frozen restricted potential $U_N^{\alpha\beta}$ for the planar diatom-diatom reaction, with $\mathbb{T}^2$ represented as $[0,1) \times [0,1)$. Darker regions represent lower energies. Left: case 1. Simplest possible Morse function on $\mathbb{T}^2$ (assuming distinct saddles). Right: case 2. Possible restricted potential for dipole-dipole reaction.

with approximate dividing manifold

$$S_0 = \{z \in M_\lambda | x = \bar{x}_c(\lambda)\}$$

spanning it.

Let us consider the transition states N_E, given by $H_N^{-1}(E)$. The positive definite terms of H_N, which are not involved in any Morse bifurcations, can be removed by minimising over the intramolecular degrees of freedom, setting $a = \bar{a}$, $v_a = 0$, $b = \bar{b}$, $v_b = 0$, and over the intermolecular momenta, setting $v_\alpha = 0$, $v_\beta = 0$. We therefore want to find the diffeomorphism class of the level sets of the restricted frozen potential $U_N^{\alpha\beta} : \mathbb{T}^2 \to \mathbb{R}$ on the 2-torus of (α, β). The Betti numbers of a torus $\mathbb{T}^2$ are 1, 2, 1. Thus, by the Morse inequalities, the simplest possible Morse function on $\mathbb{T}^2$ has four critical points of index 0, 1, 1, 2. Assuming distinct saddle energies, such a Morse function is depicted in Figure 3.4. Taking this as the simplified, restricted potential $U_N^{\alpha\beta}$ over $\mathbb{T}^2$, we see that $N_{\leq E}^{\alpha\beta}$ bifurcates from

$$\mathbb{B}^2 \text{ to } \mathbb{S}^1 \times \mathbb{B}^1 \text{ to } \mathbb{T}^2 - \mathbb{B}^2 \text{ to } \mathbb{T}^2 \times \mathbb{B}^0,$$

where $\mathbb{T}^2 - \mathbb{B}^2$ is given by Theorem A.3.4 as the handlebody $\left(\mathbb{S}^1 \times \mathbb{B}^1\right) \cup_\psi \left(\mathbb{B}^1 \times \mathbb{B}^1\right)$. Therefore the transition manifold $N_{\leq E}$ bifurcates from

$$\mathbb{B}^8 \text{ to } \mathbb{S}^1 \times \mathbb{B}^7 \text{ to } X \text{ to } \mathbb{T}^2 \times \mathbb{B}^6,$$

where X has no standard name, and the transition manifolds N_E from

$$\mathbb{S}^7 \text{ to } \mathbb{S}^1 \times \mathbb{S}^6 \text{ to } \partial X \text{ to } \mathbb{T}^2 \times \mathbb{S}^5.$$

Finally, the dividing surfaces S_E bifurcate from

$$\mathbb{S}^8 \text{ to } \mathbb{S}^1 \times \mathbb{S}^7 \text{ to } \partial P \text{ to } \mathbb{T}^2 \times \mathbb{S}^6,$$

with P again given by Theorem A.3.4.

A more realistic frozen restricted potential $U_N^{\alpha\beta}$ for the case of two interacting dipoles will likely have more than 4 critical points, thus leading to a longer sequence of Morse bifurcations. A possible example restricted potential with eight critical points at distinct heights is given in Figure 3.4. This has a sequence of critical points of index 0, 0, 1, 1, 1, 1, 2, 2. The transition state N_E therefore bifurcates from

$$\mathbb{S}^7 \text{ to } \mathbb{S}^0 \times \mathbb{S}^7 \text{ to } \mathbb{S}^7 \text{ to } \mathbb{S}^1 \times \mathbb{S}^6 \text{ to } \partial X \text{ to } \partial Y \text{ to } \partial X \text{ to } \mathbb{T}^2 \times \mathbb{S}^5,$$

where again ∂X and ∂Y are the boundaries of handlebodies given by Theorem A.3.4. The dividing surface changes from

$$\mathbb{S}^8 \text{ to } \mathbb{S}^0 \times \mathbb{S}^8 \text{ to } \mathbb{S}^8 \text{ to } \mathbb{S}^1 \times \mathbb{S}^7 \text{ to } \partial P \text{ to } \partial Q \text{ to } \partial P \text{ to } \mathbb{T}^2 \times \mathbb{S}^6,$$

again ending up diffeomorphic to $\mathbb{T}^2 \times \mathbb{S}^6$.

3.3 Symmetries and reduction (of n-body systems)

Let us consider the symmetries and reduction of general Hamiltonian system for two interacting polyatomic molecules A and B with n_a and n_b atoms, respectively. These are molecular $n = n_a + n_b$ body Hamiltonian systems $(T^*\mathbb{R}^{3n}, \omega_0, K + U)$ with a molecular (Born-Oppenheimer) potential U for the interaction of the atoms in the A and B molecules. We shall therefore consider the symmetries and reduction of general molecular n-body systems. Though these results are well known, some confusion, especially regarding singular reduction, is still found in the literature.

The Hamiltonian system representing n bodies interacting via a given potential U is a simple mechanical system with Hamiltonian function

$$H(X, Y) = \sum_{i=1}^{n} \frac{1}{2M_i} |Y_i|^2 + U(X_1, \cdots, X_n),$$

where X_i is the position vector of the i-th body and Y_i the conjugate momentum.

Bimolecular n-body systems with no background (electro-magnetic) field are invariant under translations and rotations, i.e. the action of the Euclidean group $SE(3) = \mathbb{R}^3 \times SO(3)$ on state space is a symmetry of the system. The translational symmetry is the action of the Abelian[*33] additive group $\mathbb{R}^3$,

$$T : \mathbb{R}^3 \times T^*\mathbb{R}^{3n} \to T^*\mathbb{R}^{3n}$$
$$: (\gamma, X_1, \cdots, X_n, Y_1, \cdots, Y_n) \mapsto (X_1 + \gamma, \cdots, X_n + \gamma, Y_1, \cdots, Y_n),$$

---

*33 Abelian groups G are those that satisfy commutativity, namely $g \cdot h = h \cdot g$ for g, $h \in G$.

and the rotational symmetry is the action of the special orthogonal group $SO(3)$,

$$A : SO(3) \times T^*\mathbb{R}^{3n} \to T^*\mathbb{R}^{3n}$$
$$: (g, X_1, \cdots, X_n, Y_1, \cdots, Y_n) \mapsto (g \cdot X_1, \cdots, g \cdot X_n, g \cdot Y_1, \cdots, g \cdot Y_n).$$

The combined Euclidean action is $A_{(\gamma,g)}(X, Y) = (g \cdot X + \gamma, g \cdot Y)$.

These symmetries are both lifted actions obtained from the translations and rotations of configuration space. For example, the rotational symmetry is obtained from the action of $SO(3)$ on $\mathbb{R}^{3n}$

$$\tilde{A} : SO(3) \times \mathbb{R}^{3n} \to \mathbb{R}^{3n} : (g, X_1, \cdots, X_n) \mapsto (g \cdot X_1, \cdots, g \cdot X_n)$$

as the left-lift, namely

$$A_g(X, Y) = (\tilde{A}_g(X), (T^*_{\tilde{A}_g(X)} \tilde{A}_{g^{-1}})(Y)) = (g \cdot X, g \cdot Y),$$

for $g \in SO(3)$, $Y \in T^*_X \mathbb{R}^{3n}$ and $T^* \tilde{A}_{g^{-1}}$ the cotangent lift of the diffeomorphism $\tilde{A}_{g^{-1}}$, see e.g. [AM78, page 283]. Similarly, the translational symmetry is the left-lift of the action of $\mathbb{R}^3$ on $\mathbb{R}^{3n}$. Cotangent lifts are symplectomorphisms, in fact they preserve the action one form.

When dynamical systems admit a symmetry they can generally be reduced to a system with less dimensions. In the case of mechanical systems with smooth lifted symmetries, Noether's theorem allows us to associate with these a conserved quantity (or integral of motion), and therefore further reduce the system [Arn89, Appendix 5], [Mar92, Section 2.7]. The integral associated with translational symmetry is linear momentum

$$P : T^*\mathbb{R}^{3n} \to \mathrm{Lie}(\mathbb{R}^3)^* \cong \mathbb{R}^3 : (X, Y) \mapsto P(X, Y) = \sum_{i=1}^{n} Y_i = P_0,$$

and the one associated with rotational symmetry is angular momentum

$$J : T^*\mathbb{R}^{3n} \to \mathfrak{so}(3)^* \cong \mathbb{R}^3 : (X, Y) \mapsto J(X, Y) = \sum_{i=1}^{n} X_i \times Y_i = L,$$

where we have chosen parametrisations of the dual Lie algebras of the symmetry groups in order to write out the momenta in coordinates. Parametrising the group actions, i.e. considering the one-parameter subgroups of the symmetry group individually, allows us to parametrise Noether's theorem and the momenta, see e.g. [Mey73], [Arn89, Appendix 5].

For general Hamiltonian systems with symmetries, the associated conserved quantities are referred to as *momentum maps*[*34] because of the archetypal examples of linear

---

[*34] Some of the literature calls them *moment maps*. This started as an "incorrect" translation of the French *application moment* proposed by Soriau. Note that linear and angular momentum are called moment linéaire and cinétique in French. See Marsden and Weinstein [MW01] for the history of the terminology.

and angular momentum. Note however that general Hamiltonian systems require further conditions for the existence (and equivariance) of momentum maps [OR04, Section 4.5.16].

The Euclidean symmetry group $SE(3)$ is the product of $\mathbb{R}^3$ and $SO(3)$ with non-commutative group multiplication. It is a special example of a *semi-direct product* Lie symmetry group $S = \Gamma \circledS G$, where Γ is a vector space and G a Lie group. For symmetries produced by such groups, reduction by stages allows us to reduce first by Γ and then by an appropriate subgroup of G in this order, see e.g. [MM$^+$07, Chapter 4]. For n-body systems, this means reducing the translational symmetry first and then the rotational one.

Let us therefore first consider the reduction of the translational symmetry. Symplectic reduction can be carried out essentially in two ways, we shall consider point reduction. This involves first fixing the momentum to a chosen regular value, considering the submanifold $P^{-1}(P_0)$, and then taking the quotient by the subgroup Γ_{P_0} that leaves $P^{-1}(P_0)$ invariant, in this case $\mathbb{R}^3$. Thus obtaining the reduced space $P^{-1}(P_0)/\mathbb{R}^3$. The subgroup Γ_{P_0} is actually the isotropy group of $P_0 \in \text{Lie}(\mathbb{R}^3)^*$ under the (coadjoint) action of $\mathbb{R}^3$ on $\text{Lie}(\mathbb{R}^3)^*$, i.e. $\Gamma_{P_0} = \{\gamma \in \Gamma | Ad^*_\gamma(P_0) = P_0\}$, where $Ad^*_\gamma(P_0) = \gamma \cdot P_0$ is the coadjoint action. This follows from P being the momentum of a lifted action, and so equivariant with respect to the coadjoint action of $\mathbb{R}^3$. That is, the momentum map and the $\mathbb{R}^3$ action commute, $P(T_\gamma(z)) = Ad^*_{\gamma^{-1}}(P(z))$.

The translational symmetry is both proper, since $\hat{T} : \mathbb{R}^3 \times T^*\mathbb{R}^{3n} \to T^*\mathbb{R}^{3n} \times T^*\mathbb{R}^{3n} : (\gamma, X, Y) \mapsto (X + \gamma, Y, X, Y)$ is a proper map, and free, meaning that no points of M are invariant under any set of translations. Thus the (quotient) reduced space $P^{-1}(P_0)/\mathbb{R}^3$ is a smooth symplectic manifold and the reduction is said to be regular. The symplectic form ω_{P_0} satisfies $\pi^*_{P_0}\omega_{P_0} = i^*_{P_0}\omega$, where $i_{P_0} : P^{-1}(P_0) \hookrightarrow M$ and $\pi_{P_0} : P^{-1}(P_0) \to P^{-1}(P_0)/\mathbb{R}^3$ are the inclusion and projection maps, respectively. We can then define the reduced Hamiltonian function H_{P_0} satisfying $H_{P_0} \circ \pi_{P_0} = H \circ i_{P_0}$, and the reduced Hamiltonian system is $(M_{P_0}, \omega_{P_0}, H_{P_0})$.

Actually, we can say more because the state space is a cotangent bundle and the symmetry is a lifted action. (Regular) Cotangent bundle reduction theory tells us that, since the symmetry group is Abelian, the reduced space is also a contangent bundle

$$ P^{-1}(P_0)/\mathbb{R}^3 \cong T^*(\mathbb{R}^{3n}/\mathbb{R}^3) \cong T^*\mathbb{R}^{3(n-1)}, $$

so if we define $Q = \mathbb{R}^{3(n-1)}$, $M = T^*Q$, then the translation-reduced system is $(M, \omega_0, H, SO(3))$. This is again a simple mechanical system.

Having an Abelian symmetry group corresponds to having the momenta P_i associated to the one-parameter subgroups γ_i in involution, i.e. $\{P_i, P_j\} = 0$ for all $i, j = 1, 2, 3$ [Mey73]. Thus the translation symmetry can be reduced classically by finding new coordinates including the integrals and the subgroups. One set of such coordinates are the Jacobi vectors and their associated momenta. The transformation to these coordinates

is a linear transformation on configuration space

$$(X_1, \cdots, X_n) \mapsto (R_0, R_1, \cdots, R_{n-1}),$$

that is then extended canonically to state space (see e.g. [Mar92, Section 3.2]). These vectors can be chosen in a number of ways, but the one that feels most natural for bimolecular systems is to choose vectors between the atoms within the two molecules hierarchically, via partial centres of mass of the cluster, and finally a vector between the line of centres of the two molecules. It is well known that in these new coordinates, the Hamiltonian splits into

$$H(\hat{R}_0, R, P_0, P) = \frac{1}{2M_0}|P_0|^2 + \frac{1}{2m_i}|P_i|^2 + U(R)$$

$$\omega_0 = \mathrm{d}R_0 \wedge \mathrm{d}P_0 + \mathrm{d}R_i \wedge \mathrm{d}P_i,$$

where R_0 is the position of the centre of mass of the system. Thus setting $R_0 = 0$, $P_0 = 0$, we obtain the translation reduced Hamiltonian system. This is a specific choice of barycentric coordinates, i.e. with the centre of mass placed at the origin. The celestial mechanics literature, which considers gravitational n-body systems, tends to prefer heliocentric coordinates with the sun (helios) at the origin.

The next stage is the reduction of the $SO(3)$ symmetry from the translation-reduced system $(M, \omega_0, H, SO(3))$. This lifted action is also proper, but not free since collinear configurations with parallel momenta are invariant under rotations about the line of syzygy, and n-body collisions with zero momentum are invariant under all rotations. This is expressed in terms of the isotropy subgroups of points $z = (R, P) \in M$

$$G_z = \{g \in SO(3) | g \cdot z = z\} = \begin{cases} \{Id\} & \text{for } \mathrm{span}\{(R, P)\} = \mathbb{R}^3, \mathbb{R}^2, \\ SO(2) & \text{for } \mathrm{span}\{(R, P)\} = \mathbb{R}^1, \\ SO(3) & \text{for } \mathrm{span}\{(R, P)\} = \mathbb{R}^0. \end{cases}$$

Thus, state space M can be subdivided into isotropy-type submanifolds M_{Id}, $M_{SO(2)}$, $M_{SO(3)}$. Actually, we note that M_{Id} can be subdivided into M_3 and M_2 with span $\mathbb{R}^2$ and $\mathbb{R}^3$ respectively. M_2 is the subset of M_{Id} consisting of planar reactions, and is invariant.

Recall that the quotient of a manifold by a group whose action is proper but not free is a singular manifold. Thus reduction of symmetries that are not free requires more care. Fortunately, quotient manifolds are *(Whitney) stratified space*, i.e. topological spaces that decomposes into a locally finite collection of disjoint, closed submanifolds which are ordered and satisfy Whitney's conditions, see e.g. [SL91], [OR04, Chapter 1]. These are particularly simple types of singular manifolds. For stratifications of symplectic manifolds, we define a *stratified symplectic space* to be a stratified space with symplectic strata and a smooth structure, i.e. a Poisson algebra of functions that restrict to smooth functions on the strata [SL91].

Singular (point) reduction states that the reduced space $M_L = J^{-1}(L)/G_L$ is a

stratified symplectic space with symplectic strata $M_L^{(K)} = (J^{-1}(L) \cap G_L \cdot M_K^i)/G_L$, where M_K^i is a connected components of the K-isotropy submanifold M_K whose point have momentum L. Moreover, M_L is a cone space. The unique symplectic form $\omega_L^{(K)}$ on $M_L^{(K)}$ again satisfies $\pi_L^{(K)*}\omega_L^{(K)} = i_L^{(K)*}\omega_L^{(K)}$. The Hamiltonian flow h_t leaves the connected components of the strata $M_L^{(K)}$ invariant, and reduces to Hamiltonian flows $h_L^{(K)}(t)$ on $M_L^{(K)}$ with reduced Hamiltonian function $H_L^{(K)} : M_L^{(K)} \to \mathbb{R}$ defined by

$$H_L^{(K)} \circ \pi_L^{(K)} = H \circ i_L^{(K)}.$$

Thus, the reduced dynamics can be studied on the individual strata separately. Actually, by what is now generally referred to as Sjamaar's principle, the reduction of the individual strata is regular relative to a natural action, see e.g. [OR04, Section 8.2].

The translation-reduced state space $M \cong T^*\mathbb{R}^{3(n-1)}$ is connected, as are the isotropy-type submanifolds M_K, so the reduced space has three strata. On the two singular strata, the angular momentum is zero by definition, whereas the angular momentum of points in M_{Id} spans the whole of $\mathbb{R}^3$. Actually, the angular momentum of points in $M_2 \subset M_{Id}$ is restricted to the line perpendicular to the (invariable) plane. The points with non-zero angular momentum constitute a subset of the principal stratum. For non-zero L, the isotropy subgroup $G_L = SO(2)$, the rotations about L, whereas for points with zero angular momentum, the isotropy subgroup is the full $SO(3)$. In either case, the G_L-saturation, $G_L \cdot M_K = M_K$.

As for the reduction of the translation symmetry, we would like a hierarchical and clusterable (canonical) transformation of the coordinates, such that two of the new coordinates are ignorable and the reduction can be obtained by fixing their value and that of their conjugate momenta. However, the angular momenta L_i are not in involution and finding charts is not straight forward, with the exception of two-body and planar systems, which both lie in the invariable plane perpendicular to L.

In the celestial mechanics literature, the well known method to find reduced charts is Jacobi's elimination of the node for the three-body system, which was generalised to n-bodies by Deprit [Dep83]. The method is however of little use for bimolecular systems because the charts it produces do not cover the necessary regions of the reduced space. Chierchia and Pinzari have shown that via a Poincaré-regularisation some of the singularities can be removed [CP11], however the regularised charts are still not sufficient for all the motions seen in molecular systems. It would be interesting to check whether this method could be adapted for molecular systems, though it is not clear to us whether clusters could be introduced into the kinetic frame tree by adding branches, or whether the charts could be extended to cover the desired regions of state space.

Another approach to finding charts is to recall that the translation-reduced system is mechanical and the symmetry is lifted. However, the action is not free and there are no singular cotangent bundle reduction theorems that we can invoke. In fact, even for points in M_{Id}, the configuration space isotropy G_q is not always trivial. That is, collinear configurations, though part of the principal stratum when the momenta are not aligned, are invariant under rotations of configuration space about the collinearity.

Note that, this non-trivial configuration space isotropy does not cause any issues when reducing the system, seeing as we are considering the lifted action of $SO(3)$ on state space. The problems arise when trying to reduce via cotangent bundle reduction, in which we consider the action on configuration space. This distinction is not clear in a lot of the molecular literature, which often states that collinear configurations are confined to the singular strata. Generally, the configuration and state space isotropy subgroups for a given Lie group action are not the same, instead we have that $G_z \subset G_q$, for $z = (q, p)$. This is one of the main issues in singular cotangent bundle reduction. Furthermore, by the equivariance of J, if $L = J(z)$, then $G_z \subset G_L$. The only way to obtain charts via regular cotangent bundle reduction is therefore to restrict our attention to non-collinear configurations.

The gauge theoretic, or orbit bundle, approach to cotangent bundle reduction gives the reduced state space as a fibre bundle over the cotangent bundle of the quotient configuration space $Q_{Id}/SO(3)$ with fibres the angular momentum spheres $\mathbb{S}^2$, see e.g. [MM$^+$07, Section 2.3]. This bundle is in general not a product bundle, see discussion in [LR97]. The reduced charts obtained this way are outlined in Appendix A.4, which follows Littlejohn and Reinsch's nice review [LR97]. This method gives coordinates that are physically meaningful, as it does not mix coordinates and momenta.

3.4 Spatial atom-molecule reactions

Now, we consider bimolecular reactions in full spatial generality. In particular, we shall consider reactions between an atom and a normal (i.e. with rigid equilibrium configuration) polyatomic molecule, consisting of n_b atoms. The molecule shall be assumed to have a non-collinear equilibrium about which it is vibrating fast, and the system to be in the capture regime with energy below that at which the molecule dissociates. Thus, we can use the charts provided by the bundle approach to cotangent bundle reduction, see Appendix A.4. We only need one molecule to be non-collinear, which is why we chose to consider the simple case of a molecule B interacting with an atom A. Non-collinearity is not a significant restriction for large molecules, as collinear molecules are codimension $2n - 5$, for $n \geq 3$, not taking into account any chemical effects. However, collinearity is common for small molecules, such as diatoms, so larger molecules with more degrees of freedom are actually easier to consider. This however is only a limitation of our choice of coordinates!

The reduced molecular $n = n_b + 1$ body Hamiltonian system shall be denoted $(\tilde{M}_\lambda, \omega_\lambda, H_\lambda)$. The reduced state space $\tilde{M}_\lambda$ is the subset of the principal stratum with non-collinear configurations and thus a smooth manifold of dimension $6n_b - 4$, which is diffeomorphic to a (generally non-trivial) $\mathbb{S}^2$ fibre bundle

$$T^*(\tilde{Q}/SO(3)) \times_{\tilde{Q}/SO(3)} \mathbb{S}^2_\lambda,$$

where $\tilde{Q} = Q_{Id}$ is the non-collinear subset of the translation reduced configuration space Q, and $\mathbb{S}^2_\lambda$ is the angular momentum sphere [MM$^+$07, Section 2.3].

Choosing non-canonical coordinates, we have

$$H\left(z;\lambda\right) = \frac{1}{2}\sum_{i,j=1}^{3n-6} v_i K^{ij}(q)v_j + V(q,z_\lambda;\lambda)$$

$$V(q,z_\lambda;\lambda) = \frac{1}{2}\sum_{i,j=1}^{3} l_i(z_\lambda;\lambda)I^{ij}(q)l_j(z_\lambda;\lambda) + U\left(q\right),$$

and

$$\omega = \sum_{i=1}^{3n-6} \mathrm{d}q_i \wedge \mathrm{d}v_i + \sum_{i=1}^{3n-6}\sum_{j,k=1}^{3} A_{ij}(q)\partial_{z_{\lambda k}} l_j(z_\lambda;\lambda)\mathrm{d}q_i \wedge \mathrm{d}z_{\lambda k}$$

$$+ \frac{1}{2}\sum_{i,k=1}^{3n-6}\sum_{j=1}^{3} l_j(z_\lambda;\lambda)\left(B_{kij}(q) + \epsilon_{juv}A_{ku}(q)A_{iv}(q)\right)\mathrm{d}q_i \wedge \mathrm{d}q_k + \mathrm{d}q_\lambda \wedge \mathrm{d}p_\lambda,$$

where q are the reduced internal coordinates and v their non-canonical momenta, λ the magnitude of the angular momentum and $z_\lambda = (q_\lambda, p_\lambda)$ canonical Serret-Andoyer coordinates on the angular momentum sphere, such that e.g.

$$l(z_\lambda;\lambda) = (p_\lambda, \sqrt{\lambda^2 - p_\lambda^2}\sin q_\lambda, \sqrt{\lambda^2 - p_\lambda^2}\cos q_\lambda).$$

We will need more than one chart, due to the inevitable coordinate singularities in both the internal coordinates, for $n \geq 4$ bodies, as well as in the angular momentum degree of freedom, when $p_\lambda = \lambda$. $V(q,z_\lambda;\lambda)$ is the effective potential with the centrifugal terms, $K(q)$ is the reduced metric, $I(q)$ is the moment of inertia tensor, $A(q)$ is the gauge potential and $B(q)$ is the Coriolis tensor, both present in the Coriolis terms found in the symplectic form. These are introduced in Apprendix A.4, and are actually defined as functions of the rotating Jacobi vectors $r(q)$ and the reduced masses m_i, e.g. $K(q) = K(r(q);m)$. However, seeing as we are uninterested in scaling effects due to the mass, we shall set $m_i = 1$.

The capture scenario requires the same assumptions as for the planar case, plus a few more, namely that the energy E is below that at which the molecule dissociates, so the molecule is well defined and we have a two-body capture problem, and that the molecule is normal and in the small vibrations regime, which requires assumptions on the centrifugal and Coriolis terms and so on the angular momentum, as we shall soon explain. Furthermore, we assume that V has a non-degenerate maximum with respect to the intermolecular distance, and that this is large compared to the size of the molecule.

The rotating frame for the reduction is chosen such that the Jacobi vector along the line of centres $r_{n_b}(q)$ is parallel to the x_1 axis, and the remaining $SO(2)$ symmetry about the x_1-axis is used to orient the equilibrium configuration of the molecule B in order to simplify the moment of inertia. The most natural choice of internal coordinates q is the distance between atom and molecule x and two angles $\beta = (\beta_1, \beta_2)$ for the attitude of the molecule with respect to the atom, which are intermolecular coordinates, as well

65

as some $3(n_b - 2)$ coordinates b for the intramolecular degrees of freedom of B, so $q = (x, \beta, b)$, unless B has further symmetries of its own that can be reduced.

3.4.1 Molecular and capture scaling

As for planar systems, scaling the coordinates introduces our assumptions into the system, and working in canonical coordinates makes it easier to tell the relative size of different terms. In canonical coordinates, the Hamiltonian function is

$$H(z; \lambda) = \frac{1}{2} \sum_{i,j=1}^{3n-6} \sum_{k=1}^{3} (p_i - A_{ik}(q) l_k(z_\lambda; \lambda)) K^{ij}(q) (p_j - A_{jk}(q) l_k(z_\lambda; \lambda)) + V(q, z_\lambda; \lambda)$$

$$V(q, z_\lambda; \lambda) = \frac{1}{2} \sum_{i,j=1}^{3} l_i(z_\lambda; \lambda) I^{ij}(q) l_j(z_\lambda; \lambda) + U(q).$$

We are interested in a neighbourhood of the large capture maximum $\bar{x}_c$, where A and B are distant, so we scale $x = \varepsilon_c^{-1} \tilde{x}$ and therefore also $p_x = \varepsilon_c \tilde{p}_x$. This is the simpler way of introducing the relative scale between the intermolecular distance and the size of the molecule. Then, by passing to the intermolecular time, we can scale the Hamiltonian such that x is of order one.

Secondly, we are assuming that the molecule is normal, so U has non-degenerate minima with respect to the intramolecular degrees of freedom b, and considering the system when the molecule is in the small vibrations regime. We therefore shift the intramolecular coordinates to have $b = 0$ at equilibrium, and then scale $b = \varepsilon_b \tilde{b}$ and $p_b = \varepsilon_b^{-1} \tilde{p}_b$.

Thus, the scaled Jacobi vectors in the rotating frame are

$$r_{n_b}(q) = \varepsilon_c^{-1} \rho_{n_b}(x) = \varepsilon_c^{-1} x(1, 0, 0)$$

$$r_i(q) = g_b(\beta) \cdot \rho_i(b) = g_b(\beta) \cdot (\rho_i^0 + \varepsilon_b \sum_{j=1}^{3n_b-6} \rho_{ij}^1 b_j) + \mathcal{O}(\varepsilon_b^2), \quad i = 1, \cdots, n_b - 1,$$

where ρ_i^0 are the equilibrium configuration vectors, $g_b(\beta) \in SO(3)/SO(3) \cong \mathbb{S}^2$ determines the orientation of B and shall be chosen shortly, and the $3(n_b - 1)(3n_b - 6)$ constants $\rho_{\beta ijk}^1$ determine the intramolecular coordinates b and shall be chosen in order to simplify the Hamiltonian along the lines of the Eckart [Eck35] and Sayvetz [Say39] conventions for normal and anomalous molecules in the small vibration regime. Essentially, we shall consider an Eckart convention for a normal molecule in the small vibrations regime interacting with an atom, for which the intermolecular coordinates are similar to the large amplitude coordinates of anomalous molecules considered by Sayvetz. In the Eckart convention, which is used throughout the molecular literature, the rotations and vibrations are decoupled to leading order since the intramolecular coordinates b are chosen to be Riemann normal coordinates for which the gauge potential $A_b(q)$ vanishes at the equilibrium configuration. This is discussed from a geometric perspective by Littlejohn and Mitchell [LM02]. They also discuss the scaling from a molecular Born-Oppenheimer perspective.

As for the planar case, we assume that the potential scales to

$$U(q; \varepsilon) = U_b(b) + \varepsilon_c^2 U_c^0(x) + \varepsilon_c^4 U_c^2(q; \varepsilon),$$

and then choose ε_b such that

$$U(q; \varepsilon) = \bar{U}_b^0 + \varepsilon_b^{-2} \sum_{i=1}^{3n_b-6} \bar{U}_{bi}^2 b_i^2 + \varepsilon_c^2 U_c^0(x) + \varepsilon_c^4 U_c^2(q; \varepsilon) + \mathcal{O}\left(\varepsilon_b^5\right).$$

That is, we are assuming that the molecule is strongly bonded, $\bar{U}_{bij}^2 \sim \varepsilon_b^{-4}$. Note also, that we have chosen normal mode intramolecular coordinates for which $\bar{U}_{\beta ij}^2 = \tilde{U}_{\beta i}^2 \delta_{ij}$, which determines $\frac{1}{2}(3n_b - 7)(3n_b - 6)$ of the $\rho_{\beta ijk}^1$ constants.

The reduced kinetic energy and centrifugal energy contain both intermolecular and intramolecular terms and so must be scaled with care.

Recall that the moment of inertia tensor is defined as

$$I(q) = \sum_{k=1}^{n-1} (r_k(q) \cdot r_k(q) I_d - r_k(q) \otimes r_k(q)),$$

where $\otimes$ is the tensor, or outer, product for which $r_k \otimes r_k = r_k r_k^T$. This is a real, symmetric ($I = I^T$), positive definite ($\forall y \in \mathbb{R}^3/\{0\}$, $y^T I y > 0$) matrix, since B is assumed to be non-collinear.

If we write $I(q) =: I_c(q) + I_\beta(q)$, then

$$
\begin{aligned}
I_\beta &= \sum_{k=1}^{n_b-1} (r_k \cdot r_k I_d - r_k \otimes r_k) \\
&= \sum_{k=1}^{n_b-1} ((G_b \rho_k) \cdot (G_b \rho_k) I_d - (G_b \rho_k) \otimes (G_b \rho_k)) \\
&= G_b (\sum_{k=1}^{n_b-1} (\rho_k \cdot \rho_k I_d - \rho_k \otimes \rho_k)) G_b^T,
\end{aligned}
$$

where $G_b \rho_k = g_b \cdot \rho_k$. Thus, the moment of inertia tensor scales to

$$I(q) = \varepsilon_c^{-2} I_c(x) + G_b(\beta) I_b^0 G_b^T(\beta) + \mathcal{O}\left(\varepsilon_b^1\right)$$

where $I_c(x) = \varepsilon_c^{-2} m_1 x^2 \mathrm{Diag}(0, 1, 1)$, and $I_b^0 = \mathrm{Diag}(\mu_{b1}, \mu_{b2}, \mu_{b3})$ with $\mu_{b1} > \mu_{b2} > \mu_{b3}$. This choice of I_b^0 defines $g_b(\beta)$ and the rotation of B about x_1.

The inverse moment of inertia matrix exists and is also symmetric. We are interested in the scale, and find that

$$I^{-1} \sim \begin{pmatrix} \varepsilon^0 & \varepsilon_c^2 & \varepsilon_c^2 \\ \varepsilon_c^2 & \varepsilon_c^2 & \varepsilon_c^4 \\ \varepsilon_c^2 & \varepsilon_c^4 & \varepsilon_c^2 \end{pmatrix} + \cdots.$$

The gauge potential is defined as

$$A(q) = I^{-1}(q)a(q),$$

where $a(q) = (a_x(q), a_\beta(q), a_b(q))^T$ and

$$a_i(q) = \sum_{k=1}^{n-1} r_k(q) \times \frac{\partial r_k(q)}{\partial q_i}.$$

Therefore

$$a_x(q) = 0,$$

$$a_{bi}(q) = G_b(\beta) \sum_{k=1}^{n_b-1} \rho_k^0 \times \rho_{ki}^1 + \varepsilon_b G_b(\beta) \sum_{k=1}^{n_b-1} \sum_{j=1}^{3n_b-6} (\rho_{kj}^1 \times \rho_{ki}^1)b_j = a_{bi}^0(\beta) + \varepsilon_b a_{bi}^1(\beta, b)$$

$$a_{\beta i}(q) = a_{\beta i}^0(\beta) + \mathcal{O}(\varepsilon_b),$$

and we ask that $a_{bi}^0(\beta) = 0$ for all $i = 1, \cdots, 3n_b - 6$, i.e.

$$\sum_{k=1}^{n_b-1} \left(\rho_k^0 \times \rho_{ki}^1 \right) = 0, \quad \forall i = 1, \cdots, 3n_b - 6.$$

This is known as the Eckart condition, and it imposes $3(3n_b - 6)$ conditions on ρ_{kij}^1.

Thus, the gauge potential scales to

$$A(q) \sim \begin{pmatrix} 0 & \varepsilon_c^0 & 0 \\ 0 & \varepsilon_c^2 & 0 \\ 0 & \varepsilon_c^2 & 0 \end{pmatrix} + \cdots,$$

where $A_{\beta 1}^0(\beta)$ and $A_{\beta i}^0(x, \beta)$ for $i = 2, 3$.

Finally, the reduced metric is $K(q) = \tilde{K}(q) - A^T(q)I(q)A(q)$ with

$$\tilde{K}_{ij}(q) = \sum_{k=1}^{n-1} \frac{\partial r_k(q)}{\partial q_i} \cdot \frac{\partial r_k(q)}{\partial q_j}.$$

This is a real, symmetric, positive definite matrix. We write

$$\tilde{K}(q) = \tilde{K}_c(q) + \tilde{K}_\beta(q),$$

where

$$\tilde{K}_c = \begin{pmatrix} 1 & 0 & 0 \\ 0 & 0 & 0 \\ 0 & 0 & 0 \end{pmatrix}, \quad \tilde{K}_\beta = \begin{pmatrix} 0 & 0 & 0 \\ 0 & \tilde{K}_\beta & \tilde{K}_{\beta b} \\ 0 & \tilde{K}_{\beta b}^T & \tilde{K}_b \end{pmatrix},$$

68

and

$$\tilde{K}_{\beta ij}(q) = \sum_{k=1}^{n_b-1} \frac{\partial G_b}{\partial \beta_i} \rho_k^0 \cdot \frac{\partial G_b}{\partial \beta_j} \rho_k^0 + \mathcal{O}(\varepsilon_b) = \tilde{K}_{\beta ij}^0(\beta) + \mathcal{O}(\varepsilon_b)$$

$$\tilde{K}_{\beta bij}(q) = \sum_{k=1}^{n_b-1} \frac{\partial G_b}{\partial \beta_i} \rho_k^0 \cdot G_b \rho_{kj}^1 + \mathcal{O}(\varepsilon_b) = \tilde{K}_{\beta bij}^0(\beta) + \mathcal{O}(\varepsilon_b)$$

$$\tilde{K}_{bij}(q) = \sum_{k=1}^{n_b-1} \rho_{ki}^1 \cdot \rho_{kj}^1 + ... = \tilde{K}_{bij}^0 + ...$$

We ask that $\tilde{K}_{bij}^0 = (\bar{U}_{\beta i}^2)^{-1} \delta_{ij}$ for all i, j. That is we are choosing Williamson normal form coordinates for the intramolecular degrees of freedom. These are $(3n_b - 5)(3n_b - 6)/2$ conditions on ρ_{kij}^1. Furthermore, $\tilde{K}_{\beta bij}^0(\beta) = 0$ for all i, j, i.e.

$$\sum_{k=1}^{n_b-1} \frac{\partial G_b}{\partial \beta_i} \rho_k^0 \cdot G_b \rho_{kj}^1 = 0,$$

due to Eckart condition. Let us consider the case with $i = 1$. The Euler angles β can be chosen in a number of ways, and the rotation matrix $G_b(\beta)$ can then be written as

$$G_b(\beta) = G_1(\beta_1) G_2(\beta_2),$$

where $G_i(\beta_i)$ is a rotation by β_i about some axis y_i. Recall that the symmetry about x_1 has been reduced and $G_b(\beta) \in \mathbb{S}^2$. Thus

$$\partial_{\beta_1} G_b(\beta) = \partial_{\beta_1} G_1(\beta_1) G_2(\beta_2) = G_1(\beta_1) \tilde{G}_1(\frac{\pi}{2}) G_2(\beta_2),$$

where $\tilde{G}_1(\frac{\pi}{2})$ is a rotation about y_1 by $\frac{\pi}{2}$ and simultaneously a contraction in the y_1 direction to zero. This can be seen by considering planar rotation matrices. Then

$$\sum_{k=1}^{n_b-1} \frac{\partial G_b}{\partial \beta_1}(\beta) \rho_k^0 \cdot G_b(\beta) \rho_{kj}^1 = \sum_{k=1}^{n_b-1} \tilde{G}_1(\frac{\pi}{2}) G_2(\beta_2) \rho_k^0 \cdot G_2(\beta_2) \rho_{kj}^1 = \sum_{k=1}^{n_b-1} \tilde{G}_1(\frac{\pi}{2}) \tilde{\rho}_k^0 \cdot \tilde{\rho}_{kj}^1,$$

where $\tilde{\rho}_{kj}^i = G_2(\beta_2) \rho_{kj}^i$ and

$$\sum_{k=1}^{n_b-1} \tilde{\rho}_k^0 \times \tilde{\rho}_{kj}^0 = G_2(\beta_2) \sum_{k=1}^{n_b-1} \rho_k^0 \times \rho_{kj}^0 = 0,$$

by the Eckart condition. Thus $\tilde{K}_{\beta bij}^0(\beta) = 0$, and the same is true for $i = 2$.

The gauge dependent term scales to

$$A^T I A \sim \begin{pmatrix} 0 & 0 & 0 \\ 0 & \varepsilon_c^0 & 0 \\ 0 & 0 & 0 \end{pmatrix} + \cdots,$$

so

$$K(q) = \begin{pmatrix} 1 & 0 & 0 \\ 0 & \tilde{K}_\beta^0(\beta) + F_0(\beta) + \varepsilon_c^2 F_2(x,\beta) + \varepsilon_c^4 F_4(x,\beta) & 0 \\ 0 & 0 & \tilde{D}_b^{-1} \end{pmatrix} + \mathcal{O}(\varepsilon_b)$$

and

$$K^{-1} = \begin{pmatrix} 1 & 0 & 0 \\ 0 & K_{\beta 0}^{-1}(\beta) - \varepsilon_c^2 J_2(x,\beta) + \varepsilon_c^4 J_4(x,\beta) & 0 \\ 0 & 0 & \tilde{D}_b \end{pmatrix} + \mathcal{O}(\varepsilon_b),$$

by inverting the matrix block-wise, and expanding inverse matrices in formal power series.

We can finally write out the Hamiltonian function in terms of our new scaled coordinates. First however, we scale the time such that the intermolecular time is order one, and therefore the Hamiltonian function becomes

$$H(z;\lambda,\varepsilon) = \frac{\varepsilon_c^{-2}}{2} \left(\varepsilon_b^{-2} \sum_{i=1}^{3n_b-6} \bar{U}_{bi}^2 (p_{bi}^2 + b_i^2) + \sum_{i,j=1}^{2} v_{\beta i}(z;\lambda,\varepsilon) J_{\beta 0}^{ij}(\beta) v_{\beta j}(z;\lambda,\varepsilon) + I_0^{11}(\beta) p_\lambda^2 \right)$$

$$+ \frac{p_x^2}{2} + \frac{1}{2} \sum_{i,j=1}^{3} l_i(z_\lambda;\lambda) I_2^{ij}(x,\beta) l_j(z_\lambda;\lambda) + U_c^0(x) - \frac{1}{2} \sum_{i,j=1}^{2} v_{\beta i}(z;\lambda,\varepsilon) J_{\beta 2}^{ij}(x,\beta) v_{\beta j}(z;\lambda,\varepsilon)$$

$$+ \frac{\varepsilon_c^2}{2} \left(\sum_{i,j=1}^{2} v_{\beta i}(z;\lambda,\varepsilon) J_{\beta 4}^{ij}(x,\beta) v_{\beta j}(z;\lambda,\varepsilon) + \sum_{i,j=1}^{3} l_i(z_\lambda;\lambda) I_4^{ij}(x,\beta) l_j(z_\lambda;\lambda) + U_c^2(q;0) \right)$$

$$+ \text{ h.o.t.}$$

Note that we are using the non-canonical momenta v_β and the angular momenta l as place-holders, where

$$v_{\beta i}(z;\lambda,\varepsilon) = p_{\beta i} - \sum_{j=1}^{3} A_{\beta ij}(x,\beta;\varepsilon) l_j(z_\lambda;\lambda),$$

and

$$A_{\beta ij}(q) = (A_{\beta i1}(\beta), \varepsilon^2 A_{\beta i2}(x,\beta), \varepsilon^2 A_{\beta i3}(x,\beta)) + \cdots.$$

3.4.2 Angular momentum degree of freedom

The angular momentum degree of freedom z_λ lives on the 2-sphere $\mathbb{S}_\lambda^2$. It's dynamics is coupled to the internal dynamics, and is determined by both centrifugal and Coriolis terms.

Considering the atom and the molecule as constituting a single "body", the internal dynamics gives its deformations and the z_λ degree of freedom its angular momentum. With this analogy, if the molecule is in equilibrium with itself and with respect to the atom, then we obtain a rigid-body and the Hamiltonian, which reduced to the
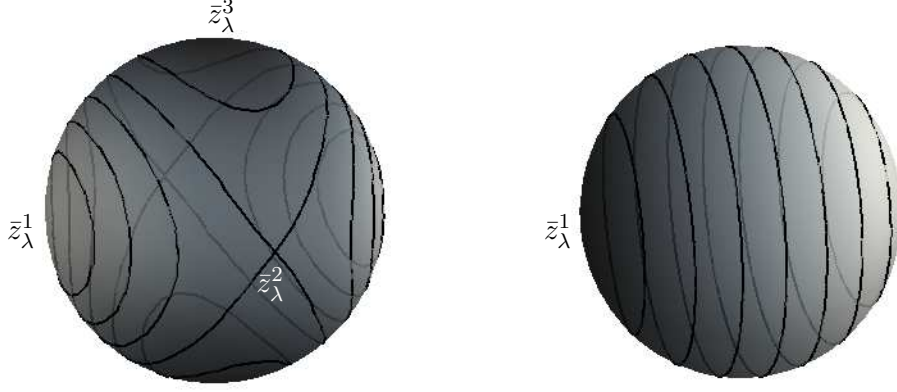
Figure 3.5: Angular momentum sphere with equipotential lines of the centrifugal energy, when the moment of inertia has three distinct principal moments (left), or two equal moments (right).

centrifugal terms, represents rigid body motion. We recall that rigid-bodies follow closed curves on the angular momentum sphere with critical points when l is parallel to the eigenvectors of I^{-1} (or equivalently I), called *principal axes*, see e.g. [Dep67]. Typical rigid-body dynamics for the case of distinct eigenvalues, or *principal moments*, is depicted in Figure 3.5.

For the full system, the angular momentum degree of freedom doesn't follow closed curves on $\mathbb{S}^2_\lambda$ anymore, instead it is coupled with the internal "defomation" dynamics. The equilibria of the system occur when q is a critical point of the effective potential V, $v = 0$, and again l is parallel to the principal axes. We shall now consider the centrifugal energy

$$E_\lambda = \frac{1}{2} l^T(z_\lambda; \lambda) I^{-1}(q; \varepsilon) l(z_\lambda; \lambda),$$

which we point out once more is not preserved.

The eigenvectors η_i of I^{-1}, which are now functions of q, are the same as those of I, whereas the eigenvalues μ_i are the reciprocal, i.e.

$$I\eta = \mu^{-1}\eta \quad \Rightarrow \quad \mu\eta = I^{-1}\eta.$$

So we consider I, which has real eigenvalues, since it is a real positive definite matrix, and if these are distinct then the eigenvectors are orthogonal. We find that, to order ε_b^0, the eigenvalues and eigenvectors of I^{-1} are

$$\mu_1(q) = I_\beta^{11}(\beta) + \cdots, \qquad\qquad \eta_1(q) = x_1 + \mathcal{O}\left(\varepsilon_c^2\right),$$
$$\mu_2(q) = \varepsilon_c^2 x^{-2} + \varepsilon_c^4 x^{-4} \mu_{24}(\beta) + \cdots, \qquad \eta_2(q) \in \{x_2, x_3\} + \mathcal{O}\left(\varepsilon_c^2\right),$$
$$\mu_3(q) = \varepsilon_c^2 x^{-2} + \varepsilon_c^4 x^{-4} \mu_{34}(\beta) + \cdots, \qquad \eta_3(q) \in \{x_2, x_3\} + \mathcal{O}\left(\varepsilon_c^2\right),$$

71

where

$$\mu_{24}(\beta) = \frac{1}{2}(I_{22}^\beta(\beta) + I_{33}^\beta(\beta)) + \sqrt{\frac{1}{4}(I_{22}^\beta(\beta) - I_{33}^\beta(\beta))^2 + I_{23}^\beta(\beta)^2},$$

$$\mu_{34}(\beta) = \frac{1}{2}(I_{22}^\beta(\beta) + I_{33}^\beta(\beta)) - \sqrt{\frac{1}{4}(I_{22}^\beta(\beta) - I_{33}^\beta(\beta))^2 + I_{23}^\beta(\beta)^2}.$$

Thus in order to have distinct principal moments and axes, we require either $I_{22}^\beta(\beta) \neq I_{33}^\beta(\beta)$, or $I_{23}^\beta(\beta) \neq 0$.

Consider a 3D molecule B with three distinct moments, that is with no rotational symmetries. As it rotates relative to the distant atom, we expect to find three pairs of points (on the attitude sphere $\mathbb{S}_B^2$) at which the combined configuration of the atom and the molecule is such that two of the moments of $I(q)$ and so $I^{-1}(q)$ are non-distinct.

Consider a fixed configuration $\hat{q}$ with distinct $\mu_1(\hat{q}) > \mu_2(\hat{q}) > \mu_3(\hat{q})$, and write

$$l(\hat{q}, Z_\lambda; \lambda) = P_\lambda \eta_1(\hat{q}) + \sqrt{\lambda^2 - P_\lambda^2} \sin Q_\lambda \eta_2(\hat{q}) + \sqrt{\lambda^2 - P_\lambda^2} \cos Q_\lambda \eta_3(\hat{q}),$$

i.e. consider Serret-Andoyer coordinates obtained by projecting onto the principal axes, cf. Appendix A.4. Then

$$E_\lambda = \frac{1}{2} \left(\mu_1(\hat{q}) P_\lambda^2 + \mu_2(\hat{q})(\lambda^2 - P_\lambda^2) \sin^2 Q_\lambda + \mu_3(\hat{q})(\lambda^2 - P_\lambda^2) \cos^2 Q_\lambda \right),$$

so the critical points are $\bar{Z}_\lambda^2 = (0,0)$, $(0,\pi)$, $\bar{Z}_\lambda^3 = (\frac{\pi}{2}, 0)$, $(\frac{3\pi}{2}, 0)$, and $\bar{Z}_\lambda^1 = (q_\lambda, \pm\lambda)$. The superscript denotes which principal axis l is parallel to at the given critical point. The symmetry of the centrifugal term, inherited from the moment of inertia tensor, is clear from the existence of two critical points for each axis. That is, the direction of the angular momentum is irrelevant. The critical energies are

$$\bar{E}_\lambda^i = H_\lambda(\bar{Z}_\lambda^i) = \frac{\mu_i}{2}\lambda^2.$$

For the non-distinct eigenvalues case $\mu_2(\hat{q}) = \mu_3(\hat{q})$, choosing some generalised eigenvectors for η_2, η_3, the centrifugal energy is

$$E_\lambda = \frac{1}{2}((\mu_1(\hat{q}) - 2\mu_2(\hat{q}))P_\lambda^2 + 2\mu_2(\hat{q})\lambda^2,$$

so the critical points are $(Q_\lambda, 0)$, which is degenerate, and $(Q_\lambda, \pm\lambda)$. This is depicted in Figure 3.5.

For the capture problem, considering arbitrary $\lambda \sim 1$, forces us to restrict our attention to energies below the centrifugal energy $\bar{E}_\lambda^1$ such that the angular momentum degree of freedom is confined to an small annulus $\mathbb{A}_{\lambda, \varepsilon_c^2}^2$ that doesn't contain $\bar{Z}_\lambda^1$. Roughly speaking l must be almost perpendicular to the line of centres. This is necessary in order to ensure that the intermolecular distance degree of freedom (x, p_x) is more hyperbolic than the angular momentum degree of freedom, which we need for the capture transition manifold about $\bar{x}_c$. Also, large $P_\lambda \sim 1$ forces $p_{\beta i}$ to be large at the critical point with $v_{\beta i} = 0$, so the attitude degrees of freedom might also be more

hyperbolic than the (x, p_x) one. This can be seen by considering the scaled Hamiltonian function of the previous Subsection. The limit of normal hyperbolicity of the transition manifold is considered in the disconnecting example of Subsection 2.4.1.

Take fixed $\hat{q}$ and energy just above

$$\bar{E}_\lambda^2 = \frac{\mu_2}{2}\lambda^2 = \frac{\lambda^2}{2}(\varepsilon_c^2 x^{-2} + \varepsilon_c^4 x^{-4}\mu_{24}(\beta)) + \cdots \sim \varepsilon_c^2 \lambda^2.$$

If all the energy of the system is in E_λ, then for the non-distinct case we have $P_\lambda = 0$ at $E_\lambda = \bar{E}_\lambda^2$, whereas for the distinct case,

$$P_\lambda^2 = \frac{2E_\lambda - \lambda^2(\mu_2 \sin^2 Q_\lambda + \mu_3 \cos^2 Q_\lambda)}{\mu_1 - (\mu_2 \sin^2 Q_\lambda + \mu_3 \cos^2 Q_\lambda)},$$

so

$$P_\lambda^2(0, \bar{E}_\lambda^2) = \frac{\varepsilon_c^4 \lambda^2(\mu_{24} - \mu_{34})}{x^4 \mu_1} + \cdots \sim \varepsilon_c^4 \lambda^2.$$

Furthermore, the projection of the angular momentum to the x_1 axis, $p_\lambda = P_\lambda + \mathcal{O}(\varepsilon)$, so bounding $E < \bar{E}_\lambda^2 + \Delta$, with Δ small, gives $p_\lambda = 0 + \mathcal{O}(\varepsilon_c^2) + \mathcal{O}(\varepsilon_c^4)$.

3.4.3 Centrifugal and Coriolis scaling

In order to ensure that we have a normally hyperbolic capture transition manifold about $\bar{x}_c$, given the considerations of Subsection 3.4.2, we shall consider the case when the angular momentum is order one, but far from being aligned with the line of centres along x_1, i.e. $p_\lambda \sim \varepsilon_c^2$, by restricting our attention to energies up to values just above the centrifugal energy at the middle principal moment $\bar{E}_\lambda^2$.

Thus $z_\lambda \in \mathbb{A}_{\lambda, \varepsilon_c^2}^2$ and we scale $p_\lambda = \varepsilon_c^2 \tilde{p}_\lambda$, so

$$l = \lambda(0, \sin q_\lambda, \cos q_\lambda) + \varepsilon_c^2 p_\lambda(1, 0, 0) + \mathcal{O}(\varepsilon_c^4)$$

and

$$H(z; \lambda, \varepsilon) = \varepsilon_c^{-2}\varepsilon_b^{-2} \sum_{i=1}^{3n_b-1} \frac{\bar{U}_{bi}^2}{2}(p_{bi}^2 + b_i^2) + \varepsilon_c^{-2}\frac{1}{2}\sum_{i,j=1}^{2} v_{\beta i}(z; \lambda, \varepsilon)J_{\beta 0}^{ij}(\beta)v_{\beta j}(z; \lambda, \varepsilon)$$

$$+ \frac{1}{2}p_x^2 + \frac{\lambda^2}{2x^2} + U_c^0(x) - \frac{1}{2}\sum_{i,j=1}^{2} v_{\beta i}(z; \lambda, \varepsilon)J_{\beta 2}^{ij}(x, \beta)v_{\beta j}(z; \lambda, \varepsilon)$$

$$+ \varepsilon_c^2 \left(\frac{1}{2}\sum_{i,j=1}^{2} v_{\beta i}(z; \lambda, \varepsilon)J_{\beta 4}^{ij}(x, \beta)v_{\beta j}(z; \lambda, \varepsilon) + \frac{1}{2}I_0^{11}(\beta)p_\lambda^2 \right.$$

$$+ \sum_{j=2}^{3} p_\lambda I_2^{1j}(x, \beta)l_j^0(q_\lambda; \lambda) + \frac{1}{2}\sum_{i,j=2}^{3} l_i^0(q_\lambda; \lambda)I_4^{ij}(x, \beta)l_j^0(q_\lambda; \lambda) + U_c^2(q; 0) \Bigg)$$

$$+ \text{ h.o.t.}$$

Finally, we consider the rotational momentum of B, i.e.

$$v_{\beta i}(z; \lambda, \varepsilon) = p_{\beta i} - \varepsilon_c^2 \left(A_{\beta i 1}(\beta) p_\lambda + A_{\beta i 2}(x, \beta) \lambda \sin q_\lambda + A_{\beta i 3}(x, \beta) \lambda \cos q_\lambda \right) + \cdots$$

We note that, even though we have removed the coupling of vibrations and rotations to first orders, already up to order ε^0, $\dot{p}_{\beta i}$ is not zero, since the reduced metric K is a function of β. However, the rate of change of p_β is a function of p_β^2 up to order ε_c^2, so if we consider a molecule that is initially rotating slowly, it will be a long time before it increases its rotational velocity. Thus, as for the planar case, we consider a slowly rotating molecule with $p_{\beta i} = \varepsilon_c^2 \tilde{p}_{\beta i}$, so $v_{\beta i} \sim \varepsilon_c^2$. Then

$$H(z; \lambda, \varepsilon) = \varepsilon_c^{-2} \varepsilon_b^{-2} \sum_{i=1}^{3n_b - 6} \frac{\bar{U}_{bi}^2}{2}(p_{bi}^2 + b_i^2) + \frac{1}{2}p_x^2 + \frac{\lambda^2}{2x^2} + U_c^0(x)$$

$$+ \varepsilon_c^2 \left(\frac{1}{2} \sum_{i,j=1}^{2} v_{\beta i}(z; \lambda, 0) J_{\beta 0}^{ij}(\beta) v_{\beta j}(z; \lambda, 0) + \frac{1}{2} I_0^{11}(\beta) p_\lambda^2 \right.$$

$$+ \sum_{j=2}^{3} p_\lambda I_2^{1j}(x, \beta) l_j^0(q_\lambda; \lambda) + \frac{1}{2} \sum_{i,j=2}^{3} l_i^0(q_\lambda; \lambda) I_4^{ij}(x, \beta) l_j^0(q_\lambda; \lambda) + U_c^2(q; 0) \Bigg)$$

$$+ \mathcal{O}\left(\varepsilon_c^4, \varepsilon_b^1\right),$$

and

$$\omega = \sum_{i=1}^{3n_b - 6} \mathrm{d}b_i \wedge \mathrm{d}p_{bi} + \varepsilon_c^2 \sum_{i=1}^{2} \mathrm{d}\beta_i \wedge \mathrm{d}p_{\beta i} + \mathrm{d}x \wedge \mathrm{d}p_x + \varepsilon_c^2 \mathrm{d}q_\lambda \wedge \mathrm{d}p_\lambda.$$

This gives, the equations of motion

$$\dot{b}_i = \varepsilon^{-2} \varepsilon_b^{-2} \bar{U}_{bi}^2 p_{bi}, \qquad \dot{\beta}_i = \partial_{p_{\beta i}} H_2(z; \lambda), \qquad \dot{x} = p_x, \qquad \qquad \dot{q}_\lambda = \partial_{p_\lambda} H_2(z; \lambda),$$

$$\dot{p}_b = -\varepsilon^{-2} \varepsilon_b^{-2} \bar{U}_{bi}^2 b_i, \quad \dot{p}_{\beta i} = -\partial_{\beta_i} H_2(z; \lambda), \quad \dot{p}_x = -\partial_x V_c^0(x; \lambda), \quad \dot{p}_\lambda = \partial_{q_\lambda} H_2(z; \lambda),$$

up to order ε^0.

3.4.4 Capture transport problem and transition states

We are interested in the capture dynamics for an atom and a distant molecule, and have restricted our attention to the simplest case in which the molecule is rotating slowly and the angular momentum is not aligned with the line of centres, by scaling the reduced $n_b + 1$ body system accordingly.

From the equations of motion, we note that provided the (x, p_x) degree of freedom is more hyperbolic than both the attitude (β, p_β) and the z_λ angular momentum degrees of freedom, the submanifold

$$N_0 = \{z \in M_\lambda | x = \bar{x}_c(\lambda), \ p_x = 0\}$$

is almost invariant and normally hyperbolic.

Taking N_0 as an approximation to the true normally hyperbolic submanifold N

nearby, and considering the approximate dividing manifold S_0 spanning it

$$S_0 = \{z \in M_\lambda | x = \bar{x}_c(\lambda)\},$$

we can find the restricted Hamiltonian functions

$$
\begin{aligned}
H_N\left(z; \lambda, \varepsilon\right) = {}& \varepsilon_c^{-2}\varepsilon_b^{-2} \sum_{i=1}^{3n_b-6} \frac{\bar{U}_{bi}^2}{2}(p_{bi}^2 + b_i^2) + \varepsilon_c^2 \Bigg(\frac{1}{2} \sum_{i,j=1}^{3} v_{\beta i}(z; \lambda, 0) G_{\beta 0}^{ij}(\beta) v_{\beta j}(z; \lambda, 0) \\
& + \frac{1}{2} I_0^{11}(\beta) p_\lambda^2 + \sum_{j=2}^{3} p_\lambda I_2^{1j}(\bar{x}_c, \beta) l_j^0(q_\lambda; \lambda) + \frac{1}{2} \sum_{i,j=2}^{3} l_i^0(q_\lambda; \lambda) I_4^{ij}(\bar{x}_c, \beta) l_j^0(q_\lambda; \lambda) \\
& + U_c^2(q; 0)\Bigg) + \mathcal{O}\left(\varepsilon_c^4, \varepsilon_b^1\right),
\end{aligned}
$$

modulo constant terms, and H_S to leading orders. These give the transition states and dividing surfaces, respectively.

As for the planar examples, it is simpler to study the Morse bifurcations if we minimise the reduced Hamiltonians over the positive definite coordinates, namely b, p_b and v_β. Actually, since we are considering energies $E < \bar{E}_\lambda^1$, only one of the angular momentum coordinates is involved in Morse bifurcations, so we can also minimise over p_λ. This can be simplified by using canonical angular momentum coordinates Z_λ aligned with the principal axes, as done in Subsection 3.4.2. Thus setting $b = p_b = v_\beta = P_\lambda = 0$ in H_N, we obtain

$$
V_N^c\left(\beta, Q_\lambda; \lambda, \varepsilon\right) = \varepsilon_c^2 \left(\frac{\lambda^2}{2} \left(\mu_{24}(\beta) \sin^2 Q_\lambda + \mu_{34}(\beta) \cos^2 Q_\lambda\right) + \bar{U}_c^2(\beta; 0)\right) + \mathcal{O}\left(\varepsilon_c^4, \varepsilon_b^1\right).
$$

We are therefore interested in the level-sets of V_N^c and their Morse bifurcations, which we can then use to find those of the transition states and dividing surfaces. We have been careful not to specify the domain of V_N^c, which is a subset of N and so codimension-2 in the reduced state space $\tilde{M}_\lambda$. The latter is a $\mathbb{S}_\lambda^2$ fibre bundle over the cotangent bundle of the reduced configuration space $\tilde{Q}$, so also N and S will in general be non-trivial bundles. However, we restrict our attention to subsets of these manifolds for which the bundle is trivial. Furthermore, we are considering energies below that at which the molecules dissociates, and up to just above the centrifugal energy for the angular momentum aligned with the $\eta_2(\beta)$ principal axis with $Q_\lambda = k\pi + \pi/2$, $k \in \mathbb{Z}$. Whichever is the smaller value will serve as an upper limit to the energy.

The critical points $(\bar{\beta}, \bar{Q}_\lambda)$ of the frozen, restricted effective potential V_N^c are given by

$$(\mu_{24}(\bar{\beta}) - \mu_{34}(\bar{\beta})) \sin \bar{Q}_\lambda \cos \bar{Q}_\lambda = 0,$$

$$\frac{\lambda^2}{2}(\partial_\beta \mu_{24}(\bar{\beta}) \sin^2 \bar{Q}_\lambda + \partial_\beta \mu_{34}(\bar{\beta}) \cos^2 \bar{Q}_\lambda) + \partial_\beta U_c^2(\bar{\beta}; 0) = 0.$$

The first equation is satisfied trivially for $\hat{\beta}$ at which the two principal moments are equal $\mu_{24}(\hat{\beta}) = \mu_{34}(\hat{\beta})$. We shall consider examples of V_N^c that are Morse functions,
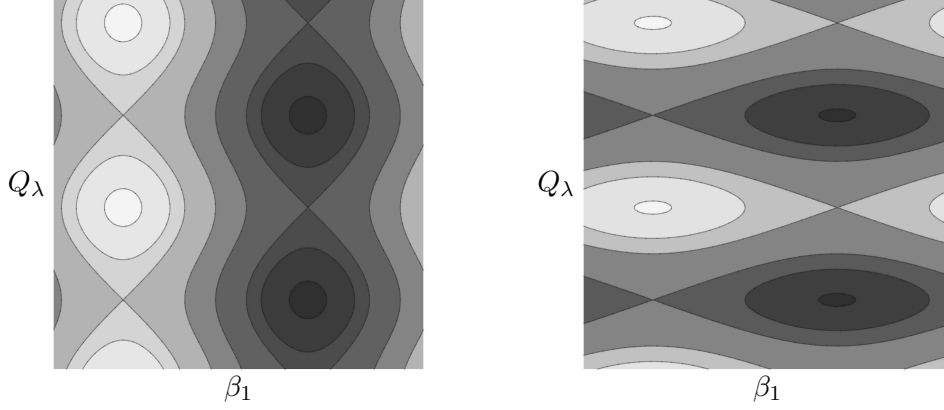
Figure 3.6: Contour plots of an example function on the (β_1, Q_λ) torus, where darker regions represent lower energies and there are no values $\hat{\beta}_1$ with non-distinct principal moments. Case in which the value of the function at $(\bar{\beta}_1^0, \bar{Q}_\lambda^2)$ is smaller than that at $(\bar{\beta}_1^1, \bar{Q}_\lambda^3)$, i.e. the first Morse bifurcation involves the angular momentum angle on the left, and vice-versa on the right.

i.e. have non-degenerate critical points $(\bar{\beta}, \bar{Q}_\lambda)$ and so $\hat{\beta} \neq \bar{\beta}$. Given this non-degeneracy assumption, the critical points satisfy either

$$\bar{Q}_\lambda^3 = k\pi \quad \text{and} \quad \partial_\beta \left(\frac{\lambda^2}{2} \mu_{34} + U_c^2 \right) (\bar{\beta}) = 0,$$

or

$$\bar{Q}_\lambda^2 = k\pi + \frac{\pi}{2} \quad \text{and} \quad \partial_\beta \left(\frac{\lambda^2}{2} \mu_{24} + U_c^2 \right) (\bar{\beta}) = 0,$$

for $k \in \mathbb{Z}$, cf. [LR97, Section IV.E]. Furthermore, the Morse function V_N^c has at least two non-degenerate minima at $(\bar{\beta}^0, \bar{Q}_\lambda^3)$ due to the symmetry of the centrifugal terms, as $Q_\lambda \in \mathbb{S}^1$.

The sequence of Morse bifurcations of the level sets of the frozen restricted effective potential V_N^c, and therefore of the transition states and dividing surfaces, depends on the relative size of the centrifugal and the reduced potential U_c^2 energies. This will determine the relation of the different critical energies. Critical points with the same attitude β and the angular momentum aligned with different principal axes have energies that differ by λ^2, whereas the difference in energy for critical points with different attitudes depends on the atom-molecule pair.

The simplest case is when the first Morse bifurcation encountered as the energy is increased from the minima involves the angular momentum angle, and the system goes from rotating about the $\eta_3(\bar{q})$ axis to rotating more freely about $\eta_2(\bar{q})$ as well. This bifurcation occurs at the critical energy for the $(\bar{\beta}^0, \bar{Q}_\lambda^2)$ critical points. In this case both the domain of V_N^c and the subsets of N and S of interest are bundles over a contractible base space and so trivial [Ste51, Theorem 11.6]. The frozen energy levels $\tilde{N}_{\leq E}$ bifurcate from $\mathbb{S}^0 \times \mathbb{B}^3$ to $\mathbb{S}^1 \times \mathbb{B}^2$, so the transition states N_E go from $\mathbb{S}^0 \times \mathbb{S}^{6n_b-7}$ to $\mathbb{S}^1 \times \mathbb{S}^{6n_b-8}$, and similarly the dividing surfaces.

As the energy is increased further, we will reach critical values at which also the
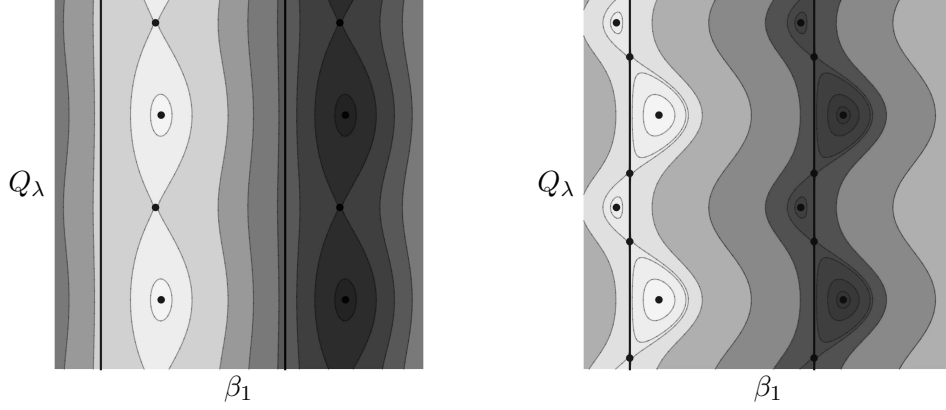
Figure 3.7: Contour plots of an example function on the (β_1, Q_λ) torus, where darker regions represent lower energies and vertical back lines non-distinct principal moments. Case in which the value of the function at $(\bar\beta_1^0, \bar Q_\lambda^2)$ is smaller than that at $(\bar\beta_1^1, \bar Q_\lambda^3)$, i.e. the first Morse bifurcation involves the angular momentum angle on the left, and vice-versa on the right.

attitude coordinates are involved in Morse bifurcations. We will consider the case in which the energy does not change significantly as the molecule rotates in one direction, with respect to the atom, but does when it tries to rotate in the other direction. Specifically, we shall consider potentials U_c^2 on $\mathbb{S}^2$ that have a minimum $\bar\beta^0$, a saddle $\bar\beta^1$ and two maxima $\bar\beta_2$, and restrict our attention to the annulus $\mathbb{A}^2 \subset \mathbb{S}^2$ containing $\bar\beta^0$ and $\bar\beta^1$. Choosing the attitude angles appropriately, only one coordinate is involved in Morse bifurcations, whereas the other contributes positive definite terms. The subset of the transition manifold N of interest is a bundle over $\mathbb{S}^1 \times \mathbb{B}^{6n_b-9}$ which we claim is trivial. Firstly, we note that it is equivalent to the product of a bundle over $\mathbb{S}^1$ with $\mathbb{B}^{6n_b-9}$ via homotopy-type arguments [Ste51, Theorem 11.4], cf. bundles over contractible spaces being trivial. The characterisation of bundles over spheres with structure group G depends on certain homotopy groups of G [Ste51, Theorem 18.5]. Our fibres are diffeomorphic to $\mathbb{S}^2$, or subsets of it, and the diffeomorphism group of $\mathbb{S}^2$ is the orthogonal group $O(3)$. However, N is orientable so both elements of the product must be orientable. Thus, given that the bundle over the circle must be orientable, we restrict our attention to the orientation preserving diffeomorphisms $SO(3)$ and find that the bundle over the circle is a product, and therefore our original bundle is also trivial [Ste51, Section 26]. Note however that not all orientable surface bundles over the circle are product bundles, as we can construct non-trivial bundles with fibres diffeomorphic to $\mathbb{T}^2$, for example.

V_N^c can be minimised over the irrelevant attitude to obtain a function on the torus $\mathbb{T}^2$ for (β_1, Q_λ), say. There are two possible scenarios for this case, the first is that $\mathbb{T}^2$ does not contain points $\hat\beta$ at which the μ_2, μ_3 principal moments become equal. The order of the bifurcations then depends on the relative heights of the critical energies, and both cases are straight forward, see Figure 3.6. The other scenario is when $\mathbb{T}^2$ does contain $\hat\beta$. We shall consider the case in which it contains only one pair of such points. Contour plots for the restricted function on $\mathbb{T}^2$ are given in Figure 3.7. If the centrifugal

energy is smaller than the attitude potential, then the points $\hat{\beta}_1$ at which the moments μ_2, μ_3 are not distinct do not play a role in the Morse bifurcations, which are the same as those for the case when $\mathbb{T}^2$ does not contain $\hat{\beta}$, as we can by comparing the left hand side of Figures 3.6 and 3.7. Instead, when the molecular potential is smaller than the centrifugal one, depicted on the right in Figure 3.7, we see that the points $\hat{\beta}_1$ do play a significant role in the bifurcations and the sub-level sets of the torus bifurcate as follows

$$\mathbb{S}^0 \times \mathbb{B}^2 \text{ to } \mathbb{S}^0 \times \mathbb{S}^0 \times \mathbb{B}^2 \text{ to } \mathbb{S}^1 \times \mathbb{B}^1 \text{ to } X \text{ to } Y \text{ to } \mathbb{T}^2,$$

where X and Y can be written as handlebodies using Theorem A.3.4. Therefore, the sub-level sets of the capture transition manifold $N_{\leq E}$ have the following sequence of bifurcations

$$\mathbb{S}^0 \times \mathbb{B}^{6n_b-6} \text{ to } \mathbb{S}^0 \times \mathbb{S}^0 \times \mathbb{B}^{6n_b-6} \text{ to } \mathbb{S}^1 \times \mathbb{B}^{6n_b-7} \text{ to } X \text{ to } Y \text{ to } \mathbb{T}^2 \times \mathbb{B}^{6n_b-8},$$

and the transition states

$$\mathbb{S}^0 \times \mathbb{S}^{6n_b-7} \text{ to } \mathbb{S}^0 \times \mathbb{S}^0 \times \mathbb{S}^{6n_b-7} \text{ to } \mathbb{S}^1 \times \mathbb{S}^{6n_b-8} \text{ to } \partial X \text{ to } \partial Y \text{ to } \mathbb{T}^2 \times \mathbb{S}^{6n_b-9}.$$

Similarly for the dividing surfaces.

Finally, if we were to consider higher energies in this scenario, the other attitude would also become involved in Morse bifurcations. Here again the $\hat{\beta}$ points would most likely lead to interesting sequences of Morse bifurcations, however we would also have to deal with the non-trivial nature of the fibre bundle. After the Morse bifurcations at the index-2 critical points $\bar{\beta}^2$, the base space would contain a 2-sphere, and many examples of non-trivial orientable bundles over these can be found. Thus before we can consider the full sequence of Morse bifurcations of the dividing surfaces and transition states and the transport for a larger range of energies, the bundle class of the reduced state space needs to be understood.

3.5   Comment. Spatial reactions for collinear molecules

By considering normal molecules, with a fixed equilibrium configuration and energies below that at which either of the molecules dissociates, collinearity becomes a decreasing concern with increasing size of the molecules, namely codimension-$(2n_i - 5)$ where $n_i \geq 3$ is the number of atoms in the ith molecule, not taking into account the chemistry of the molecule. However, for smaller molecules, higher energies, or other transport problems we may need to consider collinear configurations.

For non-zero angular momentum, collinear configurations are a subset of the principal reduced stratum, thus no different to non-collinear configurations. However due to collinear configurations having non-trivial configuration space isotropy, we cannot find charts via the gauge theoretic approach to cotangent bundle reduction of Appendix A.4. The issue is therefore not one of reduction per se, but only of finding suitable coordinates. The transport problem and bifurcations of transition states will be the

same as those considered in Section 3.4.

For more than seventy years, chemists have been using charts obtained by modifying gauge theoretic cotangent bundle reduction [Say39]. The idea is to pass to a rotating frame in which the collinear (equilibrium) configuration is along a chosen axis, say the x_1-axis, but retain the remaining rotational symmetry (about x_1) as an internal coordinate. Then by choosing the Eckart convention and the non-gauge invariant form of the kinetic energy, we find that the Lagrangian is not a function of the angular velocity about the collinear axis ω_1, so we can obtain a Hamiltonian that is not a function of the first angular momentum component l_1. That is, l_1 is replaced by the canonical momentum conjugate to the "internal" rotation about the x_1-axis. These charts were first considered by Sayvetz [Say39], though nowadays they are often attributed to Watson [Wat70].

This procedure can be justified geometrically by applying the slice theorem (see e.g. [OR04, Section 2.3.14]) to configuration space in a neighbourhood of the collinear configurations, and then lifting the charts obtained to the cotangent bundle [RSS06]. Actually, with this understanding, charts can be obtained that are not those of the Eckart convention, i.e. other gauges and internal coordinates. This was used in examples by Kozin et al. [KRT00] to find charts in the collinear neighbourhood.

Note that this is just the splitting of coordinates into internal coordinates and rotations, not an actual reduction, cf. Appendix A.4. With these chart, we cannot simply pass to Serret-Andoyer coordinates to reduce the symmetry seeing as the Hamiltonian is not a function l_1. This is generally not addressed in literature.

Chapter 4

Conclusions and discussion

We have shown the existence of a class of systems for which the dividing surface method can be extended beyond the well known basic transport scenario by using Morse theory.

A natural question given these bifurcations is how the flux of ergode through the dividing surface varies, as a function of energy, through a Morse bifurcation. In Section 2.5, we see that except in the 2 degree of freedom case, the Morse bifurcations do not have a significant effect on the flux, which varies C^{m-2} smoothly through these. In 2 degrees of freedom, the flux has a $-\Delta E \ln |\Delta E|$ infinite-slope singularity at an index-1 saddle on the transition manifold.

These bifurcations can be used to study many important transport problems for larger ranges of energies than previously thought possible. An example is bimolecular reactions, as seen from the capture rates considered in Chapter 3. By considering the various different sequences of Morse bifurcations we were able to find interesting new transition states and dividing surfaces for general reactions with non-zero angular momentum.

The bimolecular reactions that we considered possessed Euclidean symmetry and were reduced accordingly. Even though symplectic reduction theory is an old and much studied subject, when considering these examples we faced a number of difficulties. Setting aside the fact that these examples require singular reduction, due to the nature of the rotational symmetry, and that singular cotangent bundle reduction is still not a complete theory, there is a large gap between the reduction theory literature and applications. Finding suitable charts for the reduced n-body system, even if we restrict our attention to the principal non-singular stratum, is not an easy task. Some of the literature avoids charts altogether focusing instead on the global geometric properties of the reduced spaces, whereas the celestial mechanics literature considers different regions of the reduced space. The most common approach in the literature concerning reaction dynamics is to restrict ones attention to non-collinear configuration such that the gauge theoretic approach to cotangent bundle reduction provides a set of charts, as reviewed in Appendix A.4. This can even be extended to collinear configurations, as commented in Section 3.5. However, here we face the opposite issue, namely the reduced space is an $\mathbb{S}^2$ fibre bundle, due to the extra angular momentum degree of freedom, but the global nature of this bundle is generally not discussed in the literature. We feel that

more work is needed, both on charts for the reduced spaces and on their global nature, and that this would improve our understanding of molecular reactions, and also other n-body systems.

The usefulness of capture rates as a bound on actual reaction rates is debatable, but largely depends on the reaction being considered. However, the moral of our study is that the attitude and angular momentum degrees of freedom are important, seeing as the most common examples found in the literature are collinear bimolecular reactions, and that critical energy values and Morse bifurcations are (mostly) not an issue.

Generally, we expect to see Morse bifurcations in a large class of transport problems from various applications. In the context of applications, numerical methods to find and continue transition manifolds (through the Morse bifurcations) would be ideal. Some numerical methods for normally hyperbolic submanifolds do exist, and others are being developed, however the high dimensionality of the transition manifolds and the global nature of the problem pose serious problems.

We have concentrated here on how the transition state and dividing surface vary with energy, but in a system depending smoothly on other parameters, a Morse bifurcation at energy E_b for parameter value λ_b implies a Morse bifurcation at some nearby smoothly varying energy $E(\lambda)$ for parameter λ near λ_b. Thus for generic (i.e. non-tangential) paths in the combined space (E, λ) there is a Morse bifurcation on crossing $E = E(\lambda)$. An example of another parameter is the angular momentum λ of the bimolecular reactions. The exact dependence of the capture transition states on the angular momentum and the possible loss of normal hyperbolicity for large values should be considered in detail.

This leads us to the question of bifurcations leading to the loss of normal hyperbolicity of the transition manifold (for systems with more than 2 degrees of freedom) and their effect on Hamiltonian transport. There have been some studies investigating the loss of normal hyperbolicity for submanifolds of dimension greater than one, see e.g. [LTK09, TTK11, AB12] and references therein, but it is still not understood, nor is the effect that it will have on transport problems. However, for Hamiltonian systems normally hyperbolic submanifolds (that satisfy a spectral gap condition) are symplectic (Proposition A.1.2). This may provide an alternative way of understanding these complicated situations. See e.g. the loss of symplectic nature of the transition manifold in the disconnecting example of Section 2.4.1.

Other than losing normal hyperbolicity, transition states may also develop topological properties that prevent them from being spanned by a dividing surface and so acting as a transition state. For the special case of 2 degree of freedom systems, some topological obstructions were considered in Subsection 2.3.1, however for higher degrees the topological possibilities are many more. A study of the topological obstructions of periodic orbit transition states which is under way will hopefully be the start of a series of such studies also for the higher dimensional case.

An open question regarding the dividing surface method, which is related to this work is what happens when a dividing manifold cannot be defined over a large enough region of state space, such that even though one finds a sufficiently large normally hy-

perbolic submanifold that can potentially act as a transition manifold and be restricted to transition states, one cannot find dividing surfaces spanning them above certain energies? This breakdown of the dividing manifold, brought about by the intersection of the stable and unstable submanifolds of the transition manifolds, and its effect on transport problems needs to be investigated.

There are a number of applications that cannot be studied using the dividing surface method. One may ask whether there are any possible extensions of the theory that would allow for it to be be used in these applications too. Amongst these are the reactions out of equilibrium, non-autonomous Hamiltonian systems representing for example reactions with an external field or laser pulse, and also systems for which the product kinetic approximation leading to a low dimensional Hamiltonian system is not valid, but which might instead be modelled by some quasi-Hamiltonian system.

Appendices

A.1 Normally hyperbolic submanifolds

Loosely speaking, a smooth, compact (possibly with boundary) invariant submanifold of a dynamical system is said to be normally hyperbolic if the linearised dynamics in the normal direction is hyperbolic and dominates the linearised tangent dynamics.

Here, we shall recall a precise definition of a normally hyperbolic submanifold, cf. [Fen71, HPS77], and present a method of finding approximations to normally hyperbolic (symplectic) submanifolds of Hamiltonian systems taken from MacKay's lectures on slow manifolds [Mac04].

A.1.1 Definitions and properties

We choose to work with the following

Definition. Consider a dynamical system $\left(M, h^t\right)$ consisting of a C^1 flow h^t on a smooth manifold M, and choose a Riemannian metric on M. Let N be a compact (possibly with boundary) C^1 submanifold of M that is invariant under the flow, i.e. $h^t(N) = N$. We say that N is a *normally hyperbolic submanifold* (of the dynamical system) if the tangent bundle of M restricted to N, $T_N M$, can be split continuously[*35]

$$T_N M = TN \oplus E^+ \oplus E^-,$$

such that $TN \oplus E^{\pm}$ are invariant under Dh^t for all t and there exist real numbers $k^{\pm}, k > 0$ and $0 \leq b < a$, such that for all $\tilde{z} \in N$, we have the following growth rates

$$\|\pi^+ \circ D_{\tilde{z}} h^t|_{E^+}\| \leq k^+ e^{at}, \quad \forall t \leq 0,$$
$$\|\pi^- \circ D_{\tilde{z}} h^t|_{E^-}\| \leq k^- e^{-at}, \quad \forall t \geq 0,$$
$$\|D_{\tilde{z}} h^t|_{TN}\| \leq k e^{b|t|}, \quad \forall t \in \mathbb{R},$$

where $\pi^{\pm} : T_N M \to E^{\pm}$ are the projections induced by the splitting.

This is stronger than the usual definition, say that of Fenichel [Fen71, Section IV] as we can see from his uniformity lemma, but appropriate for our purposes. The inequality satisfied by a and b is generally referred to as the spectral gap condition.

[*35] There are two opposite notations for the sign of $E^{\pm}$ in literature, plus many other notations. The one used here respects the sign of the eigenvalues, whereas the other one follows the direction of time along which trajectories approach the normally hyperbolic manifold.

Remark A.1.1 (Choice of splitting). Note that generally the normal hyperbolicity will depend on the choice of splitting. There exists an invariant splitting that simplifies the theory, and is forced upon the definition in most of the literature. However, this choice of splitting is unnecessary and when considering concrete examples finding it can be cumbersome. Like Fenichel [Fen71], which uses a Riemannian splitting, we choose a general splitting that is not invariant.

For the general properties of normally hyperbolic submanifolds, such as persistence, stable and unstable manifolds and smoothness results, see e.g. Fenichel [Fen71] or Hirsch, Pugh and Shub [HPS77].

We are interested in Hamiltonian systems with their symplectic state space. In this case, normally hyperbolic submanifolds with a spectral gap condition, as in our definition, are symplectic. This was noted by Marco [Mar], who refers to normally hyperbolic submanifolds satisfying a gap condition as *controllable*, and Gelfreich and Turaev [GT14].

Proposition A.1.2. *Normally hyperbolic submanifolds (satisfying a spectral gap condition) of Hamiltonian systems are symplectic, specifically ω_N is non-degenerate.*

The proof, which can be found in [Mar, GT14], is the following.

Proof. Recall that normally hyperbolic submanifolds N have stable and unstable submanifolds $W^\pm(N)$, which are tangent at N to $TN \oplus E^\pm$, and that $N = W^+(N) \cap W^-(N)$. Furthermore, $W^\pm(N)$ are invariantly fibred by submanifolds $W^\pm(\tilde{z})$ for $\tilde{z} \in N$, usually referred to as *strong stable* and *strong unstable manifolds*. If we consider the invariant splitting, in which $E^\pm$ are invariant under Dh_t, then $W^\pm(\tilde{z})$ are tangent at N to $E_{\tilde{z}}^\pm$ [HPS77]. We shall use the invariant splitting in what follows. Firstly, we note that $TW^\pm(N) \perp_\omega TW^\pm(\tilde{z})$ for all $\tilde{z} \in N$. Considering $\eta \in T_{\tilde{z}}W^-(\tilde{z}) = E_{\tilde{z}}^-$ and $\nu \in T_{\tilde{z}}W^-(N)$, we find that

$$|\omega(\eta,\nu)| = |\omega(Dh_t(\eta), Dh_t(\nu))| \le c|Dh_t(\eta)||Dh_t(\nu)| \le ck^- e^{-at}(k^- e^{-at} + ke^{|b|t})|\eta||\nu|,$$

for $t \ge 0$, with the same notation used previously. This tends to zero in the limit as $t \to +\infty$ since $0 \le b < a$. Thus $T_{\tilde{z}}W^-(\tilde{z}) \perp_\omega T_{\tilde{z}}W^-(N)$ and by invariance of ω under the flow h_t, $TW^-(\tilde{z}) \perp_\omega TW^-(N)$. Similarly $TW^+(\tilde{z}) \perp_\omega TW^+(N)$. Now assume that, contrary to the claim, ω_N is degenerate and there is a non-zero tangent vector $\hat{\xi} \in T_{\tilde{z}}N$ such that $\hat{\xi} \perp_\omega T_{\tilde{z}}N$. Since $\hat{\xi} \in T_{\tilde{z}}W^+(N) \cap T_{\tilde{z}}W^-(N)$, we find that $\hat{\xi} \perp_\omega T_{\tilde{z}}W^\pm(\tilde{z})$. Then, due to the splitting of TM_N,

$$T_{\tilde{z}}M = E_{\tilde{z}}^+ \oplus T_{\tilde{z}}N \oplus E_{\tilde{z}}^-,$$

we have that $\hat{\xi} \perp_\omega T_{\tilde{z}}M$, contradicting the non-degeneracy of ω. $\qquad\square$

Given a vector field X generating the flow h^t, the linearised flow Dh^t about the normally hyperbolic submanifold N satisfies the (first) variation equation

$$\frac{\mathrm{d}}{\mathrm{d}t}\left(D_{\tilde{z}}h^t(\nu)\right) = D_{h^t(\tilde{z})}X \cdot D_{\tilde{z}}h^t(\nu),$$

for $\tilde{z} \in N$, $\nu \in T_{\tilde{z}}M$. The splitting allows us to write $\nu = v_1\xi + v_2\eta_+ + v_3\eta_-$ with $v = (v_1, v_2, v_3)$ and re-write the variation equation as

$$\dot{v} = \begin{pmatrix} T & C_+ & C_- \\ 0 & V_+ & 0 \\ 0 & 0 & V_- \end{pmatrix} v,$$

where we have used the invariance of N and $TN \oplus E^{\pm}$. Thus, by asking that

$$\|V_+^{-1}\|^{-1} \geq a, \quad \|V_-^{-1}\|^{-1} \geq a, \quad \|T\| \leq b, \quad \|C_{\pm}\| \text{ bounded},$$

we recover the conditions on the linearised flow from the definition, see e.g. differential inequalities in [Hal69, Section I.6].

For Hamiltonian systems we could "re-write" the definition in terms of properties of the linearised Hamiltonian (of the variation equation).

A.1.2 Approximating (symplectic) normally hyperbolic submanifolds of Hamiltonian systems

A main theorem on normally hyperbolic submanifolds tells us that given an "almost invariant" normally hyperbolic submanifold N_0 of a dynamical system, meaning that on N_0 the normal component of the vector field is small, there exists a true normally hyperbolic submanifold N nearby. Here, we are interested in (symplectic) normally hyperbolic submanifolds of Hamiltonian systems and we want to find sufficiently good approximations to the Hamiltonian on normally hyperbolic submanifolds to deduce the sequence of Morse bifurcations as energy is increased. Thus, we will show how to find a better approximation of an almost invariant normally hyperbolic symplectic submanifold N_0, using a symplectically orthogonal fibration of its neighbourhood. The approach follows MacKay's lectures that present the slow manifold case [Mac04].

Theorem A.1.3. *Every almost invariant, normally hyperbolic submanifold N_0 of a Hamiltonian system can be improved to one that also contains all nearby equilibria and has a smaller angle to the vector field.*

Proof. Given a Hamiltonian system (M^{2m}, ω, H) with vector field X_H generating a flow h^t, and a symplectic submanifold N_0, consider a symplectic fibration of a tubular neighbourhood $U \subset M$ of N_0, $\pi : U \to N_0 : z \mapsto \tilde{z}$, as defined in Section 2.2. The vertical subbundle is given by

$$\text{Vert}_z = \ker d_z\pi = T_z F_{\tilde{z}}, \quad \forall z \in U,$$

and by choosing the horizontal subbundle to be symplectically orthogonal to the vertical subbundle, i.e.

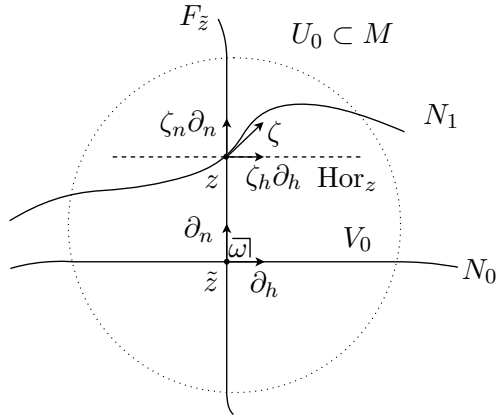$$\text{Hor}_z = \text{Vert}_z^{\omega},$$

Figure A.1: Schematic representation of the construction used to find a better approximation N_1 to a normally hyperbolic submanifold N given an almost invariant normally hyperbolic symplectic submanifold N_0. Note: finding N_1 does not require any specific coordinates.

we obtain a symplectic splitting of the tangent bundle of the neighbourhood of N_0

$$TM = \mathrm{Vert} \oplus^\omega \mathrm{Hor}.$$

Seeing as N_0 is a symplectic submanifold of M, we can choose (local) Darboux coordinates $z = (x, u, y, v)$ for a neighbourhood $U_0 \subset M$ of $\tilde{z} \in N_0$ in which $\omega = \mathrm{d}x \wedge \mathrm{d}y + \mathrm{d}u \wedge \mathrm{d}v$ and such that $N_0 = \{z \in M | x = y = 0\}$ and $F_{\tilde{z}} = \{z \in M | u = \tilde{u}, \ v = \tilde{v}\}$, where $\tilde{z} = (0, \tilde{u}, 0, \tilde{v})$ and everything is restricted to U_0. We shall often write $h = (u, v)$ and $n = (x, y)$. To justify this local chart, we must note that we have restricted to a neighbourhood $V_0 \subset N_0$ of $\tilde{z}$, such that $U_0 = \pi^{-1}(V_0)$ and by the local trivialisation is diffeomorphic to $V_0 \times F$. Then the chart is the symplectomorphism to $(\mathbb{R}^{2m}, \omega_0)$ given by the symplectic neighbourhood theorem (see e.g. [MS98, Theorem 3.30]). In these coordinates, the tangent space $\mathrm{Hor}_z = \mathrm{span}\{\partial_h\}$ for $z \in F_{\tilde{z}}$, but globally the fibration may not be trivial and the Hor subbundle is not necessarily integrable (as discussed by Guillemin et al. [GLS96, Section 1.3]). See Figure A.1 for a depiction of the above. Now, we can write the equations of motion as

$$\dot{z} = J \, DH(z),$$

and the variation equation is

$$\dot{v} = J \, D^2 H\left(h^t(\tilde{z})\right) v.$$

The assumptions of almost invariance, i.e. $\|DH|_{F_{\tilde{z}}}(\tilde{z})\| \leq \varepsilon$ small for $\tilde{z} \in N_0$, and that the normal dynamics is hyperbolic, which can be written as $\|D^2 H|_{F_{\tilde{z}}}(\tilde{z})^{-1}\|^{-1} \geq a > 0$, together with the implicit function theorem give the existence of a locally unique critical point $n_c(\tilde{h})$ of $H_{F_{\tilde{z}}}$ that is within approximately $a^{-1}\varepsilon$ of N_0 and depends smoothly on $\tilde{z} = (\tilde{h}, 0) \in N_0$. Then define the new approximate submanifold N_1 to be the graph of n_c, so in particular N_1 contains all nearby true equilibria of the system.

Note that finding N_1 does not require any special coordinates. However, our choice of Darboux coordinates will now be used to show that N_1 is a better type of approximation to the true normally hyperbolic submanifold N than N_0, in the sense that the angle of the vector field to N_1 is small (called "first order" in [Mac04]).

Firstly, the restriction ω_{N_1} of ω to N_1 is non-degenerate, and we use it to define $X_{H_{N_1}}$ tangent to N_1 via $\omega_{N_1}(X_{H_{N_1}}, \zeta) = \mathrm{d}H_{N_1}(\zeta)$ for all $\zeta \in T_z N_1$. Then, to check that $X_H - X_{H_{N_1}}$ is small compared to $X_{H_{N_1}}$, we first find that $|\omega(\zeta, \eta)| \leq ca^{-1}\delta|\zeta||\eta|$ for $\zeta \in T_z N_1$, $\eta \in T_z F_{\tilde{z}}$ with $z \in N_1$, $\delta = |\partial_{hn}^2 H(z)|$ and c slightly larger than 1. This can be seen by splitting the vectors tangent to N_1 into a horizontal and vertical part, namely $\zeta = \zeta_h \partial_h + \zeta_n \partial_n \in T_z N_1$, and writing $DH|_{F_{\tilde{z}}}(h, n_c)$ as $\partial_n H(h, n_c)$. The tangent vectors satisfy

$$\mathrm{d}(\partial_n H)(\zeta) = \partial_{hn}^2 H(h, n_c)\zeta_h + \partial_{nn}^2 H(h, n_c)\zeta_n = 0,$$

so

$$\zeta_n = -(\partial_{nn}^2 H(h, n_c))^{-1}\partial_{hn}^2 H(h, n_c)\zeta_h = D_h n_c(h)\zeta_h.$$

Then $|D_h n_c(h)| \leq ca^{-1}\delta$ and $|\omega(\zeta, \eta)| \leq ca^{-1}\delta|\zeta||\eta|$. Next, we note that due to the definition of N_1, at $z \in N_1$ the vector field satisfies $\omega(X_H, \eta) = 0$ and $\omega(X_H, \zeta) = \omega(X_{H_{N_1}}, \zeta)$.

Finally, for a general $\nu \in T_z M$, split it as $\nu = \zeta + \eta$ with $\zeta \in T_z N_1$, $\eta \in T_z F_{\tilde{z}}$, then

$$\begin{aligned}
\omega(X_H - X_{H_{N_1}}, \nu) &= \omega(X_H - X_{H_{N_1}}, \zeta + \eta) \\
&= \omega(X_H, \zeta) + \omega(X_H, \eta) - \omega(X_{H_{N_1}}, \zeta) - \omega(X_{H_{N_1}}, \eta) \\
&= \mathcal{O}(a^{-1}\delta|X_{H_{N_1}}||\eta|).
\end{aligned}$$

Thus $X_H - X_{H_{N_1}} = \mathcal{O}(a^{-1}\delta|X_{H_{N_1}}|)$, as claimed. $\qquad\square$

Note however that beyond the first iteration, the required procedure is more subtle than [Mac04] might lead one to suppose. In order to ensure that for the successive approximations the normal vector field is of the order of higher powers of the tangential vector field, one has to carefully choose a nearly symplectically orthogonal fibration at each subsequent step[*36].

A.2   Some properties of centre manifolds

This appendix highlights some of the properties of centre manifolds, namely normal hyperbolicity, uniqueness and symplectic nature, specific to Hamiltonian systems. Of the many references available, I like the straight forward introduction in Guckenheimer and Holmes [GH90, Section 3.2]. For more details, Sijbrand [Sij85] presents a thorough discussion of their properties, and has a good list of old (pre-1985) references.

[*36] Robert MacKay gave a talk at the Newton Institute in Cambridge in 2007 where this was addressed and an incomplete draft paper of March 3rd 2007 sketches the procedure, but the paper has not yet been completed.
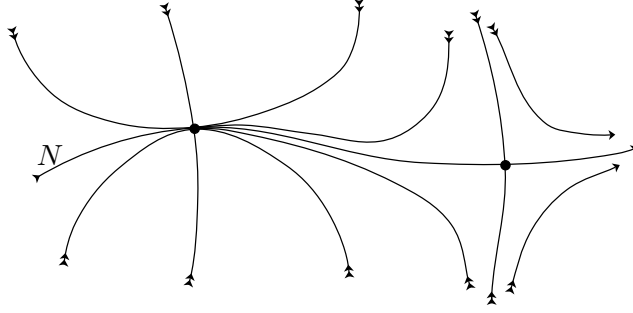
Figure A.2: Example of multiple non-unique centre manifolds for the left equilibrium point and a unique normally hyperbolic manifold, N, passing through both equilibria.

Definition. Given a non-hyperbolic equilibrium point $\bar{z}$ of a vector field X on M, the *centre subspace* $\hat{N}$ is defined as the span of eigenvectors corresponding to eigenvalues on the imaginary axis. There exists a locally invariant (under the flow) submanifold N of M, called the *centre manifold*, that passes through the critical point and is tangent to the centre subspace at this point.

See Guckenheimer and Holmes [GH90, Section 3.2] for the usual graph representation and its Taylor expansion. Note that as a submanifold, the centre manifold can actually be represented in various ways. For example, Leen gives a way of representing centre manifolds as a parametrised surface [Lee93].

Centre manifolds and normally hyperbolic manifolds have the same spectral conditions, but the definition of centre manifolds is local whereas that of normally hyperbolic manifolds is global. Namely, centre manifolds are defined in terms of the splitting of the linearised dynamics locally at an equilibrium, whereas normally hyperbolic manifolds are invariant submanifolds for which the splitting of rates holds at every point. Thus, by definition a centre manifold is normally hyperbolic at the equilibrium, and in a neighbourhood thereof.

Centre manifolds are not necessarily unique. This difference with respect to normally hyperbolic manifolds is in fact due to the local nature of the definition of a centre manifold, noted above. An example showing this difference is given in Figure A.2. Here, N is a normally hyperbolic manifold and a (generalised) centre manifold for both equilibria. However, we could also choose any other trajectory through the left equilibrium as a local centre manifold, exemplifying the non-uniqueness. These other choices are not normally hyperbolic away from the equilibrium. However, one can also have unique centre manifolds. Seeing as the definition of a centre manifold alone does not ensure uniqueness, when this is the case it is due to the dynamics of the system. Sijbrand [Sij85, Theorem 3.2], has the following

Theorem A.2.1. *Given a flow with an equilibrium $\bar{z}$ that has a non-empty centre subspace, the centre manifold N about $\bar{z}$ is unique*

  i. when $E_{\bar{z}}^{+} = \emptyset$, if the flow on N is bounded to a neighbourhood of $\bar{z}$ for all $t < 0$.

  ii. when $E_{\bar{z}}^{-} = \emptyset$, if the flow on N is bounded to a neighbourhood of $\bar{z}$ for all $t > 0$.

iii. when $E_{\bar{z}}^{\pm} \neq \emptyset$, if the flow on N is bounded to a neighbourhood of $\bar{z}$ for all $t \in \mathbb{R}$.

Sijbrand gives a proof based on the contraction mapping, and makes a remark about a more geometric proof [Sij85, Remark 1], which I couldn't find in the literature. Note that Hamiltonian systems only ever have case (iii), as dim $E_{\bar{z}}^{+} = $ dim $E_{\bar{z}}^{-}$.

Centre manifolds of non-hyperbolic equilibria of Hamiltonian systems are also symplectic. This has "always" been known, but the first reference that I could find is Mielke [Mie91, Theorem 4.1].

Proposition A.2.2. *A local centre manifold N of a non-degenerate equilibrium point $\bar{z}$ for a Hamiltonian system $\left(M^{2m}, \omega, H\right)$ is a symplectic submanifold of the state space with symplectic form ω_N, the restriction of ω.*

Proof. We must show that ω_N is a closed, nondegenerate form on N. Actually, we only need to prove nondegeneracy, since restriction and the exterior derivative commute, and so ω_N is closed ($\mathrm{d}\omega_N = 0$). At the equilibrium, nondegeneracy follows from Williamson's theorem [Arn89, Appendix 6], namely the symplectic tangent space $T_{\bar{z}}M$ decomposes into a direct sum of symplectic subspaces, one being the subspace corresponding to the elliptic eigenvalues and tangent to the centre manifold N. Then, nondegeneracy holds in a neighbourhood of the equilibrium. $\square$

Thus, the restriction of a Hamiltonian vector field to a centre manifold is the Hamiltonian vector field of the restricted system, namely

Proposition A.2.3. *The Hamiltonian vector field restricted to the centre manifold $X_H|_N$ preserves the restricted symplectic form ω_N on N and is equal to the vector field of the reduced Hamiltonian system (N, ω_N, H_N), i.e. $X_H|_N = X_{H_N}$.*

Proof. Firstly, $X_H|_N$ and ω_N are restrictions to N, and both N and ω are invariant under the flow of X_H, thus ω_N is preserved by $X_H|_N$. Then, N is invariant, so $X_H|_N \in \mathcal{T}(N)$. Hence

$$\mathrm{d}H\left(\xi\right) = \omega\left(X_H, \xi\right) = \omega_N\left(X_H|_N, \xi\right), \quad \forall \xi \in T_{\bar{z}}N$$

and

$$\mathrm{d}H\left(\xi\right) = \mathrm{d}H_N\left(\xi\right),$$

so $X_H|_N = X_{H_N}$. $\square$

A.3   Basics of Morse theory

Morse theory allows us to study the topology of a manifold by considering the properties of "height" functions on it, and vice versa. It is therefore a natural tool for Hamiltonian systems with their Hamiltonian functions. We briefly state a few of the definitions and theorems (without proofs) and mention how they can be used to study bifurcations. For details see e.g. Milnor [Mil63] or Bott [Bot82].

Consider an m-dimensional smooth manifold M and a smooth function $H : M \to \mathbb{R}$. Recall that, a point $\bar{z} \in M$ is *critical*, relative to H, if $\mathrm{d}_{\bar{z}}H = 0$. Given local coordinates

$x = (x_1, \cdots, x_m)$ about $\bar{z}$, we have that

$$\frac{\partial H}{\partial x_1}(\bar{z}) = \cdots = \frac{\partial H}{\partial x_m}(\bar{z}) = 0.$$

Also, for a critical point $\bar{z}$, we can define a symmetric bilinear form, $\text{Hess}_{\bar{z}}(H)$, called the *Hessian*. If ξ, η are tangent vectors at $\bar{z}$, and X, Y extensions to vector fields, we let $\text{Hess}_{\bar{z}}(H)(\xi, \eta) = X_{\bar{z}}(Y(H))$. This is symmetric and independent of the extensions [Mil63, Section 2].

We can now give the

Definition. The *(Morse) index* $\lambda(\bar{z})$ of a critical point $\bar{z}$, relative to H, is the maximal dimension of a subspace V of the tangent space on which the Hessian, $\text{Hess}_{\bar{z}}(H)$, is negative definite, that is $\text{Hess}_{\bar{z}}(H)(\xi, \eta) < 0$ for all $\xi, \eta \in V$. The *nullity* of $\bar{z}$ relative to H is the dimension of the null-space, i.e. the subspace consisting of all $\eta \in T_{\bar{z}}M$ such that $\text{Hess}_{\bar{z}}(H)(\eta, \xi) = 0$ for all $\xi \in T_{\bar{z}}M$.

In local coordinates, the index is the number of negative eigenvalues of the local representation of the Hessian at $\bar{z}$, $D^2 H(\bar{z})$, counting multiplicities. The nullity is given by dim M − rank $D^2 H(\bar{z})$. Recall that a critical point is called *nondegenerate* if the Hessian has nullity zero.

A smooth function H is a said to be a *Morse function* if all of its critical points, $\bar{z}_i \in Cr(H)$, are nondegenerate.

Near a nondegenerate critical point, the level sets of H are quadrics given by the

Morse Lemma. *Let $\bar{z}$ be a nondegenerate critical point, relative to H, of index λ. Then, in some open neighbourhood of $\bar{z}$, there are local coordinates (x, y) taking the critical point to the origin, and for which the local representation of H satisfies*

$$H(x, y) = H(\bar{z}) - \frac{1}{2}\left(x_1^2 + \cdots + x_\lambda^2\right) + \frac{1}{2}\left(y_1^2 + \cdots + y_{m-\lambda}^2\right).$$

Remark A.3.1. The proof gives the coordinate transformation and thus the Morse lemma coordinates. These can be useful when studying bifurcations of the level sets. A neat proof due to Palais, which uses the homotopy method, can be found in [GS90, Appendix 1] or [BH04, Section 3.1].

Remark A.3.2. The Morse lemma can be extended to include the local representation of volume forms, as done by Colin de Verdière and Vey [CV+79]. Namely, given a volume form Ω and the Morse lemma coordinates $z = (x, y)$, in which $H(z) = H(\bar{z}) + H_2(z)$, we find

$$\Omega = \psi(H_2)\Omega_0,$$

where $\Omega_0 = dz_1 \wedge \cdots \wedge dz_m$ is the standard volume form, and ψ is a smooth proper function. Alternatively, there are local coordinates $\tilde{z} = (\tilde{x}, \tilde{y})$ in which

$$H(\tilde{z}) = \Psi(H_2(\tilde{z})),$$
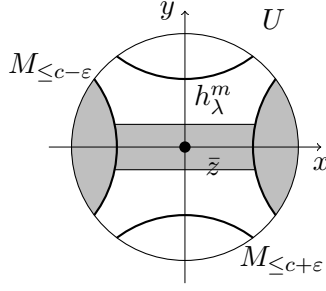$$\Omega = \Omega_0,$$

Figure A.3: Schematic representation of the handle attachment in theorem A.3.4.

where $\Psi(H_2)$ is a power series, and we have assumed that $H(\bar{z}) = 0$. The near identity transformation from this alternative representation to the Morse one is $\tilde{z} = zf(H_2(z))$ where $\Psi(H_2)^{1/2} =: H_2^{1/2}f(H_2)$. Colin de Verdière and Vey refer to these as the *iso-choric*[*37] Morse lemma [CV+79], see also [Fra88]. For two dimensional manifolds, the alternative version is often referred to as the symplectic Morse lemma, and is equivalent to a local Birkhoff normal form [Arn89, Appendix 7].

Now, for a real number a, $M_{\leq a} = \{z \in M | H(z) \leq a\}$ is the *sub-level set*, for a. If a is a regular value of H, then these are manifolds with boundary $M_a = \partial M_{\leq a} = \{z \in M | H(z) = a\}$, the *level sets*. Regarding these manifolds, we have

Theorem A.3.3. *Let $a < b$ be real numbers with $H^{-1}([a,b])$ compact. Suppose $H^{-1}([a,b])$ contains no critical points of H. Then $M_{\leq a}$ is diffeomorphic to $M_{\leq b}$, and hence so are their boundaries, $M_b \cong M_a$. Furthermore $H^{-1}([a,b]) \cong M_a \times [0,1] \cong M_b \times [0,1]$.*

To consider what happens when we "pass" a critical point, we need to recall how to attach handles. Firstly, we need the

Definition. An index-λ *handle*, or λ-handle of dimension m is $h_\lambda^m = \mathbb{B}^\lambda \times \mathbb{B}^{m-\lambda}$, where $\mathbb{B}^k$ is the unit ball in $\mathbb{R}^k$. The *axis* (also called *core*) of the handle is $\mathbb{B}^\lambda \times \{0\} \subset h_\lambda^m$.

Now, consider a manifold M^m with boundary ∂M, a handle h_λ^m and a smooth embedding $\psi : \mathbb{S}^{\lambda-1} \times \mathbb{B}^{m-\lambda} \to \partial M$, called the *attaching map*. We can form a topological space by taking the disjoint union, $M \cup h_\lambda^m$, and then identifying z in the boundary of the handle with $\psi(z) \in \partial M$. The quotient space thus obtained is denoted $M \cup_\psi h_\lambda^m$. Finally, we can show that $M \cup_\psi h_\lambda^m$ admits a unique (up to diffeomorphism) smooth dimension-m structure (see e.g. Milnor [Mil63, Section 3]). Note that attaching a 0-handle gives the disjoint union $M \cup \mathbb{B}^m$.

The effect of "passing" a critical point of the function on the diffeomorphism class of the sub-level sets is given by

Theorem A.3.4. *Suppose c is a critical value of H such that M_c contains a single nondegenerate critical point $\bar{z}$ of Morse index λ. Then for every $\varepsilon > 0$ sufficiently small,*

[*37] Of constant volume. Technically, only the alternative version of the lemma and if $\Omega = \Omega_0$ to start with.

the sub-level set $M_{\leq c+\varepsilon}$ is diffeomorphic to $M_{\leq c-\varepsilon}$ with an index-λ handle attached, i.e.

$$M_{\leq c+\varepsilon} \cong M_{\leq c-\varepsilon} \cup_\psi h_\lambda^m.$$

The handle attachment of Theorem A.3.4 is shown in Figure A.3. If we choose the Morse lemma coordinates (x, y) about $\bar{z}$ the handle is given by

$$h_\lambda^m = \{|x|^2 - |y|^2 \leq \varepsilon, \ |y|^2 \leq \delta\},$$

and the axis of the handle is given by

$$\mathbb{B}^\lambda \times \{0\} = \{|x|^2 \leq \varepsilon, y = 0\}.$$

The figure also shows how the embedding is chosen naturally without ambiguity.

The representation of the sub-level set $M_{\leq c+\varepsilon}$ given in Theorem A.3.4 is that of a *handlebody*, namely

Definition. A manifold (with boundary in general) obtained from $\mathbb{B}^m$ by attaching handles of various indices one after another

$$\mathbb{B}^m \cup_{\psi_1} \mathbb{B}^{\lambda_1} \times \mathbb{B}^{m-\lambda_1} \cup_{\psi_2} \cdots \cup_{\psi_k} \mathbb{B}^{\lambda_k} \times \mathbb{B}^{m-\lambda_k}$$

is called an m-dimensional *handlebody*.

When considering bifurcations, we want to rewrite the diffeomorphism type in a more natural way. For this, we must know the topology of the sub-level set before the bifurcation, $M_{\leq c-\varepsilon}$, and the orientation of the handle with respect to the sub-level set. This orientation is given by the Morse coordinates.

Note that, with a little care, we can also consider multiple (for a given critical value) and degenerate critical points.

Lastly, Theorem A.3.4 allows us to derive Morse inequalities[*38], which give bounds on the number of critical points and their indices, for Morse functions, based on the topology of the manifold. Firstly, we define the *Morse series of H*

$$\mathcal{M}_t(H) = \sum_{\bar{z}} t^{\lambda(\bar{z})},$$

for critical points $\bar{z} \in C_r(H)$, then we need the *Poincaré series of M*

$$P_t(M) = \sum_k t^k b_k,$$

where $b_k = \dim H_k(M; \mathbb{R})$ are the Betti numbers, i.e. the dimensions of the various homology groups of M over the real numbers. These are topological invariants of the manifold, see e.g. Frankel [Fra04, Chapter 13]. Finally, there exists a polynomial

---

[*38] Precursors to the Morse inequalities, for functions on two-spheres, can be found in the work of Maxwell on topography [Max70].

$Q_t(H)$ in t with non-negative coefficients, and the Morse inequalities are

$$\mathcal{M}_t(H) - P_t(M) = (1+t)\,Q_t(H),$$

see e.g. Bott [Bot82]. One often writes the inequality $\mathcal{M}_t(H) \geq P_t(M)$ instead, hence the name. These relations can and have been used to study the "potential energy surfaces" of molecular dynamics, see Mezey [Mez87, Chapter 2] and references therein.

A.4 Charts for reduced n-body systems in non-collinear configurations

Finding reduced charts for n body Hamiltonian systems in the non-collinear configurations region is straight forward, and can be done by considering the Euclidean action of $SE(3) = \mathbb{R}^3 \times SO(3)$ on configuration space. This gauge theoretic approach to cotangent bundle reduction is nicely reviewed by Littlejohn and Reinsch [LR97]. They however do not consider the final step required to reduce the rotational symmetry and fix the angular momentum. This is achieved by introducing Serret-Andoyer[*39] coordinates, as explained by Deprit [Dep67] (see also [DE93, CW12]). These introduce inevitable coordinate singularities (on the angular momentum sphere), which is probably why Littlejohn and Reinsch avoid them. We shall briefly review the reduction procedure for general n-body systems, and introduce our notation. A specific choice of charts for n-body systems representing bimolecular reactions is given in Section 3.4.

Consider a translation-reduced, rotation invariant n-body systems restricted to the non-collinear subset (i.e. the trivial configuration isotropy-type submanifold) of configuration space $Q_{Id} \subset Q \cong \mathbb{R}^{3(n-1)}$ and written in the Lagrangian formalism

$$L(R, \dot{R}) = \frac{1}{2}\sum_{i=1}^{n-1} m_i |\dot{R}_i|^2 - U(R),$$

where $R = (R_1, \cdots, R_{n-1})$ are some choice of Jacobi vectors. Note that we have chosen to not use normalised or mass-weighted Jacobi vectors, as done in much of the literature. We believe that the mass parameters are best dealt with by non-dimensionalising the system. The potential U is assumed to be invariant under the action of $SO(3)$.

Pass from the inertial frame $\{X_1, X_2, X_3\}$ to a convenient rotating frame $\{x_1, x_2, x_3\}$, which will depend on the problem at hand, and write

$$R_i = g(\psi) \cdot r_i, \quad i = 1, \cdots, n-1,$$

where $g \in SO(3)$ is the rotation parametrised by the Euler angles $\psi = (\psi_1, \psi_2, \psi_3)$, and r_i are the Jacobi vectors in the rotating frame.

The rotating Jacobi vectors can be expressed in terms of $3n-6$ *internal* coordinates q for $Q_{Id}/SO(3)$ by specifying $r_i(q)$, which is called the *gauge* in the physics literature

---

[*39] Often also referred to as Andoyer or Deprit coodinates. A nice account of their history is given by Deprit and Elipe [DE93].

[LR97]. We are effectively considering a fibre bundle $\pi_{Id} : Q_{Id} \to Q_{Id}/SO(3)$, and q are coordinates for the base space. Then, $\sigma(q) = g(\psi) \cdot r_i(q)$ is a section, and the Euler angles $\psi = (\psi_1, \psi_2, \psi_3)$ are coordinates for the fibre, diffeomorphic to $SO(3)$.

In the new coordinates, the kinetic energy is

$$2E_k = \sum_{i,j=1}^{3n-6} \dot{q}_i \tilde{K}_{ij}(q) \dot{q}_j + 2 \sum_{i,j=1}^{3} \sum_{k=1}^{3n-6} \omega_i I_{ij}(q) A_{kj}(q) \dot{q}_k + \sum_{i,j=1}^{3} \omega_i I_{ij}(q) \omega_j,$$

where ω is the angular velocity, that is the vector corresponding to the skew-symmetric matrix $\Omega(\psi) = g^T(\psi) \dot{g}(\psi)$, for which $\omega \times r = \Omega r$, for any 3-vector r. We are therefore considering an *anholonomic* frame (or *vielbein*) $(\dot{q}, \omega)$ for the tangent space at (q, ψ), with $\omega = \Psi(\psi)\dot{\psi}$ [LR97, Appendix C]. The pseudo-metric $\tilde{K}(q)$ satisfies

$$\tilde{K}_{ij}(q) = \sum_{k=1}^{n-1} \frac{\partial r_k(q)}{\partial q_i} \cdot \frac{\partial r_k(q)}{\partial q_j}.$$

This is the restriction of the Euclidean metric on the (translation-reduced) configuration space Q_{Id} to the section $\sigma(Q_{Id}/SO(3))$, and hence a "pseudo-metric" on the internal space $Q_{Id}/SO(3)$. It is of no importance in gauge theoretic terms, but nonetheless features prominently in the molecular literature. The moment of inertia tensor $I(q)$ is given by

$$I(q) = \sum_{k=1}^{n-1} (r_k(q) \cdot r_k(q) I_d - r_k(q) \otimes r_k(q)),$$

or

$$I_{ij}(q) = \sum_{k=1}^{n-1} \sum_{s=1}^{3} m_k \left(r_{ks}(q)^2 \delta_{ij} - r_{ki}(q) r_{kj}(q) \right),$$

and the gauge potential $A(q)$ associated with the Coriolis effect, which is caused by the coupling term, is

$$A(q) = I^{-1}(q) a(q),$$

where $a(q) = (a_1(q), \cdots, a_{3n-6}(q))$ and

$$a_i(q) = \sum_{k=1}^{n-1} r_k(q) \times \frac{\partial r_k(q)}{\partial q_i}.$$

Equivalently

$$A_{ij}(q) = \sum_{k=1}^{n-1} \sum_{s,t,u=1}^{3} I^{js}(q) m_k \epsilon_{stu} r_{kt}(q) \frac{\partial r_{ku}(q)}{\partial q_i},$$

where $I^{ks}(q)$ are components of the inverse moment of inertia tensor $I^{-1}(q)$, and ϵ_{ijk} the Levi-Civita symbols[*40].

The kinetic energy is gauge invariant, i.e. independent of the choice of internal

---

[*40] Recall, the Levi-Civita symbol ϵ_{ijk} is 1 if (i, j, k) is an even permutation of $(1, 2, 3)$, -1 if it is an odd permutation, and 0 if any index is repeated.

coordinates, but the individual terms are not (see [LR97, Section IV.A]). It is therefore rewritten, in a gauge-invariant form, as

$$2E_k = \sum_{i,j=1}^{3n-6} \dot{q}_i K_{ij}(q)\dot{q}_j + \sum_{i,j=1}^{3} \sum_{k=1}^{3n-6} (\omega_i + A_{ki}(q)\dot{q}_k) I_{ij}(q) (\omega_j + A_{kj}(q)\dot{q}_k),$$

where the metric $K(q) = \tilde{K}(q) - A^T(q)I(q)A(q)$. Note that $K(q)$ is an actual (Riemannian) metric on the internal space, obtained by projecting the metric on configuration space Q_{Id} down to the internal space. It is therefore positive definite, but non-Euclidian due to the nature of the internal space [LR97, Section IV.C].

Finally, pass to the Hamiltonian formalism. The momenta are found (via the fibre derivative of the Lagrangian) to be

$$l_i := \frac{\partial L(q, \psi, \dot{q}, \omega)}{\partial \omega_i} = \sum_{j=1}^{3} \sum_{k=1}^{3n-6} I_{ij}(q) (\omega_j + A_{kj}(q)\dot{q}_k),$$

$$p_i := \frac{\partial L(q, \psi, \dot{q}, \omega)}{\partial \dot{q}_i} = \sum_{j=1}^{3n-6} K_{ij}(q)\dot{q}_j + \sum_{j=1}^{3} A_{ij}(q)l_j,$$

where l is the angular momentum in the rotating frame, i.e. $l = g^T(\psi) \cdot L$. The Hamiltonian is then the Legendre transform of the Lagrangian, namely

$$H(q, \hat{\psi}, p, l) = \frac{1}{2} \sum_{i,j=1}^{3n-6} \sum_{k=1}^{3} (p_i - A_{ik}(q)l_k) K^{ij}(q) (p_j - A_{jk}(q)l_k)$$

$$+ \frac{1}{2} \sum_{i,j=1}^{3} l_i I^{ij}(q)l_j + U(q),$$

where the potential is a function of the internal coordinates only, due to the assumption of rotational invariance, and the Euler angles are ignorable.

The symplectic form is

$$\omega = \sum_{i=1}^{3n-6} dq_i \wedge dp_i + \sum_{i,j=1}^{3} \Psi_{ji}(\psi)d\psi_i \wedge dl_j + \frac{1}{2} \sum_{i,j,k,u,v=1}^{3} \epsilon_{ijk} l_i \Psi_{ju}(\psi)\Psi_{kv}(\psi)d\psi_u \wedge d\psi_v.$$

Alternatively, most of the literature considers the Poisson bracket instead, which for two smooth functions F, G is

$$\{F, G\} = (\partial_{q_i}F\partial_{p_i}G - \partial_{p_i}F\partial_{q_i}G) + \Psi^{ji} \left(\partial_{\psi_i}F\partial_{l_j}G - \partial_{l_j}F\partial_{\psi_i}G\right) - \epsilon_{ijk}l_i\partial_{l_j}F\partial_{l_k}G.$$

Littlejohn and Reinsch derive this in [LR97, Section IV.D].

The momenta p are gauge dependent because of the Coriolis term $A^T(q)l$. Passing to gauge-independent non-canonical momenta[*41], $v_i = p_i - A_{ij}(q)l_j$, simplifies the

---

[*41] Littlejohn and Reinsch call these "covariant shape velocities" and denote them v. We shall use the same notation, hoping that it will not lead to any confusion, even though it gives $v_i = K_{ij}(q)\dot{q}_j$.

Hamiltonian and removes this issue. The Hamiltonian becomes

$$H(q, \hat{\psi}, v, l) = \frac{1}{2} \sum_{i,j=1}^{3n-6} \sum_{k=1}^{3} v_i K^{ij}(q) v_j + V(q, l), \quad V(q, l) = \frac{1}{2} \sum_{i,j=1}^{3} l_i I^{ij}(q) l_j + U(q),$$

where V is the effective potential combining the centrifugal term and the potential, and

$$\omega = \sum_{i=1}^{3n-6} \mathrm{d}q_i \wedge \mathrm{d}v_i + \sum_{i=1}^{3n-6} \sum_{j=1}^{3} A_{ij}(q) \mathrm{d}q_i \wedge \mathrm{d}l_j$$

$$+ \frac{1}{2} \sum_{i,k=1}^{3n-6} \sum_{j=1}^{3} l_j \left(B_{kij}(q) + \epsilon_{juv} A_{ku}(q) A_{iv}(q) \right) \mathrm{d}q_i \wedge \mathrm{d}q_k$$

$$+ \sum_{i,j=1}^{3} \Psi_{ji}(\psi) \mathrm{d}\psi_i \wedge \mathrm{d}l_j + \frac{1}{2} \sum_{i,j,k,u,v=1}^{3} \epsilon_{ijk} l_i \Psi_{ju}(\psi) \Psi_{kv}(\psi) \mathrm{d}\psi_u \wedge \mathrm{d}\psi_v,$$

where we have introduced the *Coriolis tensor*

$$B_{ijk}(q) = \partial_{q_i} A_{jk}(q) - \partial_{q_j} A_{ik}(q) - \epsilon_{kst} A_{is}(q) A_{jt}(q),$$

which is a curvature form on fibre bundle (see [LR97, Section III.G]), and simplifies the equations of motion. Effectively, this transformation moves the Coriolis effect from the Hamiltonian to the symplectic form, in the second and third terms. This is similar to non-canonical coordinates for a charged particle in a magnetic field, where the effect of the Lorentz force comes from the symplectic form, see e.g. [Mar92, Section 2.10].

The molecular literature usually does not pass to the gauge-invariant form of the kinetic energy, see discussion in [LR97, Section IV.F].

Note that, by introducing the rotating frame, we have split the coordinates into internal coordinates q and (ignorable) rotations ψ, and their momenta, but we have not actually reduced the system. Since (ψ, l) are non-canonical, the fact that ψ are ignorable doesn't lead to l being constant. We can however pass from the non-canonical (ψ, l) to canonical Serret-Andoyer coordinates (θ, Θ) which consist of the total angular momentum $|l|$ plus two projections of l, which we are free to choose, and three angles. The choice of projection onto the x_1 and X_1-axis is shown in Figure A.4.

We immediately note that

$$l = l(\theta_3, \Theta_2, \Theta_3) = (\Theta_3, \sqrt{\Theta_2^2 - \Theta_3^2} \sin \theta_3, \sqrt{\Theta_2^2 - \Theta_3^2} \cos \theta_3),$$

which we need to transform the Hamiltonian function. Whereas the relations between the new angles θ and the non-canonical angular momentum coordinates is less simple and depends on the original choice of Euler angles. These are of no use to us here, but given in [Dep67] and [DE93], where (θ, Θ) are shown to be canonical coordinates.

The Hamiltonian in these new coordinates is

$$H(q, \hat{\theta}_1, \hat{\theta}_2, \theta_3, v, \hat{\Theta}_1, \Theta_2, \Theta_3) = \frac{1}{2} \sum_{i,j=1}^{3n-6} \sum_{k=1}^{3} v_i K^{ij}(q) v_j + V(q, \theta_3, \Theta_2, \Theta_3).$$
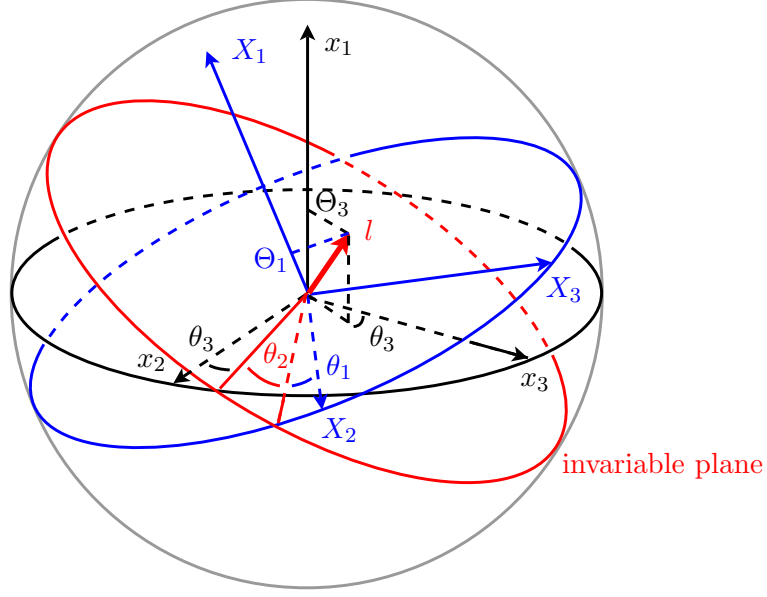
Figure A.4: Transformation to Serret-Andoyer coordinates. $\{X_1, X_2, X_3\}$ is the lab frame, $\{x_1, x_2, x_3\}$ the chosen rotating frame and l the angular momentum vector. $\Theta_2 = |l|$.

The system is reduced by eliminating the ignorable degree of freedom (θ_1, Θ_1), fixing $\Theta_2 = \lambda$, which is the constant absolute value of the angular momentum, and eliminating θ_2. The remaining angular momentum coordinates (θ_3, Θ_3) are a canonical latitude and longitude on the angular momentum sphere $\mathbb{S}^2_\lambda$, henceforth denoted $z_\lambda = (q_\lambda, p_\lambda)$, and there is a coordinate singularity at $p_\lambda = \lambda$. The reduced Hamiltonian function is

$$H\left(q, q_\lambda, v, p_\lambda; \lambda\right) = \frac{1}{2} \sum_{i,j=1}^{3n-6} \sum_{k=1}^{3} v_i K^{ij}(q) v_j + V(q, z_\lambda; \lambda),$$

$$V(q, z_\lambda; \lambda) = \frac{1}{2} \sum_{i,j=1}^{3} l_i(z_\lambda; \lambda) I^{ij}(q) l_j(z_\lambda; \lambda) + U\left(q\right),$$

and

$$\omega = \sum_{i=1}^{3n-6} \mathrm{d}q_i \wedge \mathrm{d}v_i + \sum_{i=1}^{3n-6} \sum_{j=1}^{3} A_{ij}(q) \partial_{z_{\lambda k}} l_j(z_\lambda; \lambda) \mathrm{d}q_i \wedge \mathrm{d}z_{\lambda k}$$

$$+ \frac{1}{2} \sum_{i,k=1}^{3n-6} \sum_{j=1}^{3} l_j(z_\lambda; \lambda) \left(B_{kij}(q) + \epsilon_{juv} A_{ku}(q) A_{iv}(q)\right) \mathrm{d}q_i \wedge \mathrm{d}q_k + \mathrm{d}q_\lambda \wedge \mathrm{d}p_\lambda.$$

The choice of projection is equivalent to a choice of which axis to use as a longitude for $\mathbb{S}^2_\mu$. The transformation for other projections is equivalent. Thus, by considering e.g. minor and major principal axes, we get two charts that cover whole of $\mathbb{S}^2_\mu$.

References

[AB12]   A Allahem and T Bartsch. Chaotic dynamics in multidimensional transition states. *J. Chem. Phys.*, 137(21):214310, 2012.

[AM78]   R Abraham and J E Marsden. *Foundations of Mechanics.* Addison-Wesley, second edition, 1978.

[Arn89]   V I Arnol'd. *Mathematical Methods of Classical Mechanics.* Springer-Verlag, second edition, 1989.

[Bal97]   R Balescu. *Statistical dynamics: Matter out of Equilibrium.* World Scientific, 1997.

[BCM13]   C Baesens, Y-C Chen, and R S MacKay. Abrupt bifurcations in chaotic scattering: view from the anti-integrable limit. *Nonlinearity*, 26(9):2703–2730, 2013.

[BDW96]   A Bolsinov, H R Dullin, and A Wittek. Topology of energy surfaces and existence of transversal poincaré sections. *J. Phys. A*, 29(16):4977, 1996.

[BGO90]   S Bleher, C Grebogi, and E Ott. Bifurcation to chaotic scattering. *Phys. D*, 46(1):87–121, 1990.

[BH04]   A Banyaga and D Hurtubise. *Lectures on Morse homology.* Springer-Verlag, 2004.

[BK84]   D Bensimon and L P Kadanoff. Extended chaos and disappearance of KAM trajectories. *Phys. D*, 13(1):82–89, 1984.

[Bot82]   R Bott. Lectures on Morse theory, old and new. *Bull. Amer. Math. Soc.*, 7(2):331–359, 1982.

[BUF97]   A F Brunello, T Uzer and D Farrelly. Hydrogen atom in circularly polarized microwaves: chaotic ionization via core scattering. *Phys. Rev. A*, 55(5):3730, 1997.

[Bru76]   S G Brush. *The kind of motion we call heat: a history of the kinetic theory of gases in the 19th century.* North-Holland, 1976.

[BS11]   J M Bowman and B C Shepler. Roaming radicals. *Ann. Rev. Phys. Chem.*, 62:531–553, 2011.

[BW83]   J S Birman and R F Williams. Knotted periodic orbits in dynamical systems I: Lorenz's equation. *Topology*, 22(1):47–82, 1983.

[Cay59]   A Cayley. On contour and slope lines. *Philos. Mag.*, 18(120):264–268, 1859.

[CB82]   W J Chesnavich and M T Bowers. Theory of ion-neutral interactions: Application of transition state theory concepts to both collisional and reactive properties of simple systems. In *Progress in reaction kinetics, Vol. 11*, pages 137–267. Pergamon Press, 1982.

[CEW11] P Collins, G S Ezra, and S Wiggins. Index k saddles and dividing surfaces in phase space with applications to isomerization dynamics. *J. Chem. Phys.*, 134(24):244105, 2011.

[Con68] C C Conley. Low energy transit orbits in the restricted three-body problem. *SIAM J. Appl. Math.*, 16(4):732–746, 1968.

[CP11] L Chierchia and G Pinzari. The planetary n-body problem: symplectic foliation, reductions and invariant tori. *Invent. Math.*, 186(1):1–77, 2011.

[CSB80] W J Chesnavich, T Su, and M T Bowers. Collisions in a noncentral field: A variational and trajectory investigation of iondipole capture. *J. Phys. Chem.*, 72(4):2641, 1980.

[CV+79] Y Colin de Verdière and J Vey. Le lemme de Morse isochore. *Topology*, 18(4):283-293, 1979.

[CW12] Ü Çiftçi and H Waalkens. Phase space structures governing reaction dynamics in rotating molecules. *Nonlinearity*, 25(3):791–812, 2012.

[dA+90] A M de Almeida, N De Leon, M A Mehta, and C C Marston. Geometry and dynamics of stable and unstable cylinders in hamiltonian systems. *Phys. D*, 46(2):265–285, 1990.

[Dav85] M J Davis. Bottlenecks to intramolecular energy transfer and the calculation of relaxation rates. *J. Chem. Phys.*, 83(3):1016–1031, 1985.

[Dav87] M J Davis. Phase space dynamics of bimolecular reactions and the breakdown of transition state theory. *J. Chem. Phys.*, 86(7):3978–4003, 1987.

[DE93] A Deprit and A Elipe. Complete reduction of the Euler-Poinsot problem. *J. Astronaut. Sci.*, 41:603–628, 1993.

[Dep67] A Deprit. Free Rotation of a Rigid Body Studied in the Phase Space. *Am. J. Phys.*, 35(5), 1967.

[Dep83] A Deprit. Elimination of the nodes in problems of n bodies. *Celestial Mech. Dynam. Astronom.*, 30:181–195, 1983.

[DG+90] M Ding, C Grebogi, E Ott, and J A Yorke. Transition to chaotic scattering. *Phys. Rev. A*, 42(12):7025, 1990.

[DJ+05] M Dellnitz, O Junge, W S Koon, F Lekien, M W Lo, J E Marsden, K Padberg, R Preis, S D Ross, and B Thiere. Transport in dynamical astronomy and multibody problems. *Internat. J. Bifur. Chaos*, 15(03):699–727, 2005.

[Dor99] J R Dorfman. *An introduction to chaos in nonequilibrium statistical mechanics.* Cambridge Univ. Press, 1999.

[DVB55] R De Vogelaere and M Boudart. Contribution to the theory of fast reaction rates. *J. Chem. Phys.*, 23(7):1236–1244, 1955.

[DYK04] W Domcke, D R Yarkony, and H Köppel, editors. *Conical Intersections: Electronic Structure, Dynamics & Spectroscopy.* World Scientific, 2004.

[Eas67] R W Easton. *On the existence of invariant sets inside a submanifold convex to a flow.* PhD thesis, University of Wisconsin - Madison, 1967.

[Eck35] C Eckart. Some studies concerning rotating axes and polyatomic molecules. *Phys. Rev.*, 47(7):552, 1935.

[EW09]   G S Ezra and S Wiggins. Phase-space geometry and reaction dynamics near index 2 saddles. *J. Phys. A*, 42:205101, 2009.

[Fen71]   N Fenichel. Persistence and smoothness of invariant manifolds for flows. *Indiana Univ. Math. J.*, 21:193–226, 1971.

[Fra88]   J P Françoise. Relative cohomology and volume forms. *Banach Cent. Publ.*, 20:207–222, 1988.

[Fra04]   T Frankel. *The geometry of physics: an introduction*. Cambridge Univ. Press, second edition, 2004.

[FU95]   D Farrelly and T Uzer. Ionization mechanism of Rydberg atoms in a circularly polarized microwave field. *Phys. Rev. Lett.*, 74(10), 1995.

[Gas05]   P Gaspard. *Chaos, scattering and statistical mechanics*. Cambridge Univ. Press, 2005.

[GH90]   J Guckenheimer and P J Holmes. *Nonlinear Oscillations, Dynamical Systems, and Bifurcations of Vector Fields*. Springer-Verlag, 1990.

[GHS97]   R W Ghrist, P J Holmes, and M C Sullivan. *Knots and links in three-dimensional flows*. Springer-Verlag, 1997.

[GLS96]   V Guillemin, E Lerman, and S Sternberg. *Symplectic Fibrations and Multiplicity Diagrams*. Cambridge Univ. Press, 1996.

[GPS02]   H Goldstein, C Poole, and J Safko. *Classical Mechanics*. Addison Wesley, third edition, 2002.

[GT14]   V Gelfreich and D Turaev. Arnold Diffusion in a priory chaotic Hamiltonian systems. *ArXiv preprint*, arXiv:1406.2945, 2014.

[GS90]   V Guillemin and S Sternberg. *Geometric asymptotics*. American Mathematical Society, 1990.

[Hal69]   J K Hale. *Ordinary differential equations*. John Wiley & Sons Inc., 1969.

[Han07]   H Hanßmann. *Local and Semi-Local Bifurcations in Hamiltonian Dynamical Systems: results and examples*, volume 1893 of *Lect. Notes Math.* Springer-Verlag, 2007.

[HH08]   N E Henriksen and F Y Hansen. *Theories of molecular reaction dynamics: the microscopic foundation of chemical kinetics*. Oxford Univ. Press, 2008.

[Hov08]   I Hoveijn. Differentiability of the volume of a region enclosed by level sets. *J. Math. Anal. Appl.*, 348(1):530–539, 2008.

[HPS77]   M W Hirsch, C C Pugh, and M Shub. *Invariant Manifolds*, volume 583 of *Lect. Notes Math.* Springer-Verlag, 1977.

[HU+11]   G Haller, T Uzer, J Palacián, P Yanguas, and C Jaffé. Transition state geometry near higher-rank saddles in phase space. *Nonlinearity*, 24(2):527–561, 2011.

[Jon95]   C KRT Jones. Geometric singular perturbation theory. In R Johnson, editor, *Dynamical systems*, volume 583 of *Lect. Notes Math.*, pages 44-118. Springer-Verlag, 1995.

[JR+02]   C Jaffé, S D Ross, M W Lo, J E Marsden, D Farrelly, and T Uzer. Statistical theory of asteroid escape rates. *Phys. Rev. Lett.*, 89(1):11101, 2002.

[JT09]   C KRT Jones and S-K Tin. Generalized exchange lemmas and orbits heteroclinic to invariant manifolds. *Discret. Contin. Dyn. Sys. - Series S*, 2(4):967–1023, 2009.

[Kec67]   J C Keck. Variational theory of reaction rates. In I Prigogine, editor, *Advances in Chemical Physics, Volume 13*, pages 85–121. John Wiley & Sons Inc., 1967.

[Kel65]   A Kelley. The center manifold and integral manifolds for Hamiltonian systems. *Notices Amer. Math. Soc.*, 12:143–144, 1965.

[Kin82]   M C King. Experiments with time: progress and problems in the development of chemical kinetics. Part 2. *Ambix*, 29(1):49–61, 1982.

[KK11a]   S Kawai and T Komatsuzaki. Phase space geometry of dynamics passing through saddle coupled with spatial rotation. *J. Chem. Phys.*, 134(8):084304, 2011.

[KRT00]   I N Kozin, R M Roberts, and J Tennyson. Relative equilibria of D_2H^+ and H_2D^+. *Mol. Phys.*, 98(5):295–307, 2000.

[Lai85]   K J Laidler. René Marcelin (1885-1914), a short-lived genius of chemical kinetics. *J. Chem. Educ.*, 62(11):1012, 1985.

[Lan05]   P Langevin. Une formule fondamentale de theorie cinetique. *Ann. Chim. Phys.*, 8(5):245–288, 1905.

[Lee93]   T K Leen. A coordinate-independent center manifold reduction. *Phys. Lett. A*, 174(1-2):89–93, 1993.

[Lee03]   J M Lee. *Introduction to Smooth Manifolds*. Springer-Verlag, 2003.

[LM02]   R G Littlejohn and K A Mitchell. Gauge theory of small vibrations in polyatomic molecules. In P Newton, P Holmes, and A Weinstein, editors, *Geometry, mechanics, and dynamics*, pages 407–428. Springer-Verlag, 2002.

[LR97]   R G Littlejohn and M Reinsch. Gauge fields in the separation of rotations and internal motions in the n-body problem. *Rev. Modern Phys.*, 69(1):213–275, 1997.

[LTK09]   C B Li, M Toda, and T Komatsuzaki. Bifurcation of no-return transition states in many-body chemical reactions. *J. Chem. Phys.*, 130:124116, 2009.

[Mac90]   R S MacKay. Flux over a saddle. *Phys. Lett. A*, 145(8-9):425–427, 1990.

[Mac91]   R S MacKay. A variational principle for invariant odd-dimensional submanifolds of an energy surface for Hamiltonian systems. *Nonlinearity*, 4:155–157, 1991.

[Mac94a]   R S MacKay. On transport in Hamiltonian systems. In S Benkadda, F Doveil, and Y Elskens, editors, *Transport, Chaos and Plasma Physics*, pages 30–38. World Scientific, 1994.

[Mac94b]   R S MacKay. Transport in 3D volume-preserving flows. *J. Nonlinear Sci.*, 4(1):329–354, 1994.

[Mac04]   R S MacKay. Slow Manifolds. In T Dauxois, A Litvak-Hinenzon, R S MacKay, and A Spanoudaki, editors, *Energy Localization and Transfer*, pages 149–192. World Scientific, 2004.

[Mar]   J-P Marco. Lecture notes, lecture 9: Homoclinic and heteroclinic connections. Preprint.

[Mar15]   R Marcelin. Contribution a l'étude de la cinétique physico-chimique. *Ann. Phys.-Paris*, 3:120–231, 1915.

[Mar92]   J E Marsden. *Lectures on mechanics.* Cambridge Univ. Press, 1992.

[Max70]   J C Maxwell. On hills and dales. *Philos. Mag.*, 4(269):421–427, 1870.

[MC$^+$14]   F A L Mauguiére, P Collins, G S Ezra, S C Farantos, and S Wiggins. Multiple transition states and roaming in ion-molecule reactions: a phase space perspective. *Chem. Phys. Lett.*, 592(0):282 – 287, 2014.

[MC$^+$13]   F A L Mauguière, P Collins, G S Ezra, and S Wiggins. Bifurcations of normally hyperbolic invariant manifolds in analytically tractable models and consequences for reaction dynamics. *Internat. J. Bifur. Chaos*, 23(12), 2013.

[McG69]   R McGehee. *Some homoclinic orbits for the restricted three-body problem.* PhD thesis, University of Wisconsin - Madison, 1969.

[Mei92]   J D Meiss. Symplectic maps, variational principles, and transport. *Rev. Mod. Phys.*, 64(3):795, 1992.

[Mey73]   K R Meyer. Symmetries and integrals in mechanics. In M Peixoto, editor, *Dynamical systems*, pages 259–273. Academic Press, 1973.

[Mez87]   P G Mezey. *Potential Energy Hypersurfaces.* Elsevier, 1987.

[MHO09]   K R Meyer, G R Hall, and D Offin. *Introduction to Hamiltonian Dynamical Systems and the N-body Problem.* Springer-Verlag, second edition, 2009.

[Mie91]   A Mielke. *Hamiltonian and Lagrangian Flows on Center Manifolds: with Applications to Elliptic Variational Problems*, volume 1489 of *Lect. Notes Math.* Springer-Verlag, 1991.

[Mil63]   J W Milnor. *Morse Theory.* Princeton Univ. Press, 1963.

[MM$^+$07]   J E Marsden, G Misiolek, J-P Ortega, M Perlmutter, and T S Ratiu. *Hamiltonian reduction by stages*, volume 1913 of *Lect. Notes Math.* Springer-Verlag, 2007.

[MMP84]   R S MacKay, J D Meiss, and I C Percival. Transport in Hamiltonian systems. *Phys. D*, 13(1-2):55–81, 1984.

[MS98]   D McDuff and D Salamon. *Introduction to Symplectic Topology.* Oxford Univ. Press, second edition, 1998.

[MS14]   R S MacKay and D C Strub. Bifurcations of transition states: Morse bifurcations. *Nonlinearity*, 27(5):859–895, 2014.

[MS15]   R S MacKay and D C Strub. Morse bifurcations of transition states in bimolecular reactions. *ArXiv preprint*, arXiv:1501.00266, 2015.

[MSM13]   B A Mosovsky, M F M Speetjens, and J D Meiss. Finite-time transport in volume-preserving flows. *Phys. Rev. Lett.*, 110(21):214101, 2013.

[MS$^+$81]   G Marmo, E J Saletan, A Simoni, and F Zaccaria. Liouville dynamics and poisson brackets. *J. Math. Phys.*, 22(4):835–842, 1981.

[MW01]   J E Marsden and A Weinstein. Comments on the history, theory, and applications of symplectic reduction. In N P Landsman, M Pflaum, and M Schlichenmaier, editors, *Quantization of singular symplectic quotients*, pages 1–19. Springer-Verlag, 2001.

[MX$^+$91]   R S MacKay, Q-X Xu, FJ Aoiz, and A. Bahri. Dependence of the reaction cross section on the collision energy in reactions of Sr + RX $\rightarrow$ SrX + R (R = C_2H_5, n-C_3H_7, t-C_4H_9; X = Br, I): effect of the Alkyl group. *J. Phys. Chem.*, 95:8226–8232, 1991.

[OR04]   J-P Ortega and T S Ratiu. *Momentum maps and Hamiltonian reduction.* Springer-Verlag, 2004.

[Osb08]   D L Osborn. Exploring multiple reaction paths to a single product channel. In S A Rice, editor, *Advances in Chemical Physics, Volume 138*, pages 213–266. John Wiley & Sons Inc., 2008.

[Pec76]   P Pechukas. Statistical approximations in Collision theory. In W H Miller, editor, *Dynamics of Molecular Collisions Part B*, pages 269–322. Plenum Press, 1976.

[Pec80]   P Pechukas. Orbiting trajectories in noncentral fields. *J. Chem. Phys.*, 73:993–994, 1980.

[Pet07]   M Pettini. *Geometry and topology in Hamiltonian dynamics and statistical mechanics.* Springer-Verlag, 2007.

[PM08]   D Pinheiro and R S MacKay. Interaction of Two Charges in a Uniform Magnetic Field: II. Spatial Problem. *J. Nonlinear Sci.*, 18(6):615–666, 2008.

[PP78]   E Pollak and P Pechukas. Transition states, trapped trajectories, and classical bound states embedded in the continuum. *J. Chem. Phys.*, 69(3):1218–1226, 1978.

[PT05]   E Pollak and P Talkner. Reaction rate theory: What it was, where is it today, and where is it going? *Chaos*, 15:026116, 2005.

[Rob92]   J Robbins. Winding number formula for Maslov indices. *Chaos*, 2(1):145–147, 1992.

[Rol03]   D Rolfsen. *Knots and links.* American Mathematical Society, 2003.

[RSS06]   M Roberts, T Schmah, and C Stoica. Relative equilibria in systems with configuration space isotropy. *J. Geom. Phys.*, 56(5):762–779, 2006.

[Sac69]   R J Sacker. A perturbation theorem for invariant manifolds and Hölder continuity. *J. Math. Mech.*, 18(8):705–762, 1969.

[Say39]   A Sayvetz. The Kinetic Energy of Polyatomic Molecules. *J. Chem. Phys.*, 7(6):383, 1939.

[Sij85]   J Sijbrand. Properties of center manifolds. *Trans. Amer. Math. Soc.*, 289(2):431–469, 1985.

[SK78]   D I Sverdlik and G W Koeppl. An energy limit of transition state theory. *Chem. Phys. Lett.*, 59(3):449–453, 1978.

[SL91]   R Sjamaar and E Lerman. Stratified symplectic spaces and reduction. *Ann. Math.*, 134(2):375–422, 1991.

[Sma70]   S Smale. Topology and mechanics. I. *Invent. Math.*, 10(4):305–331, 1970.

[Ste51]   N E Steenrod. *The topology of fibre bundles.* Princeton Univ. Press, 1951.

[Sto13]   A Stone. *The theory of intermolecular forces.* Oxford Univ. Press, 2013.

[Sug00]   A Sugita. Geometrical properties of maslov indices in periodic-orbit theory. *Phys. Lett. A*, 266(4):321–330, 2000.

[Sze67]   V Szebehely. *Theory of orbits. The restricted problem of three bodies.* Academic Press, 1967.

[TJ$^+$85] M Toller, G Jacucci, G DeLorenzi, and C P Flynn. Theory of classical diffusion jumps in solids. *Phys. Rev. B*, 32(4):2082–2095, August 1985.

[TS89]   D V Turaev and L P Shilnikov. On Hamiltonian systems with homoclinic saddle curves. *Soviet Math. Dokl.*, 39(1):165–168, 1989.

[TTK11]   H Teramoto, M Toda, and T Komatsuzaki. Dynamical Switching of a Reaction Coordinate to Carry the System through to a Different Product State at High Energies. *Phys. Rev. Lett.*, 106(5):1–4, 2011.

[UJ$^+$02] T Uzer, C Jaffé, J Palacián, P Yanguas, and S Wiggins. The geometry of reaction dynamics. *Nonlinearity*, 15(4):957–992, 2002.

[Van53]   L Van Hove. The occurrence of singularities in the elastic frequency distribution of a crystal. *Phys. Rev.*, 11(1941), 1953.

[VF92]   A Vanderbauwhede and B Fiedler. Homoclinic period blow-up in reversible and conservative systems. *Z. Angew. Math. Phys.*, 43, 1992.

[Vin57]   G Vineyard. Frequency factors and isotope effects in solid state rate processes. *J. Phys. Chem. Solids*, 3(1-2):121–127, 1957.

[Wat70]   J K G Watson. The vibration-rotation Hamiltonian of linear molecules. *Mol. Phys.*, 19(4):465–487, 1970.

[Wig37]   E P Wigner. Calculation of the rate of elementary association reactions. *J. Chem. Phys.*, 5(9):720–725, 1937.

[Wig38]   E P Wigner. The transition state method. *T. Faraday Soc.*, 34:29–41, 1938.

[Wil36]   J Williamson. On the algebraic problem concerning the normal forms of linear dynamical systems. *Amer. J. Math.*, 58(1):141–163, 1936.

[WW10]   H Waalkens and S Wiggins. Geometrical models of the phase space structures governing reaction dynamics. *Regul. Chaotic Dyn.*, 15(1):1–39, 2010.

[WW$^+$01] S Wiggins, L Wiesenfeld, C Jaffé, and T Uzer. Impenetrable barriers in phase-space. *Phys. Rev. Lett.*, 86(24):5478–5481, 2001.